

TU

TECHNISCHE UNIVERSITÄT WIEN

DIPLOMARBEIT

Three dimensional modelling of the lower limb of children with cerebral palsy and healthy children based on MRI - data

ausgeführt zum Zwecke der Erlangung des akademischen Grades eines Diplom –
Ingenieurs unter der Leitung von

Univ. Prof. Dipl.-Ing. Dr. techn. Margit Gföhler

E307

Institut für Konstruktionswissenschaften und Technische Logistik

Eingereicht an der Technischen Universität Wien

Fakultät für Maschinenwesen und Betriebswissenschaften

von

Clemens Stingeder

0025740

**Troppbergstraße 6B
3011 Unter-Tullnerbach**

Wien, April 2009

Acknowledgement

This work resulted from cooperation between the Institute for “Konstruktionswissenschaften und Technische Logistik” of the Technical University Vienna and the MR/CT Röntgen Institute Liesing. I want thank all people that enabled the writing of my thesis.

Special thanks go to the following people ...

... my parents and my sister for their great support and patience during the whole time of my study. Without them it would not have been possible to finish my academic studies. Thank you for going along with me during all the ups and downs over the whole time!

... my good friend and “Lieblingsbetriebsrat” Herbert Hönisch and his family for helping me in every situation and his donations that made my studies much easier. (Für Herbert: Danke dafür, dass Du immer für mich Zeit gehabt hast und mir sehr oft eine große Hilfe warst!)

... Univ. Prof. Dipl.-Ing. Dr. techn. Margit Gföhler for the allocation of the topic of my thesis.

... Reinhard Hainisch for his mentoring and guidance during the practical work for my thesis and for motivating me whenever I was down.

... M. Zubayer Karim for his support.

... my girlfriend Julia for the attendance during the last months of my studies.

Abstract

The aim of this work was to generate three dimensional models of the lower limb of a child with cerebral palsy and an age – matched healthy child for getting a better understanding of differences in muscle parameters between these two subjects. The models were based on MRI – data that was recorded in the MR/CT Institute Röntgen Liesing. For the modelling the 3D image processing software Amira version 5 from Mercury Computer Systems was used to reconstruct the muscles and the bone structures. Afterwards some muscle parameters were calculated using the data taken out of the muscle models that had been generated before.

Kurzfassung

Das Ziel der vorliegenden Diplomarbeit war es drei dimensionale Modelle der unteren Extremitäten von einem Kind mit Cerebralparese und einem gesunden Kind der gleichen Altersgruppe zu erstellen. Diese Modelle sollten in weiterer Folge dazu verwendet werden Unterschiede bei den einzelnen Muskelparametern herauszuarbeiten. Als Grundlage für die Modellierung wurden MRI – Daten, die im MR/CT Institut Röntgen Liesing aufgenommen wurden, herangezogen. Für die Erstellung der Modelle wurde das 3 dimensionale Bildverarbeitungsprogramm Amira in der Version 5.0 von Mercury Computer Systems verwendet. In weiterer Folge sollten aus den Modellen einige Muskelparameter berechnet werden.

Table of Contents

1. Introduction	5
2. Specific medical terms and definitions	7
2.1 Axes and planes in the human body	7
2.2 General anatomical terms of location.....	8
2.2.1 Directions on the trunk	8
2.2.2 Directions in the limbs	9
2.3 Muscular Tissue of the human body	10
2.3.1 Skeletal muscle	10
2.3.1.1 Forms of skeletal muscles	10
2.4 Muscles and bones of the lower limb and the pelvis.....	11
2.5 Location of left and right in MR-images.....	28
3. Data for the modelling.....	31
3.1 Description of MR – images type	33
4. Working routines with Amira 5.0	35
4.1 Viewing of the MR-images	35
4.1.1 Setting of Data range histogram and colourmap in Amira 5.0	35
4.2 Procedural method of Segmentation in Amira 5.0	37
5 Moving artefacts	41
6. Localization of the bones:.....	42
6.1 Segmentation results.....	45
7. Localization of the muscles.....	46
7.1 Problems that occurred during the separation of the muscles	49
7.2 Segmentation Results:	49
8. Separation of the tendons	51
8.1 Problems that appeared while the segmentation of tendons	55
8.2 Tendon separation results.....	56
9 Muscle parameters	57
9.1 Muscle tendon Model	57
9.2 Calculation of the muscle parameters.....	59
9.3 Results of the Calculation.....	59
9.3.1 General Explanation for the results.....	59
9.3.2 Special results of the calculation.....	60
10. Discussion	69
11. Table of figures:	71
12. Table of Tables	73
13. Bibliography:	74
14. Appendix.....	75

1. Introduction

The first goal of this work was to establish a digital computer model of the muscles and corresponding tendons of the lower limb and the pelvis from a healthy child and a child with Cerebral Palsy (CP).

According to SCPE (Surveillance of Cerebral Palsy in Europe) Cerebral Palsy occurs in 1.5 to 2 per 1000 live births in Europe. Cerebral Palsy results from a static injury caused by pre-, peri- or postnatal brain injury. This type of injury to the central nervous system commonly results in abnormal motor control associated with the delay in the onset of walking, an abnormal gait pattern and an abnormal growth of the muscles and bones. The different muscles in the lower limb of a Cerebral Palsy child do not grow and act as they should during the period of growth and in the later life of a healthy child. The results of the abnormal movement and growth are different muscle functions and gait patterns CP – children in comparison to age – matched healthy children. Consequently leg muscles of CP - children also have different parameters such as muscle volume, tendon length and maximum isometric muscle force.

For the modelling it was necessary to include all muscles of the lower limb that are responsible for human gait. Not all of the muscles that are located in the lower limb were important for the desired model because not all of them have an impact on gait. So in total there were 46 muscles, muscle groups and their proximal and distal tendons that had to be identified. The numbers and names of the muscles were chosen referring to what Wickiewicz et al said in “Muscle architecture of the Human lower Limb” [6].

The available data for the work were digital Magnetic Resonance Images taken from the lower extremities of a child with Cerebral Palsy and an age – matched healthy child in the MR/CT Institute Röntgen Liesing. In these images the muscles and tendons of the lower limb should be identified and separated with the computer program Amira 5.0. This was a necessary step on the way of getting the desired digital models of muscles, tendons and bones.

The second part was to make a comparison of the several parameters. So after the segmentation was done the muscle parameters – muscle fibre length, muscle volume, maximum isometric muscle force and tendon length – should be determined relating to the models. Later on the calculated parameters of the healthy and the handicapped child should be compared.

The reason for this comparison was to find out if there were any significant differences at the several muscle parameters in the healthy and the diseased limbs.

In another work the resulting data is used to establish electronic gait models of the lower limbs. These models are used for simulating the gait of the child and to check which parameters have to be changed to improve locomotion. So in the end the models should be used for gait analysis and to identify useful therapy methods for children with cerebral palsy.

Finally the findings should be used in a gait laboratory to determine what is different in the legs of the handicapped child in comparison to a healthy child. With the found facts it should be possible to find new innovative methods of treating the problems of the children. These methods could either be orthopaedic operations or therapies like physiotherapies or kinesitherapies.

2. Specific medical terms and definitions

2.1 Axes and planes in the human body

It is possible to define a lot of different axis and planes in the human body but in general there are three main axes that are defined. The three axes are perpendicular and they give the space coordinates in the human body. The whole main coordinate system of the human body is related to the technical x-, y-, z- coordinate system.

The axes are defined as follows:

Direct axis (vertical- or longitudinal axis): If the human stands in an upright position this axis is perpendicular to the base

Cross axis (transversal- or horizontal axis): This axis goes from the left to the right side of the body and is perpendicular to the direct axis.

Sagittal axis: Runs from the back side to the front side of the human and is perpendicular to the two aforementioned axes.

Relating to the three main coordinate axes there are also three principal planes:

Sagittal (median) plane: These are all planes that are parallel to the Sagittal axis and they divide the human body in a left- and a right side. The one that divides the corpus into two parts of equal proportions is called the **median plane**.

Transversal (horizontal) plane: All of these planes are perpendicular to the longitudinal axis. They divide the body in an upper- and a lower part.

Coronal (frontal) plane: All planes that divide the body in front- and a back part. They are all parallel to the forehead.

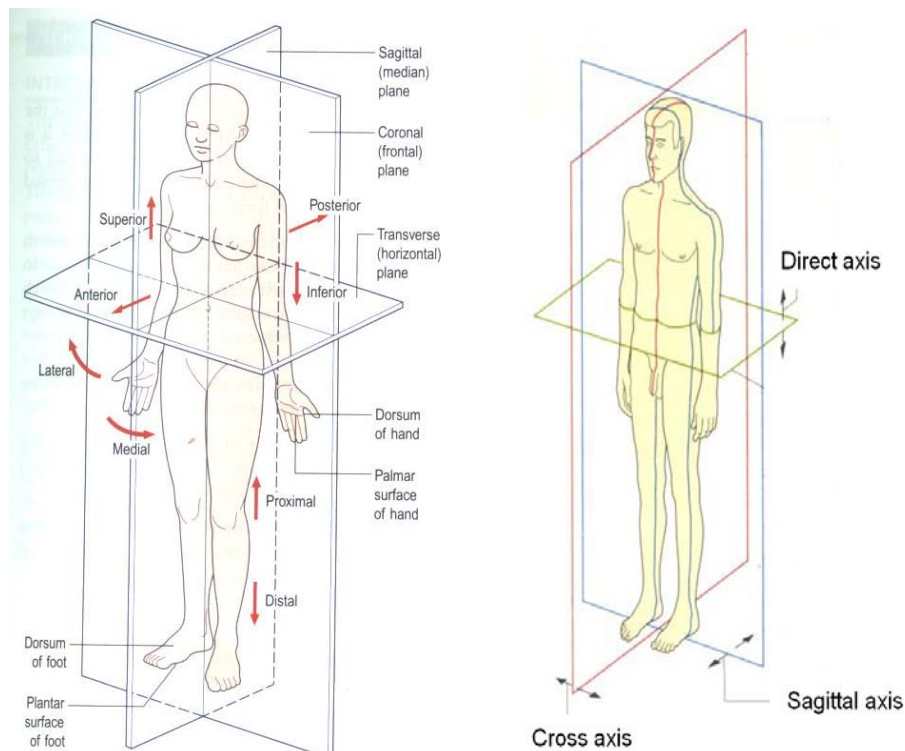


Figure 1: Left side: Planes (Anatomy and human movement, 2006) and right side: Axes (Der Körper des Menschen, 1995) in the human body

2.2 General anatomical terms of location

In medical toponymy there are some special terms for describing the location of a body component or a direction in the human body. These are also used for describing the relationship of one part, region or segment of the body, to another. So there are some special words for example for right, left, up and down and other directions or locations like this. All of these terms are in relation to the anatomical position of the body.

The anatomical position for describing these directions is: standing erect looking forward, the legs are put together and toes are pointing forward. The arms are at the side and the palms are facing forward.

The terms of location that were relevant for this work are described in the following lines.

2.2.1 Directions on the trunk

Dexter: Right side of the body and not of the observer.

Sinister: Left side of the body and not of the observer.

Cranial or superior: above, towards the top of the head; the top of the head is the superior end of the body

Caudal or inferior: below, towards the feet; the feet are the inferior end of the body.

Ventral or anterior: refers to the front of the body, towards the belly

Dorsal or posterior: refers to the back of the body, towards the spine

Medial: towards the medial plane

Lateral: away from the medial plane
Median: right in the median plane
Central: towards the inner side of the body
Peripheral: towards the surface of the body

2.2.2 Directions in the limbs

Proximal or Central: close to the point of attachment on the trunk
Distal or peripheral: away from the point of attachment on the trunk
Radial: parts of the human body which are closer to the radius
Ulnar: parts of the body those are closer to the ulna
Tibial: parts of the body those are closer to the tibia
Fibular: parts of the body those are closer to the fibula
Palmar: towards the palm
Plantar: towards the sole of foot
Dorsal: towards the back of the foot or the back of the hand

The relevant directions for this work can be seen in figure 2.

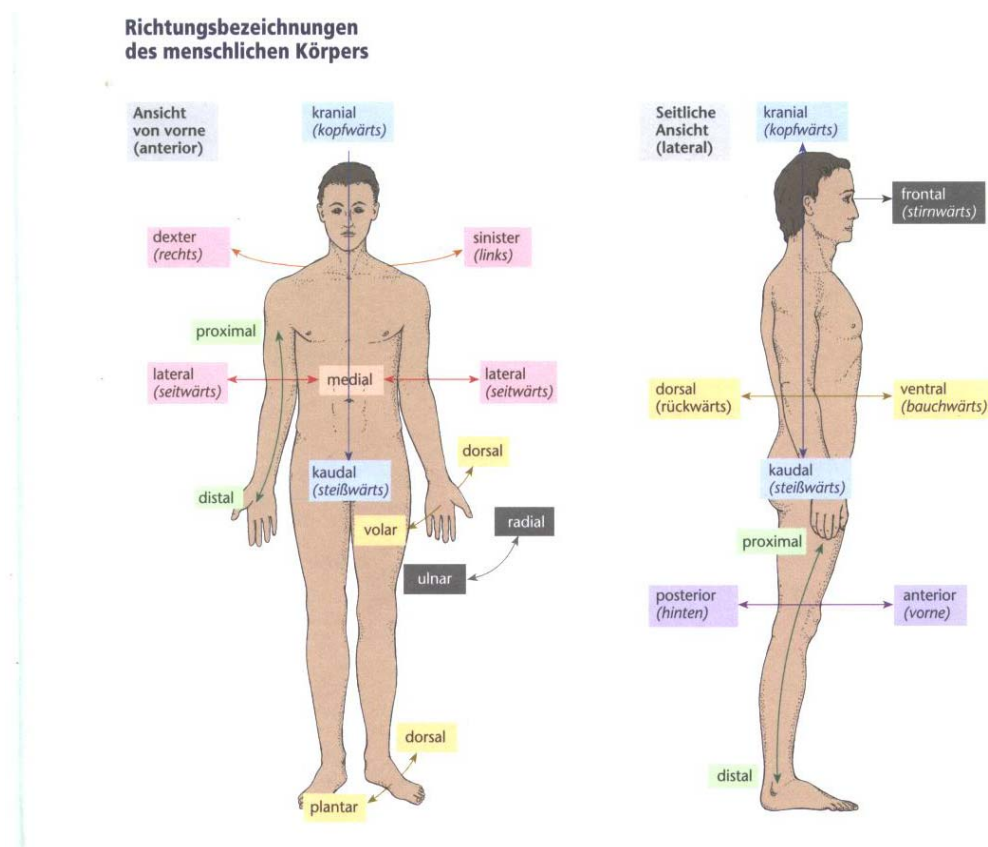


Figure 2: General anatomical terms of location (trunk and extremities),

2.3 Muscular Tissue of the human body

The following chapter is in relation to “Anatomy and human movement – structure and function” fifth edition by Nigel Palastanga, Derek Field and Roger Soames.[7]

Within the body there are three varieties of muscle:

- **Smooth muscle** also referred to as involuntary or non striated muscle
- **Cardiac muscle**
- **Skeletal muscle** also known as voluntary or striated muscle

Smooth muscle forms the muscular layer of the walls of blood vessels and of hollow organs such as the stomach. It is not under voluntary control, contracting more slowly and less powerfully than skeletal muscle. However, it is able to maintain its contraction longer. Cardiac muscle is also not under voluntary control, but although it exhibits striations it is considered to be different from skeletal muscle.

The relevant muscles for this thesis were the skeletal muscles. In the next paragraphs there are some important facts about this type of muscle.

2.3.1 Skeletal muscle

Over a third of the human body mass consist of skeletal muscles. These muscles consist of non branching striated muscle fibres that are bound together by loose areolar tissue. The muscles have different forms: some are flat and sheet - like, some are short and thick while others are long and slender. The muscle length and especially the tendon length are closely related to the distance through which it is required to contract. Some of the muscle fibres have the ability to shorten to almost the half of their length. All of the movement of the human body is an affect of the shortening of muscles. This shortening causes a pulling force over some joints and makes the involved bones move.

2.3.1.1 Forms of skeletal muscles

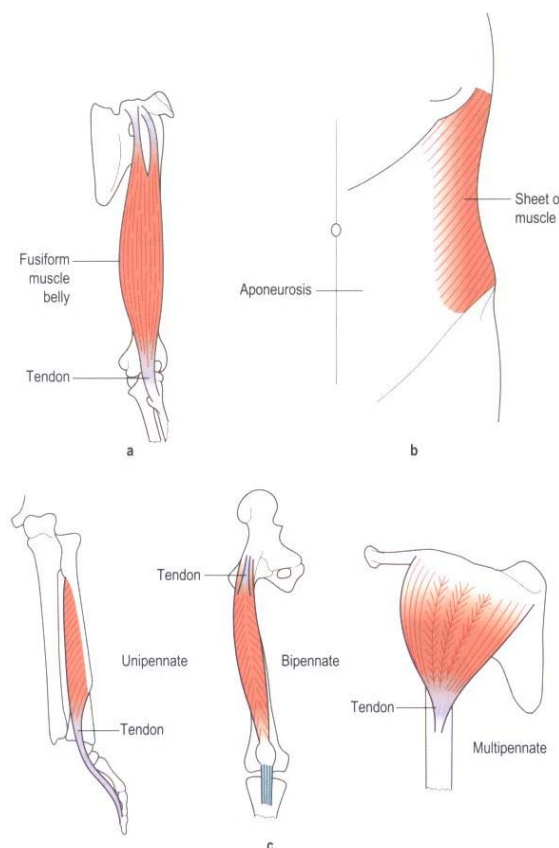
For the identification of the different muscles in the lower limb it was necessary to know the possible forms of skeletal muscles.

The fibres of the muscles can either be parallel or oblique to the pulling line of the whole muscle.

There are three big groups of muscle forms:

- **Fusiform muscle (figure 3 a):** The fibres are parallel to the line of pulling and they are grouped in discrete bundles. (e.g. biceps brachii)
- **Sheet muscle (figure 3 b):** The fibres are parallel to the line of pulling and they are spread as a broad thin sheet. (e.g. external oblique of the abdomen)

- **Pennate muscle (figure 3 c):** The fibres are oblique to the line pull. There are three main kinds of these pennate muscles:
 - *unipennate muscles:* the fibres attach to one side of the tendon only (e.g. flexor pollicis longus)
 - *Bipennate muscles:* They have a central septum with the muscle fibres attaching to both sides of the septum and to its continuous central tendon. (e.g. rectus femoris)
 - *Multipennate muscle:* They have several intermediate septa and each of these is associated with a bipennate arrangement of the fibres (e.g. deltoid)



Various arrangements of fibres within muscles: (a) fusiform; (b) sheet; (c) pennate.

Figure 3: Arrangements of fibres within muscles

2.4 Muscles and bones of the lower limb and the pelvis

For a better orientation in the MR – images it was necessary to get a very good anatomic understanding of the muscles and bones of the pelvis, the thigh and the shank. Another important thing that had to be known was the location of the Origin – the proximal attachment – and the Insertion – the distal attachment – of the desired muscles.

All this knowledge was important for the localisation of the muscles and bones in the images. The starting and endpoint was needed for identifying the tendons.

In figures 4 to 20 an overview of the required anatomy is given.

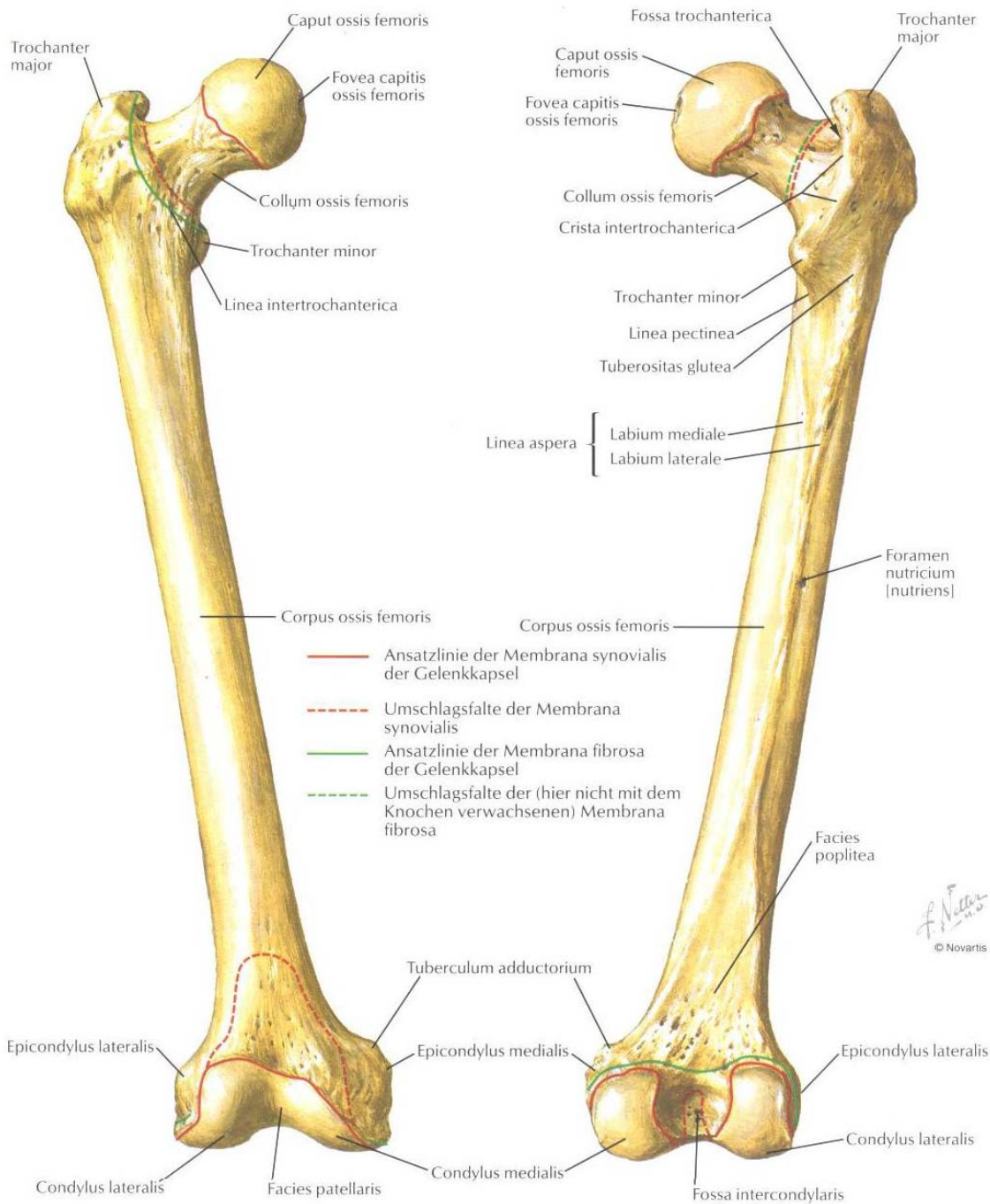


Figure 4: Bones of the thigh – Femur, left ventral view on the left side and dorsal view on the right, Netter 1999

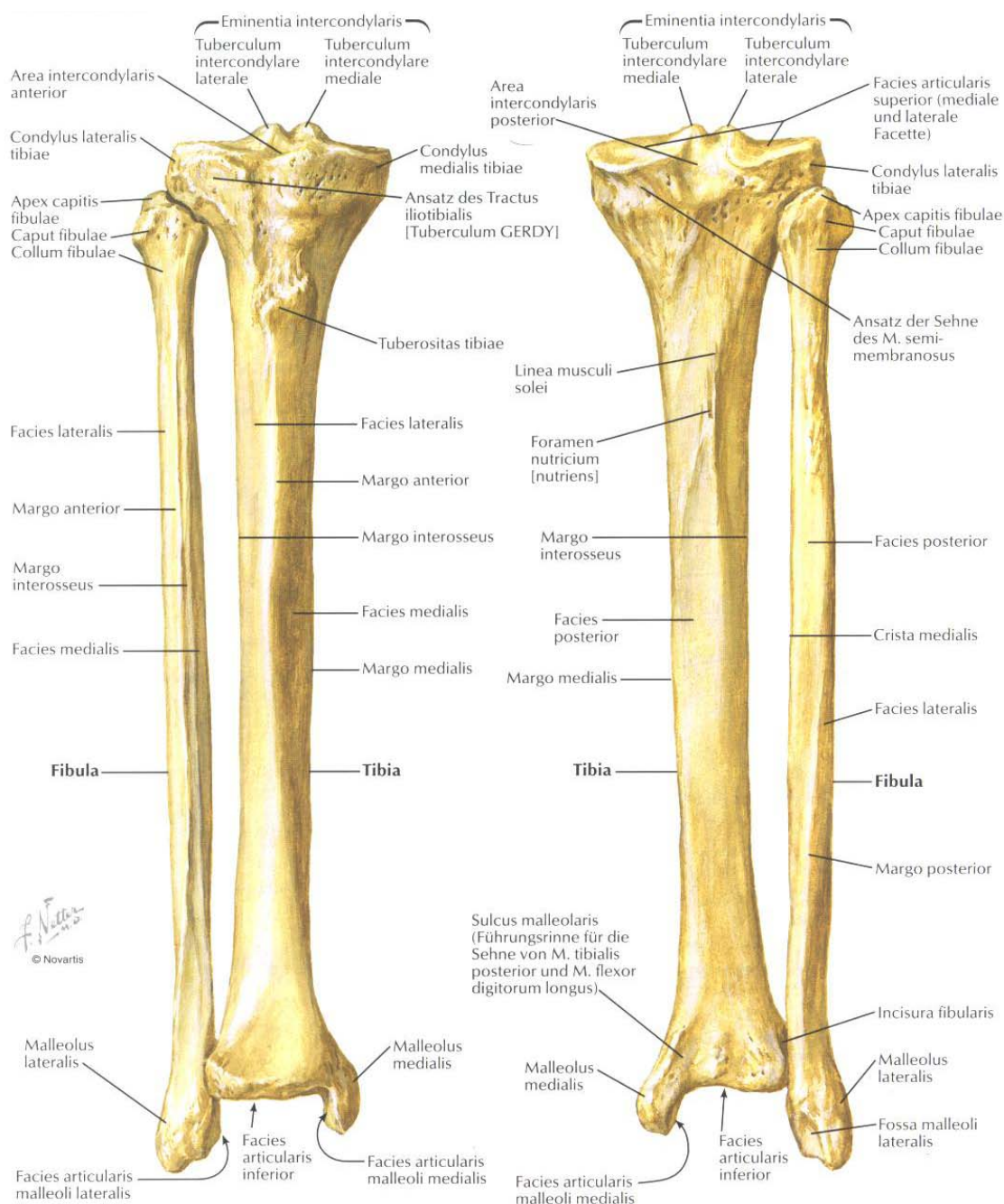


Figure 5: Bones of the shank – Fibula and Tibia, right shank, ventral view on the left and dorsal view on the right, Netter 1999

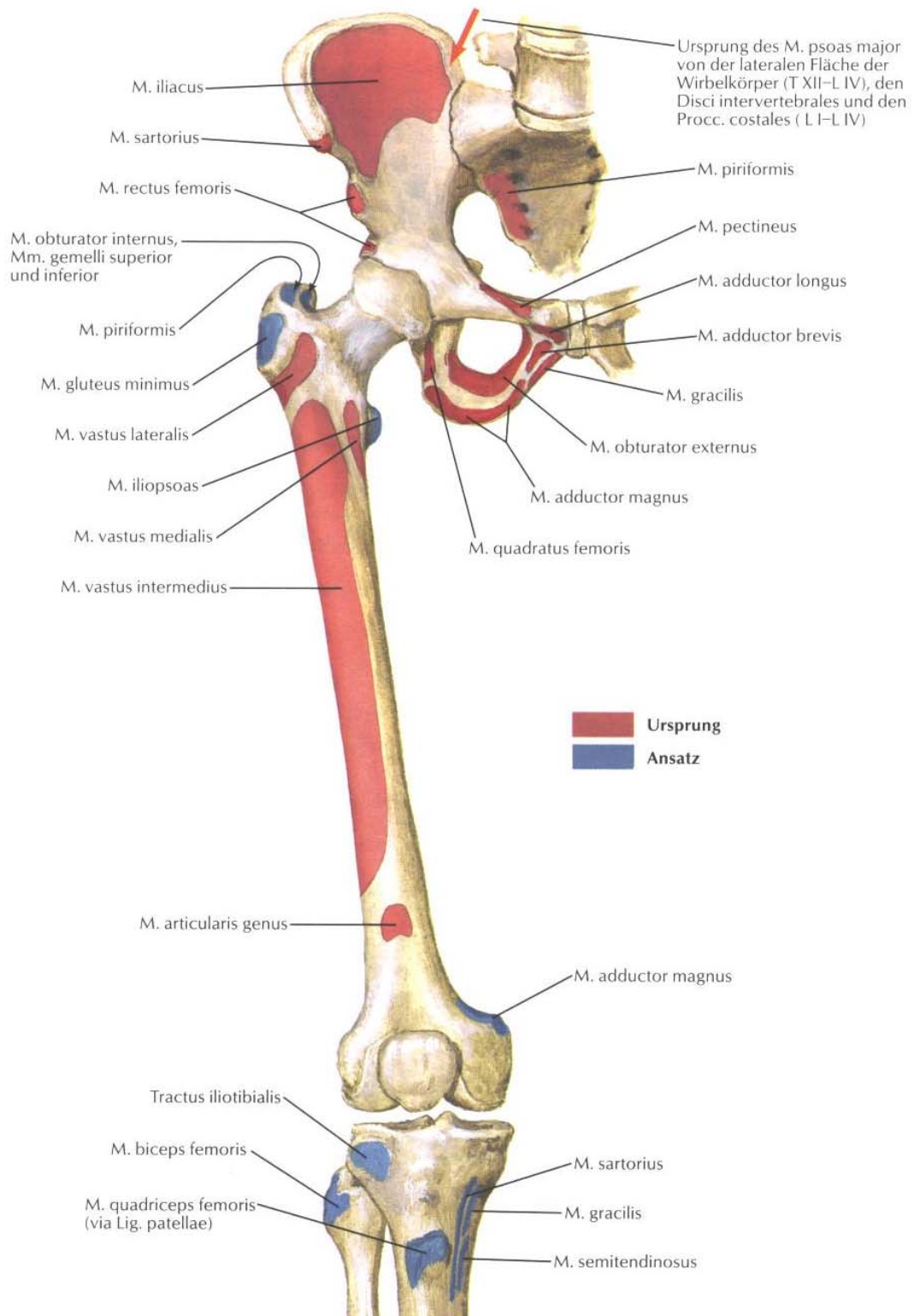


Figure 6: Muscle insertion points on the pelvis and femur, ventral view, origins are marked as red areas and insertion points are marked blue, Netter 1999

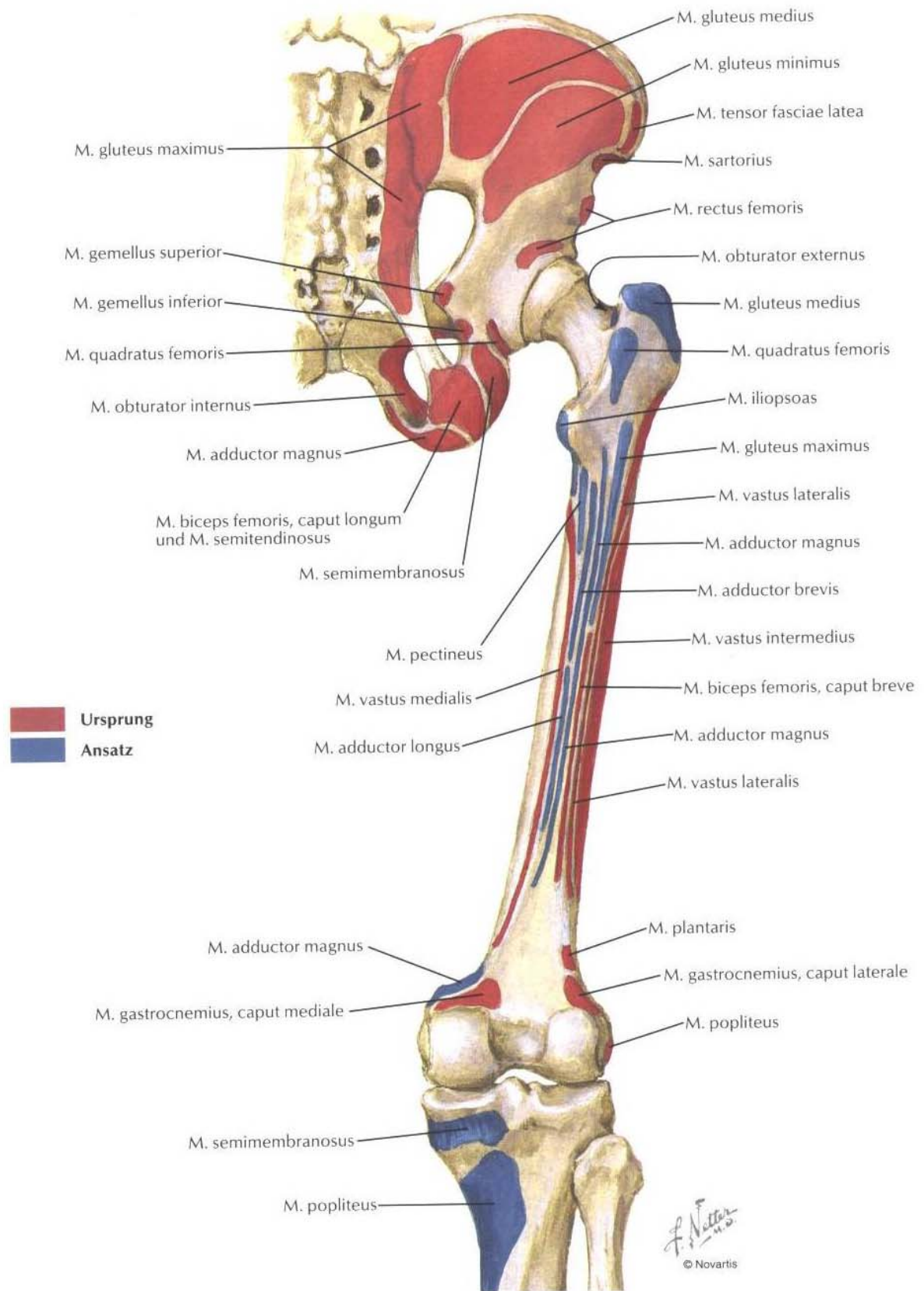


Figure 7: Muscle insertion points on the pelvis and femur, dorsal view, origins are marked as red areas and insertion points are marked blue, Netter 1999

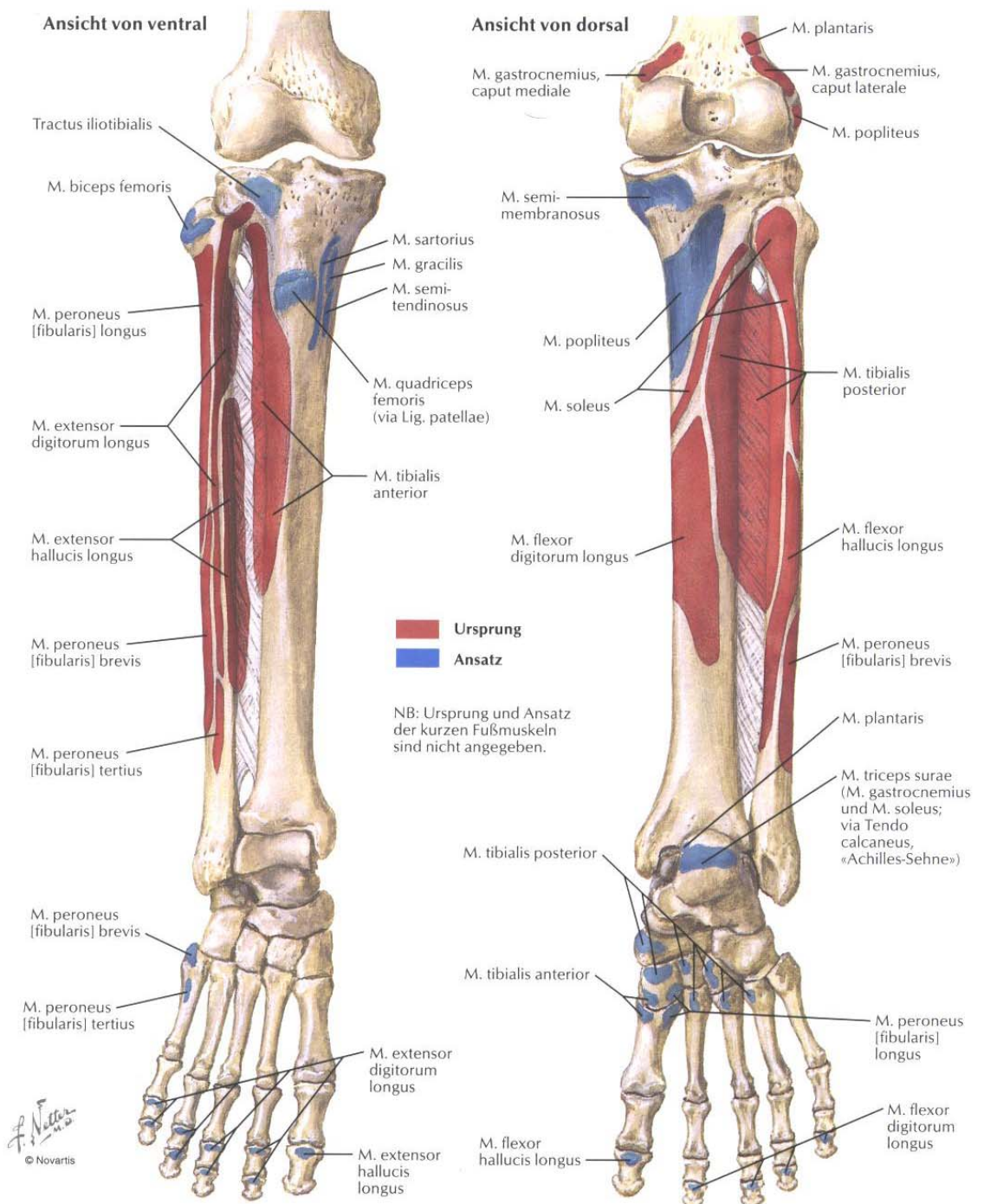


Figure 8: Muscle insertion points on the shank, ventral view on the left and dorsal view on the right, origins are marked as red areas and insertion points are marked blue, Netter 1999

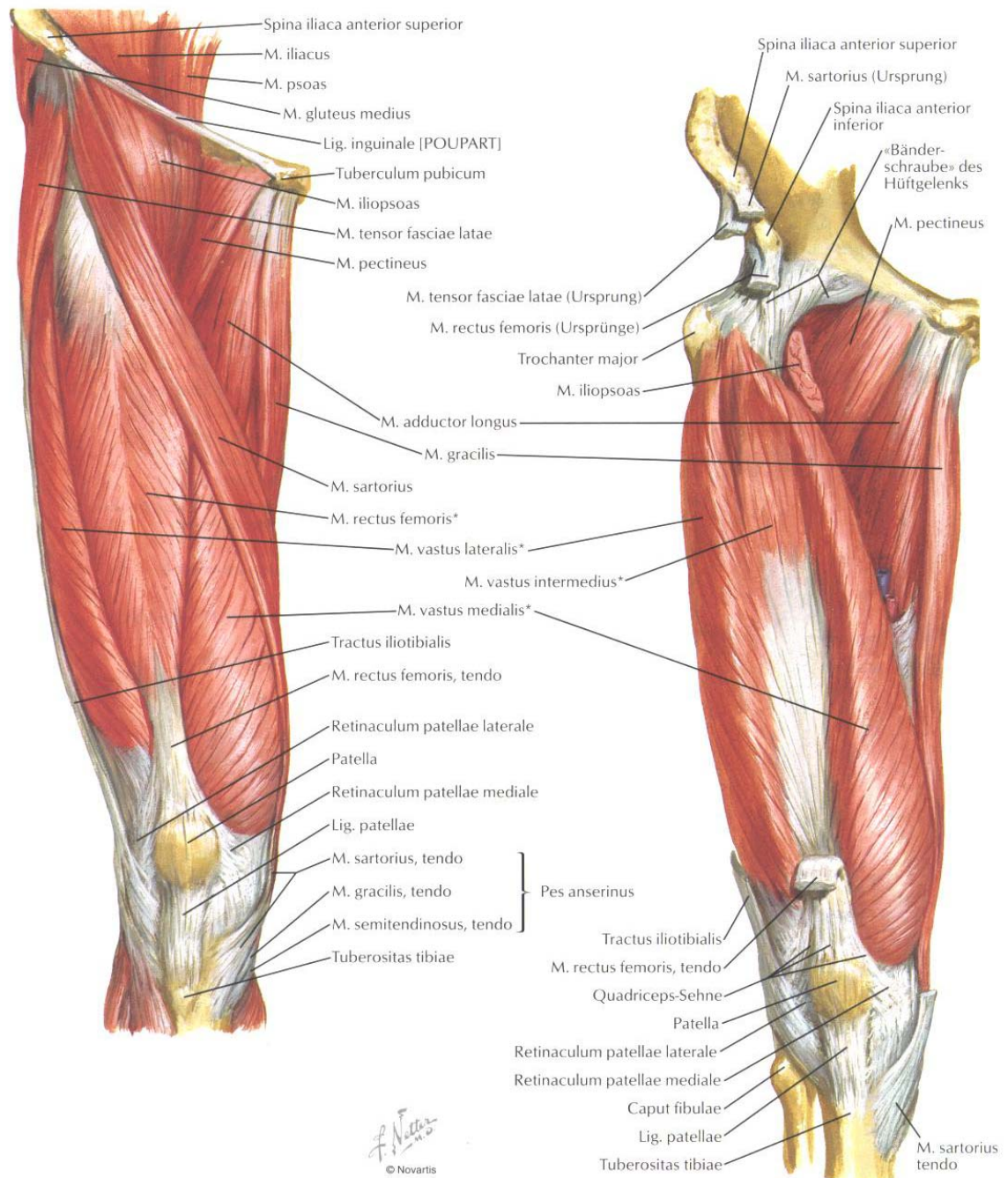


Figure 9: Muscles and tendons of the thigh; ventral view; surface layer on the left and middle layer on the right, Netter 1999

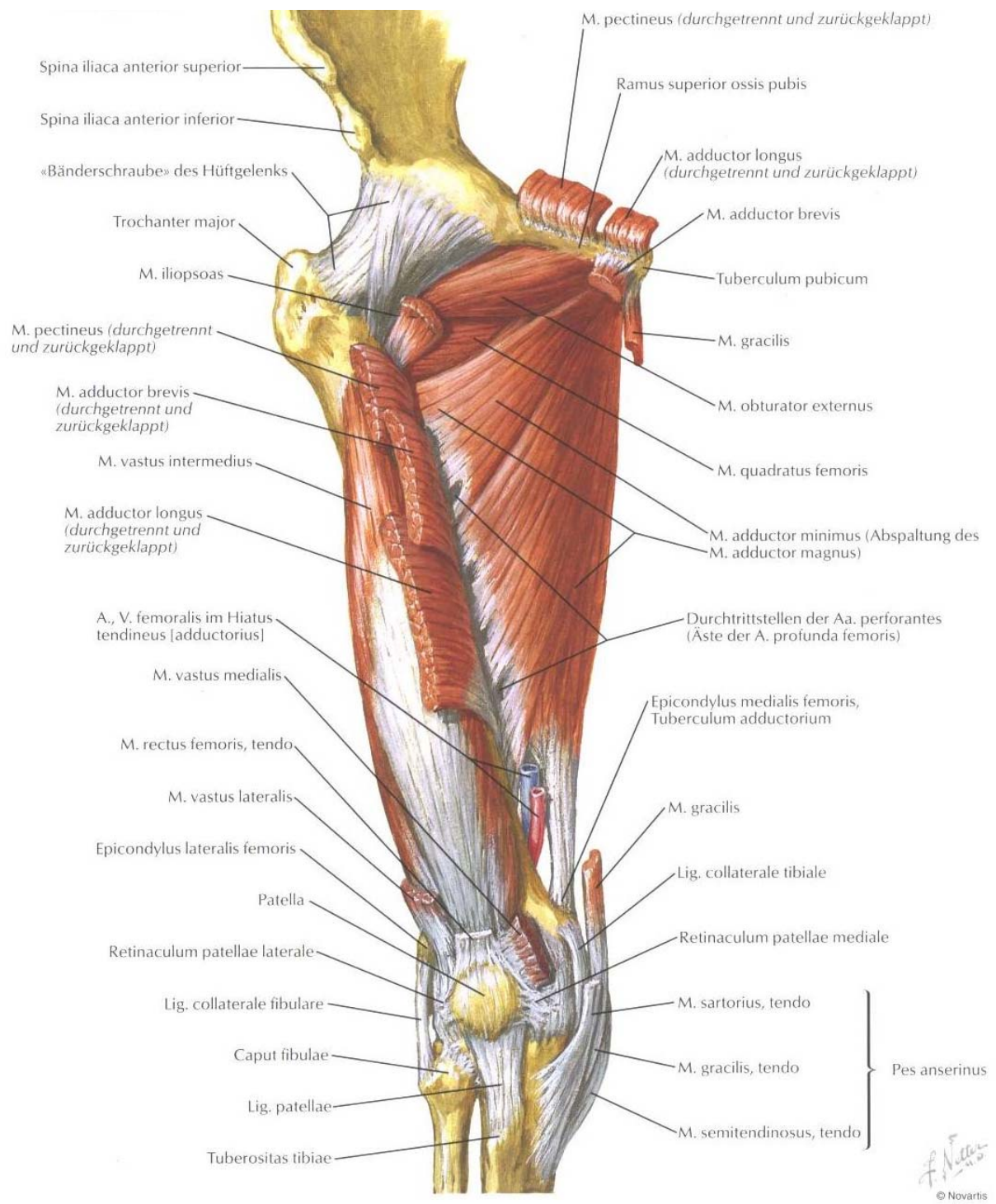


Figure 10: Muscles and tendons of the thigh; ventral view; deepest layer, Netter 1999

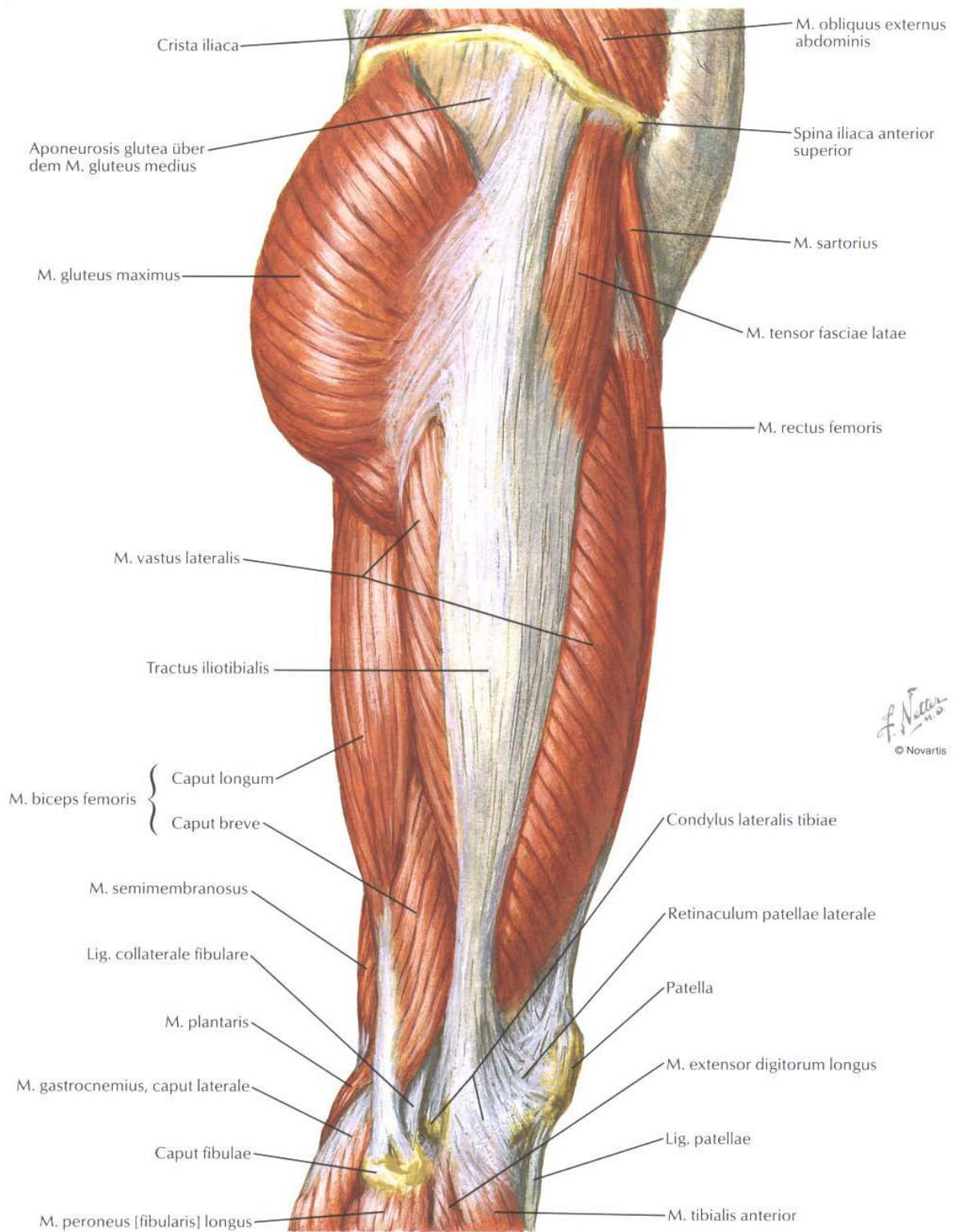


Figure 11: Muscles and tendons of the thigh and the pelvic; lateral view, Netter 1999

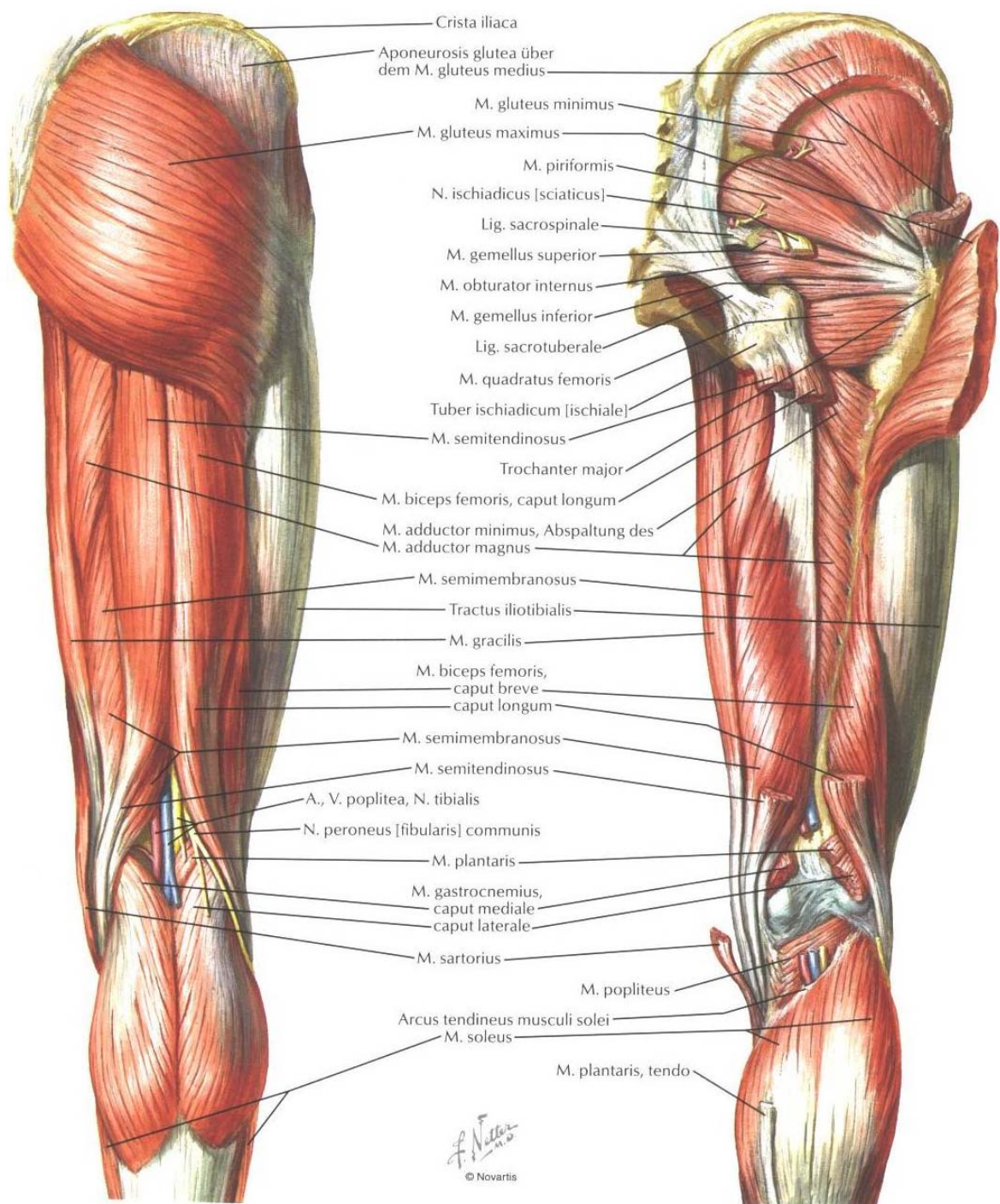


Figure 12: Muscles and tendons of the thigh and the pelvic; ventral view; surface layer on the left and deeper lay on the right, Netter 1999

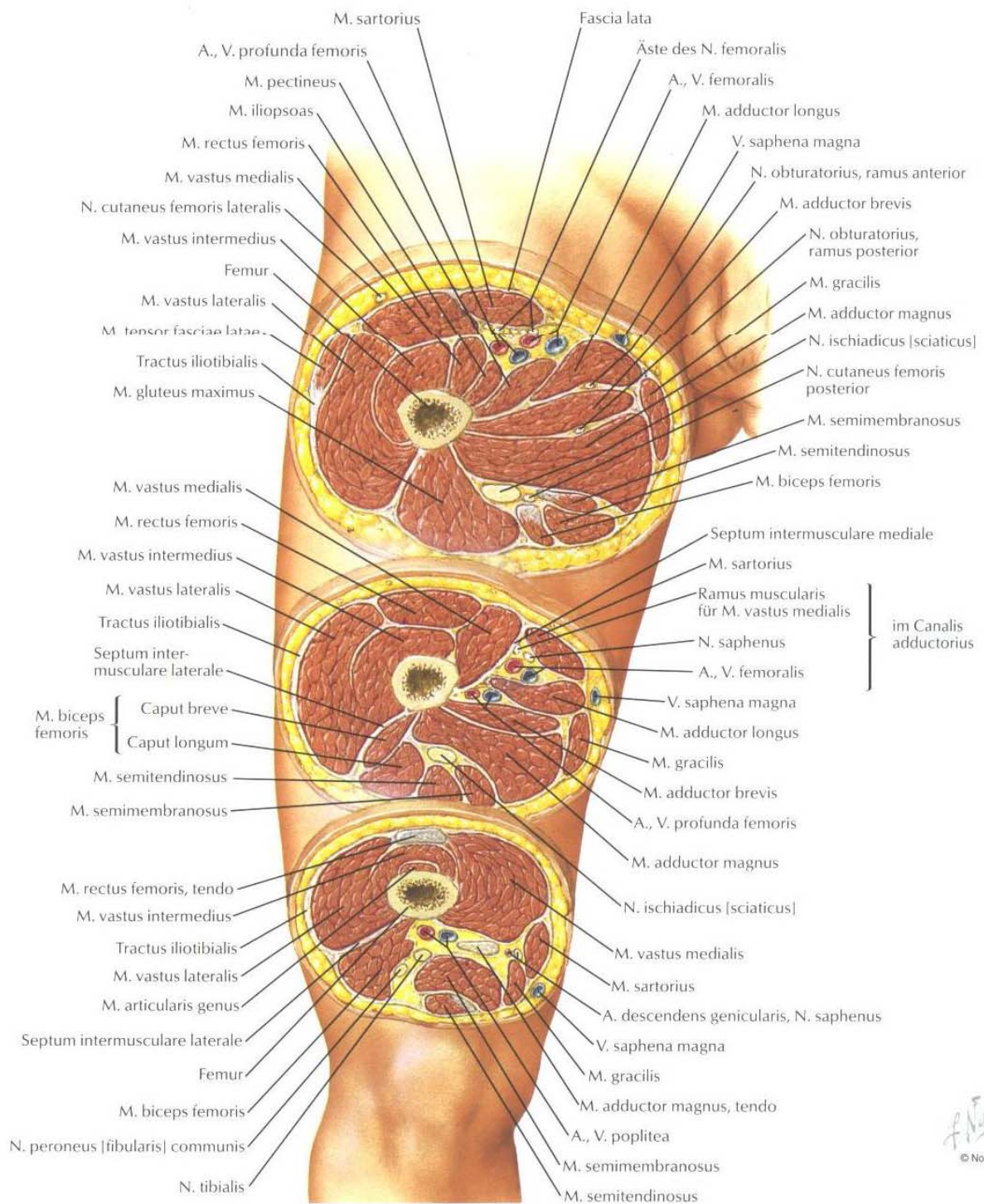


Figure 13: Muscular cross – sections of the thigh, Netter 1999

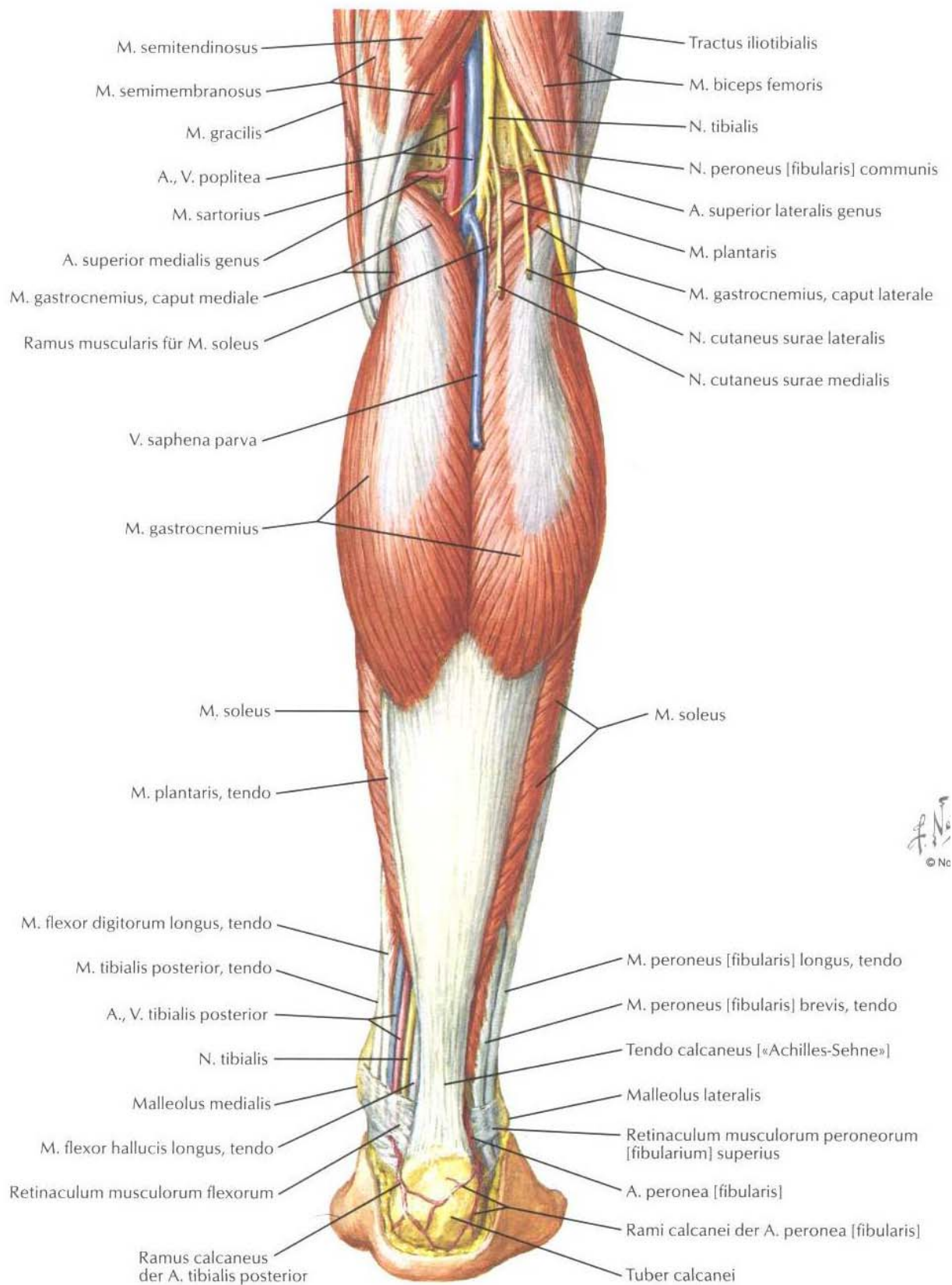


Figure 14: Muscles and tendons of the shank; dorsal view; surface layer, Netter 1999

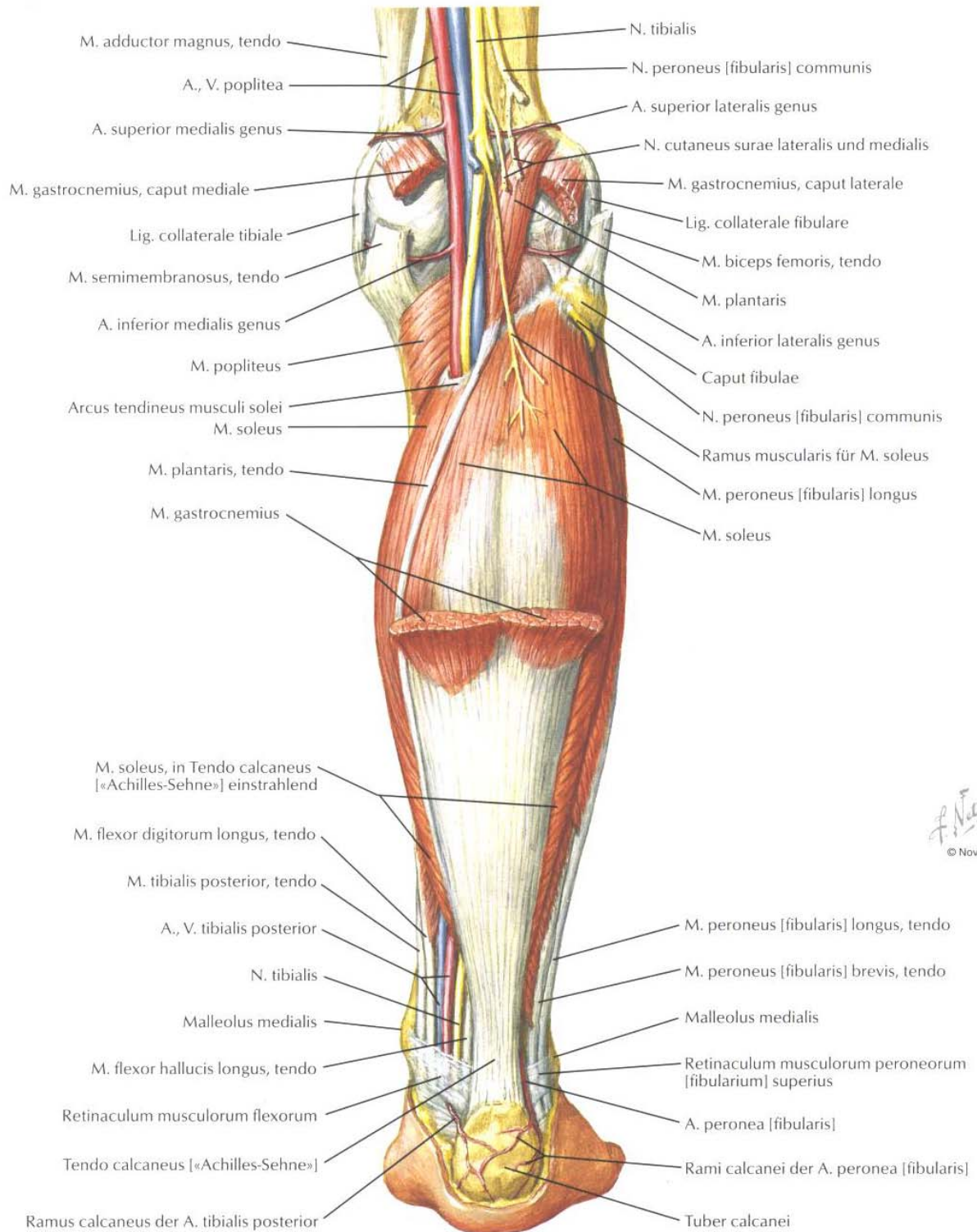


Figure 15: Muscles and tendons of the shank; dorsal view; middle layer, Netter 1999

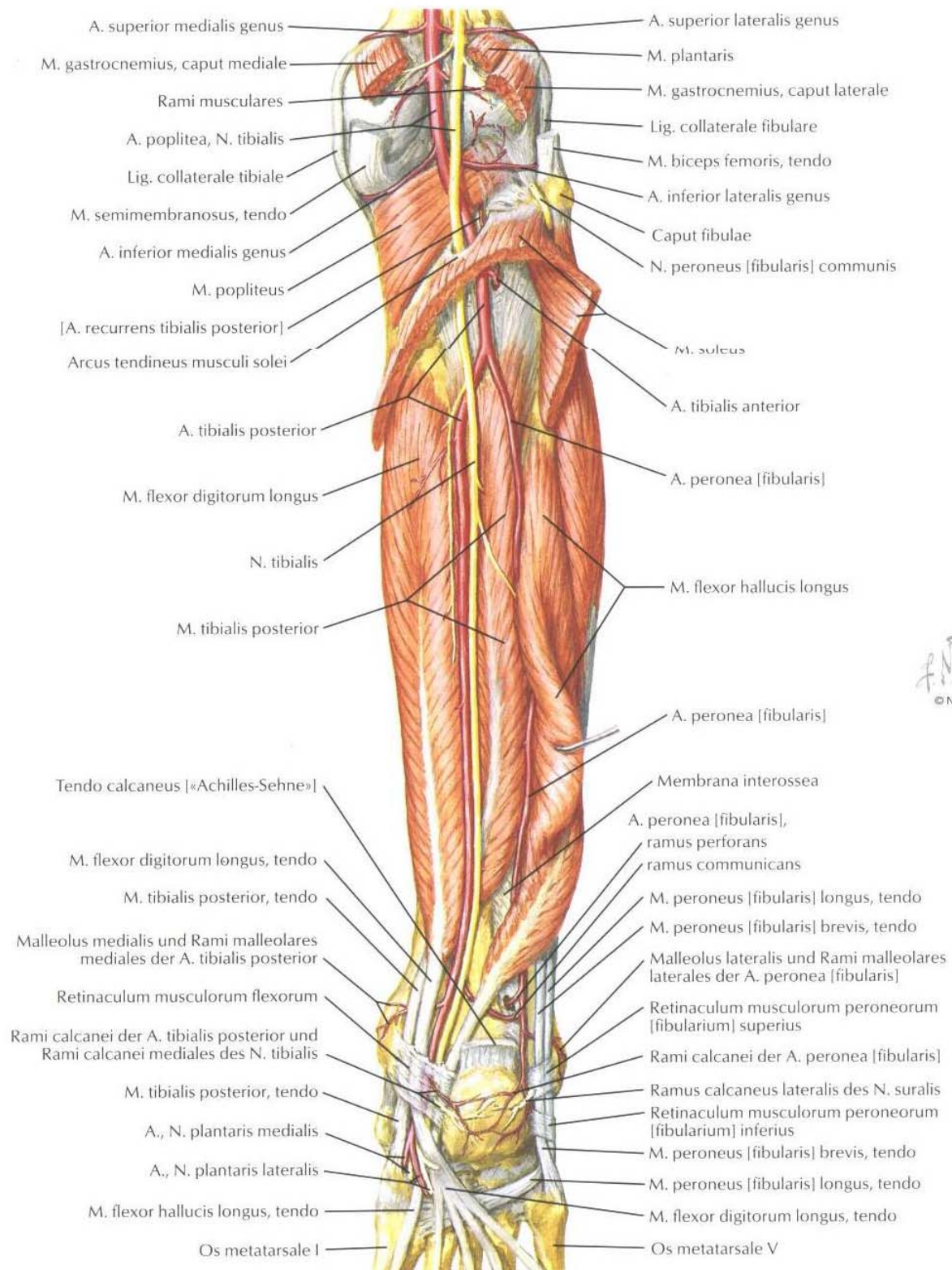


Figure 16: Muscles and tendons of the shank; dorsal view; deepest layer, Netter 1999

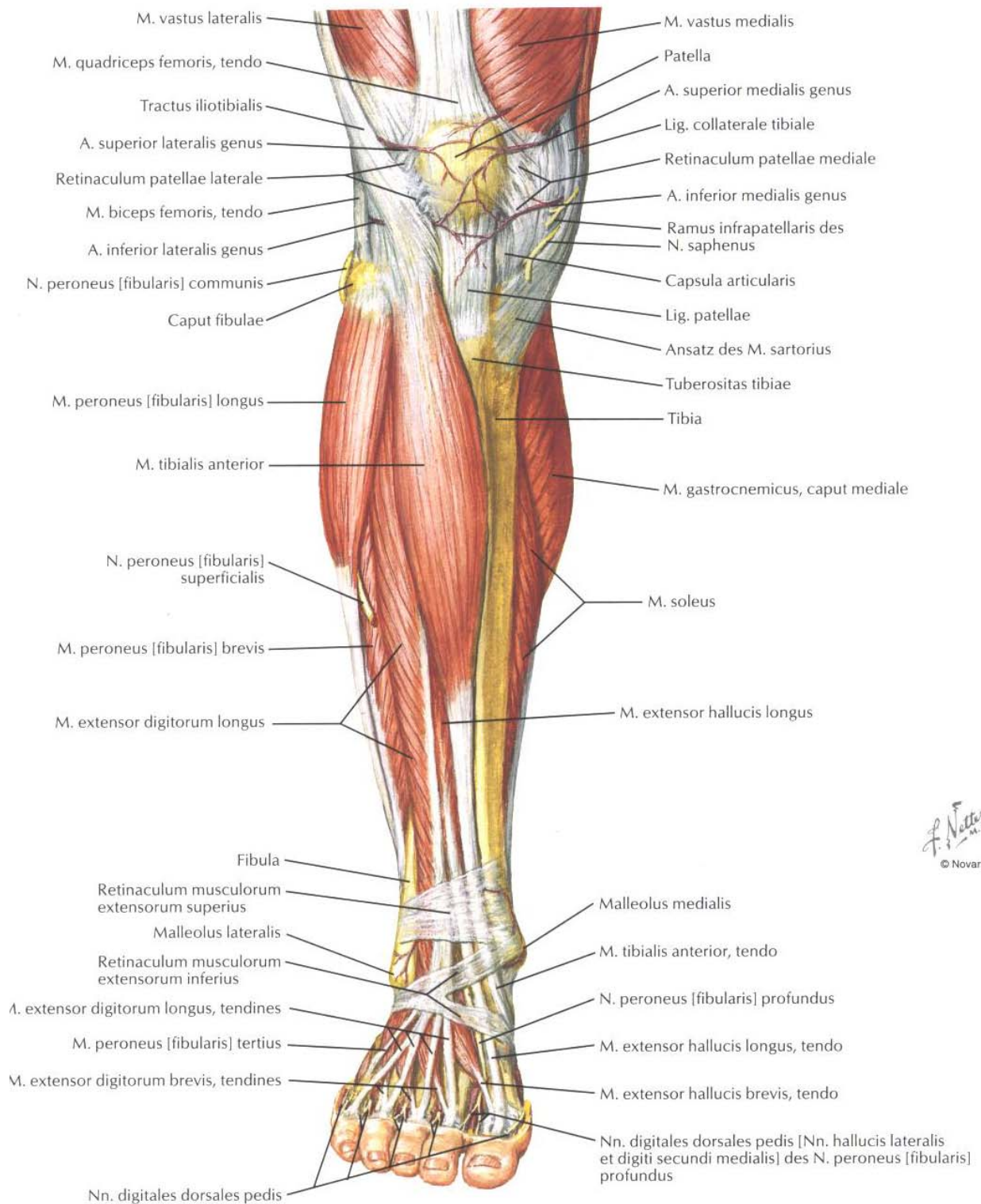


Figure 17: Muscles and tendons of the shank; ventral view; surface layer, Netter 1999

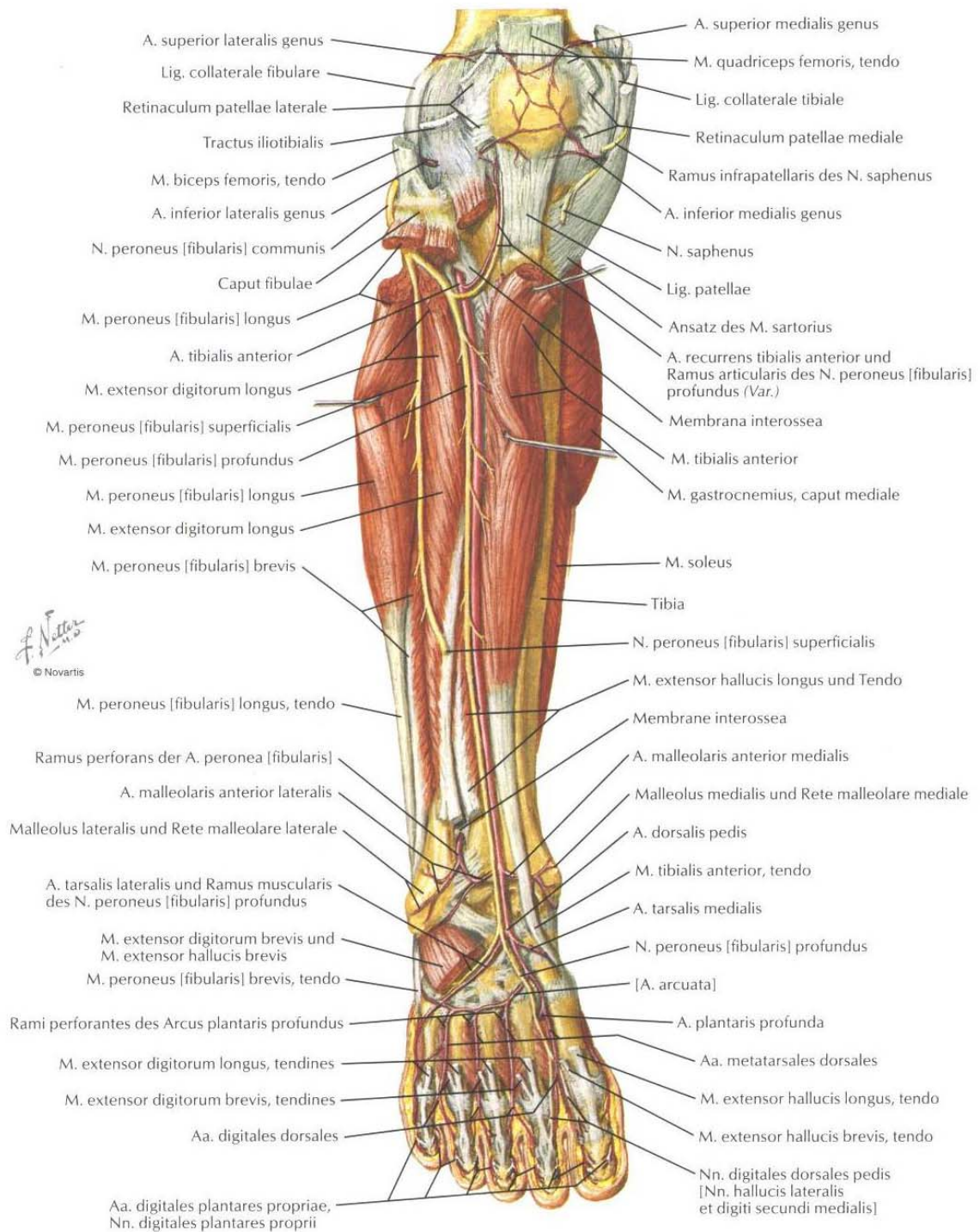


Figure 18: Muscles and tendons of the shank; ventral view; deepest layer, Netter 1999

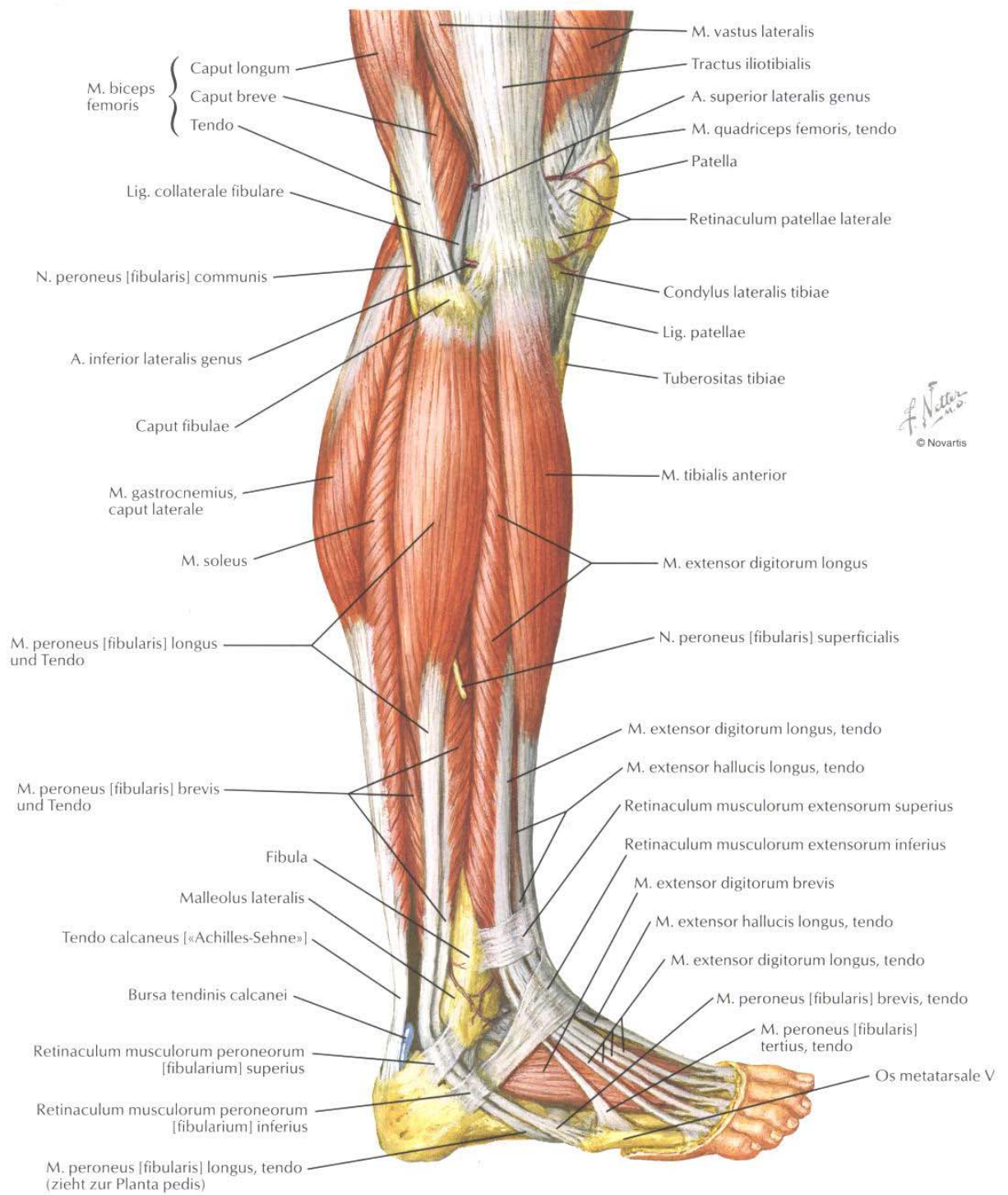


Figure 19: Muscles and tendons of the shank; lateral view, Netter 1999

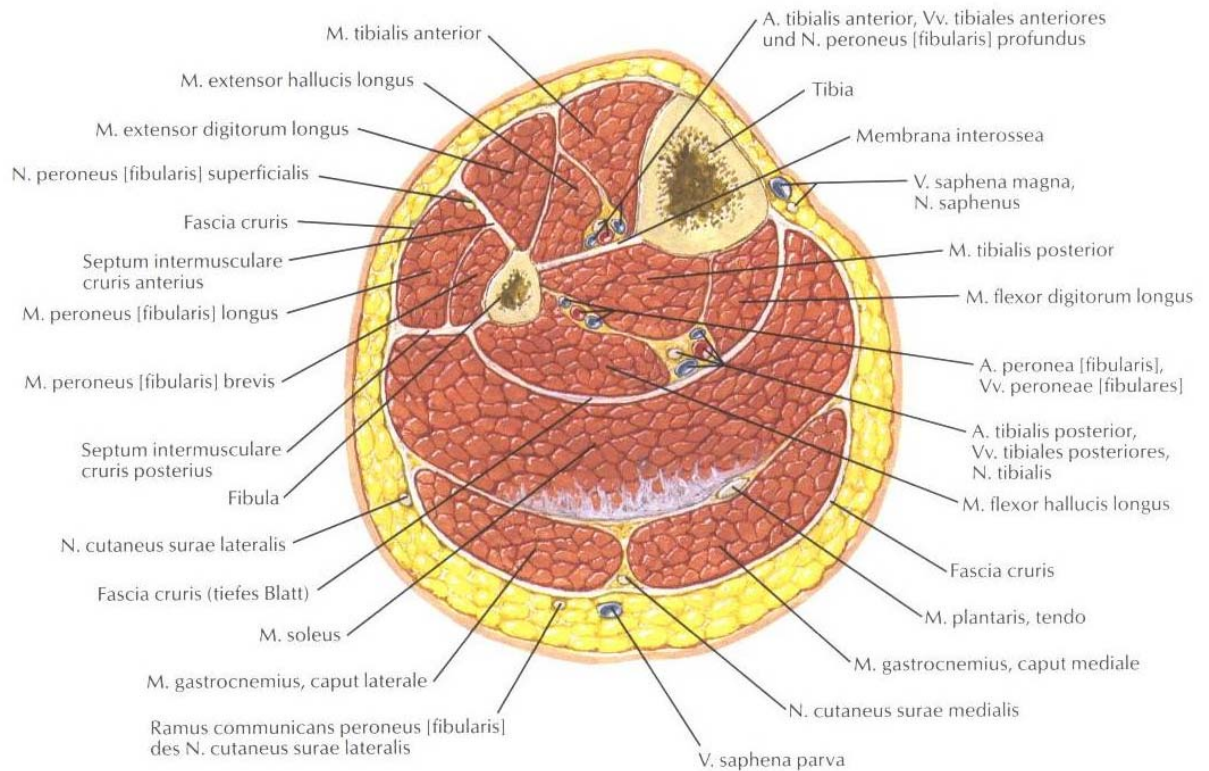


Figure 20: Muscular cross - section of the shank, Netter 1999

2.5 Location of left and right in MR-images

The view in MRI – slices is a convention in medical images and there are a few things that have to be known to read and interpret the images. If these facts are not known it is a little bit confusing for non medicinal persons and left and right are often swapped. For this reason here is a short description of the orientation in MRI – slices:

For a MRI – examination the patient normally lies on her/his back. There is always a defined area of the human body that has to be examined. During the MR – examination the area of interest is virtually sliced in panes of a defined thickness and there is a slice for each layer of the area of the human body that should be examined. In the final results of the examination there are usually images in three different planes – for this work there were only two planes necessary. These planes are the sagittal plane, the coronal plane and the transverse plane. The location of the planes in the human body can be seen in figure 1.

There is usually a stack of images for each plane. The whole area of the body that has to be examined is virtually sliced and all of the images of one direction of primary motion are parallel to the related plane in the body. Depending on the used MRI – device the gap between the single slices can be set in a defined range. The scanning parameters and consequently the resolution of the images also depend on the used device. For example in the MRI – data used for this work the gap was three millimetres and the scanning parameters were selected to enhance the brightness of fatty tissue in order to make the muscle boundaries

more visible. The used MRI device was a Siemens Symphony Maestro Class 1.5 Tesla scanner and the institute where the data was recorded was MR/CT Institute Röntgen Liesing.

Every slice has a defined number. The numeration starts with zero and goes up till there are slices over the whole area that has to be examined. In the transverse plane – which was the relevant one for this work - the first slice – which means the one with number zero - is located at the bottom which means nearest to the feet and the last slice – the one with the highest number of the whole stack – is located closest to the top of the head. So the first slice is on the distal end and the last slice on the proximal end of the examined area.

In the figure 21 there is the schematic numeration of the slices of the MR – images of the lower limb. There are four slices and their related numbers displayed as an example. The others are left out and the points in the figure 21 indicate that there are many more images in between the ones that are shown.

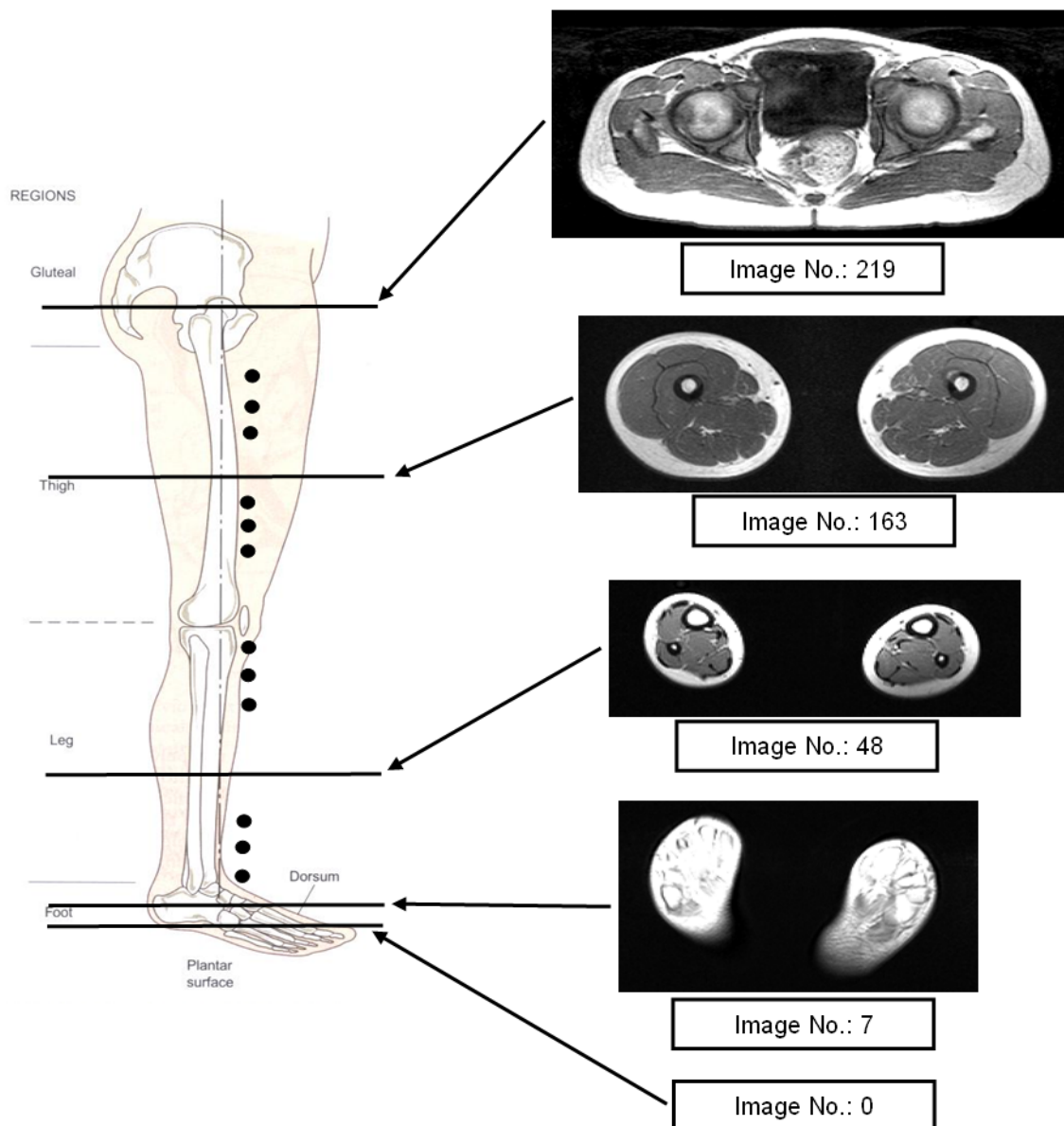


Figure 21: Schematic numeration of MR – image stack in the transverse plane

As written before the person that has to be examined normally lies on her/his back and the first slice is located on the bottom which means closest to the plantar surface of the foot. The anatomical position of the body is – as said before: Standing erect, facing forwards, legs together toes pointing forward, arms at the side palms facing forward. This is the standardised position for anatomical viewings and the MR – images are also sorted in this way. The different images in the transverse plane – which was the relevant for this work - are arranged as if the person is sliced from down up to the top.

The direction you have to look at the patient for MR – images is standing in front of the patient that is in the standardised anatomic position and the direction of view is from the feet up to the head. So in the MR-images the components of the body are located as they would be seen in a visible human that is observed in this way.

The way you have to look at the patient, the resulting directions are shown in figures 22 to 24.

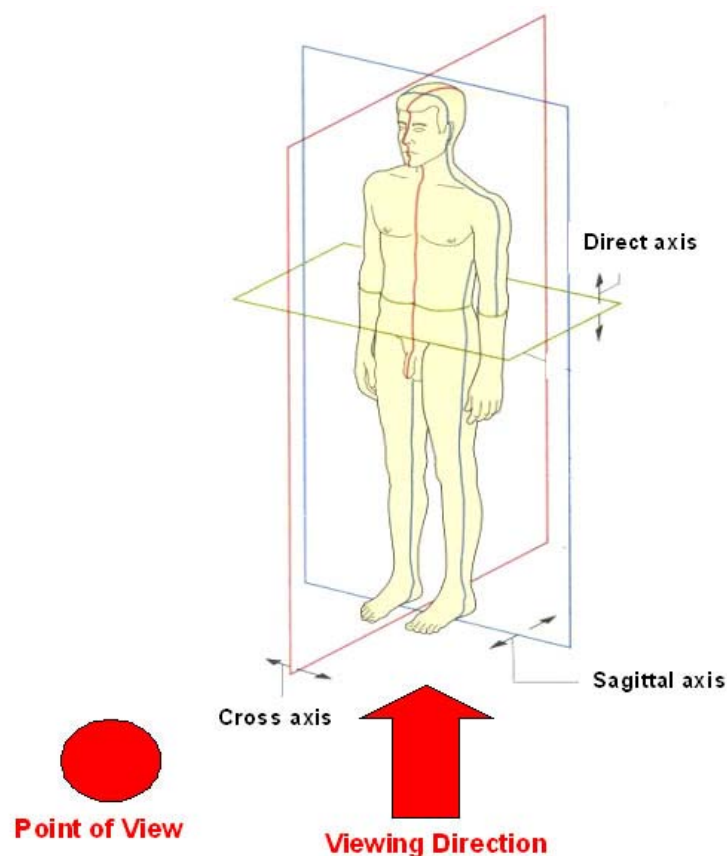


Figure 22: Point and direction of view for MR – images and anatomical terms (Der Körper des Menschen, 1995)

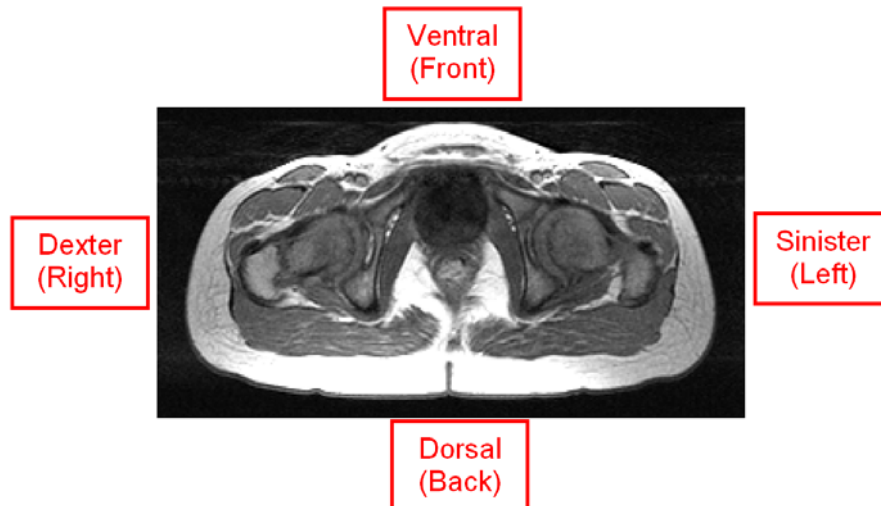


Figure 23: Directions in a MR-image of the pelvic

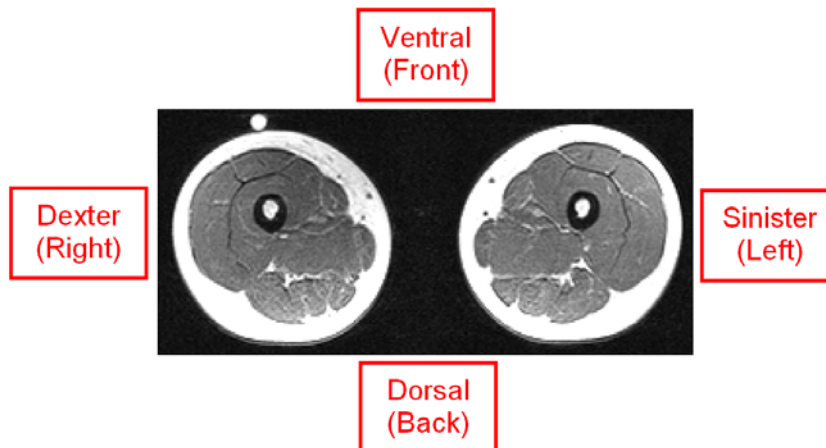


Figure 24: Directions in a MR-image of the thigh

3. Data for the modelling

The available data for the modelling were digital MR – images of the lower limb of a healthy child and a child with cerebral palsy. The CP child was 11 years old and the healthy child had an age of 9 years and both were female. They were volunteers for the experiments and their parents gave informed consents. The MRI data were collected in MR/CT Institute Röntgen Liesing. The desired Data were recorded using a Siemens Symphony Maestro Class 1.5 Tesla scanner. The scanning parameters were set to enhance the brightness of fat tissue in order to make the muscle boundaries more visible. The voxel size used for the images in the transverse plane is comparable to what Spoor and van Leeuwen [4] and Arnold et al [5] used for investigations on the lower limb. All of the used scanning parameters can be seen in table 1.

Parameter		T1 SE AXIAL	T1 SE SAGITAL
TR	ms	591	645
TE	ms	7,8	20
FOV read	mm	300	450
FOV phase	%	100	93,8
Slice		70 (100)	8
Slice Thickness	mm	5 (3)	8
Dist Factor		0	30
Concatentions		2	1
Filter		Elliptical	Elliptical
Phase enc. Dir.		R-L	A-P
Phase oversampling	%	0	0
Averages		1	1
Flip angle		70	90
Base resolution		320	256
Phase resolution	%	100	100
Voxel size	mm	0,9x0,9x5,0 (3,0)	1,8x1,8x8,0
Rel.SNR		1,00	1
Scan time		8,32	2,36
Coil		Array spine+Array body	Array spine+Array block
Workplan		4 blocks+ table movement	2 blocks+table movement

Table 1: MRI parameters

There was a series of 3 millimetres slices MR – images recorded from the lower lumbar vertebrae down to the lesser trochanter of the femur to define the muscles and bone structure of the pelvis. Three other series of 5 millimetres slices MR - images were recorded from the lesser trochanter of the femur down to the calcaneus to define the bone and muscle structures of the thigh and leg. These 4 series of data were overlapped. Nitro capsules mounted on the skin served as markers (Figure 31) to identify the corresponding slices. Two series of 8 millimetres slices images were recorded for the sagittal plane for additional information. The approximate location of the four series of images can be seen in figure 25 and the exact location of the described anatomic positions can be seen in figures 4 to 20.

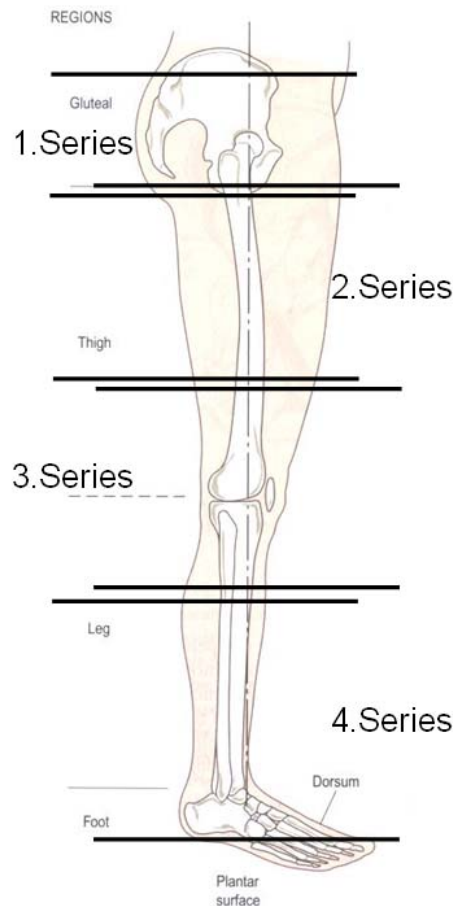


Figure 25: Schematic Location of the MRI series

The first target was to get digital models of all of the muscles and tendons that are located in the lower limb by reconstructing the muscles and bone structures. This was necessary because all of these muscles are responsible for the gait of humans. So first of all the different structures such as fat, muscles, bones and tendons had to be identified. After the identification the various structures had to be separated by defining them as different materials. The whole separation work was done by using the 3D image processing software Amira version 5.0 from Mercury Computer Systems.

As a first step the four series of images of the lower limb were put together to one big stack. The markers that had been put on the legs of the children before the examination could also be seen in the resulting MR – images and were used for a better orientation during the combination of the stacks.

3.1 Description of MR – images type

For the identification of the different components of the lower limb it was necessary to know if the available MR – images were T1- or T2- weighted. In T1 – weighted images tissues that contain water and other fluids are dark and fat – containing tissues appear as bright areas. In T2 – weighted scans the dark and bright areas are reversed.

Muscles for example are tissues that contain water and other fluids. Bones or bone marrow are fat containing tissues that are relevant for this work.

The existing scans for this paper were T1 – weighted which means muscles and tendons were dark. The other types of tissues that occurred in the MR – slices were bones, bone marrow and the fat tissue under the skin and between the muscles. These tissues appear as bright areas in the available scans. T1 – weighted MR - images are usually used for an anatomic overview of the wanted area. There is often a T1 – weighted image for an overview of the desired area also if the rest of the images were T2 – weighted.

T1 – weighted images were chosen for this work because the anatomic structure was important and it was easier to locate the borders of the muscles and to identify the different anatomic structures.

The difference of a T1 – and a T2 – weighted image of the same body region can be seen figures 26 and 27.

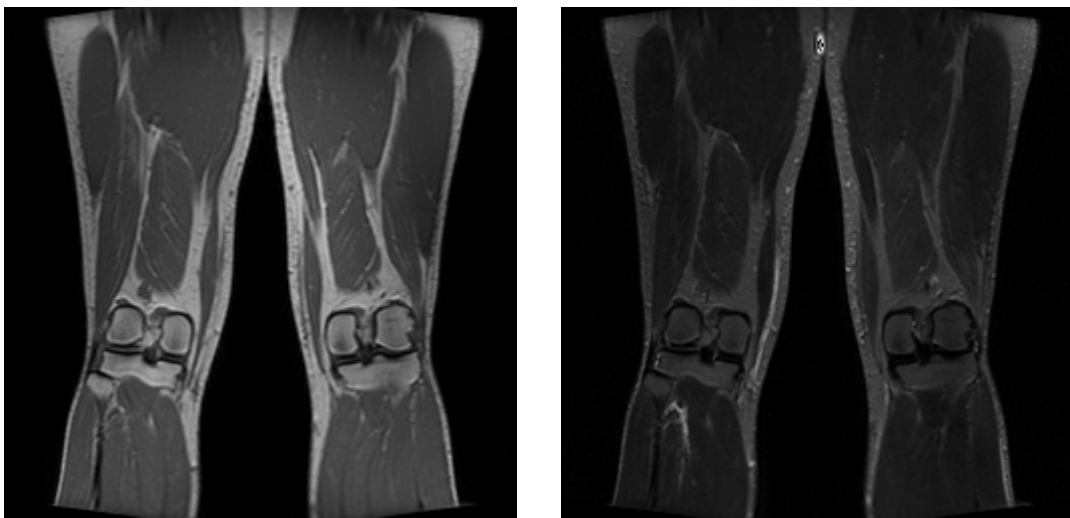


Figure 26: T1 – weighted (left image) and T2 – weighted (right image) image of the knee and the surrounding muscles, National Library of Medicine (<http://www.nlm.nih.gov/research/visible/mri.html>)

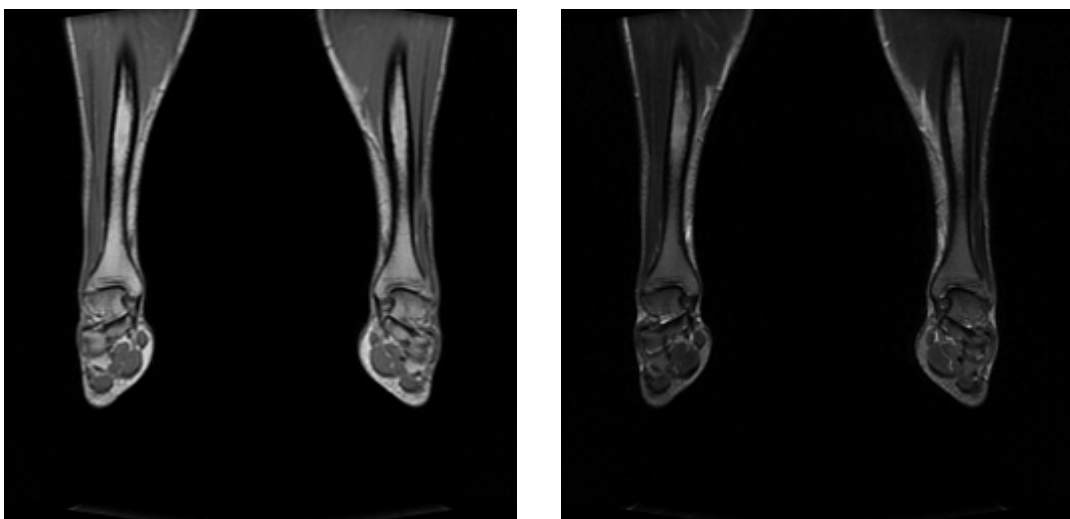


Figure 27: T1 – weighted (left image) and T2 – weighted (right image) image of the ankle and the surrounding muscles, National Library of Medicine (<http://www.nlm.nih.gov/research/visible/mri.html>)

4. Working routines with Amira 5.0

4.1 Viewing of the MR-images

To get a first overview of the MR-images the slices were displayed with the 3D image processing software Amira version 5.0 from Mercury Computer Systems which also included a viewer for MR-images. With this software it was possible to display the figures in the correct sequence. The imported images were stored in a separate object called a Data File.

This display function was used for a first check of the quality of the recorded data. It allowed validating the acuity, brightness and contrasts of the images. The validation was necessary to check if the data were good enough to generate 3-dimensional computer models out of it.

If the quality was not good enough there were some functions in Amira that made it possible to improve the contrasts and acuity. These improving potentials are described in the following paragraphs.

4.1.1 Setting of Data range histogram and colourmap in Amira 5.0

In some slices of the existing data the contrasts were insufficient and the images were very dark. So it was very difficult to differentiate the several greyscales but for this work it was necessary to have good contrasts to identify all of the muscles. The hardest part in slices with bad contrasts was to differentiate the muscles from each other.

For this reason there are functions in Amira 5.0 that made it possible to set the data range histogram and the colourmap to get better contrasts in the images. These functions are located in the "Zoom and Data Window" in the segmentation tool. The location in the Amira 5.0 user interface can be seen in figure 28.

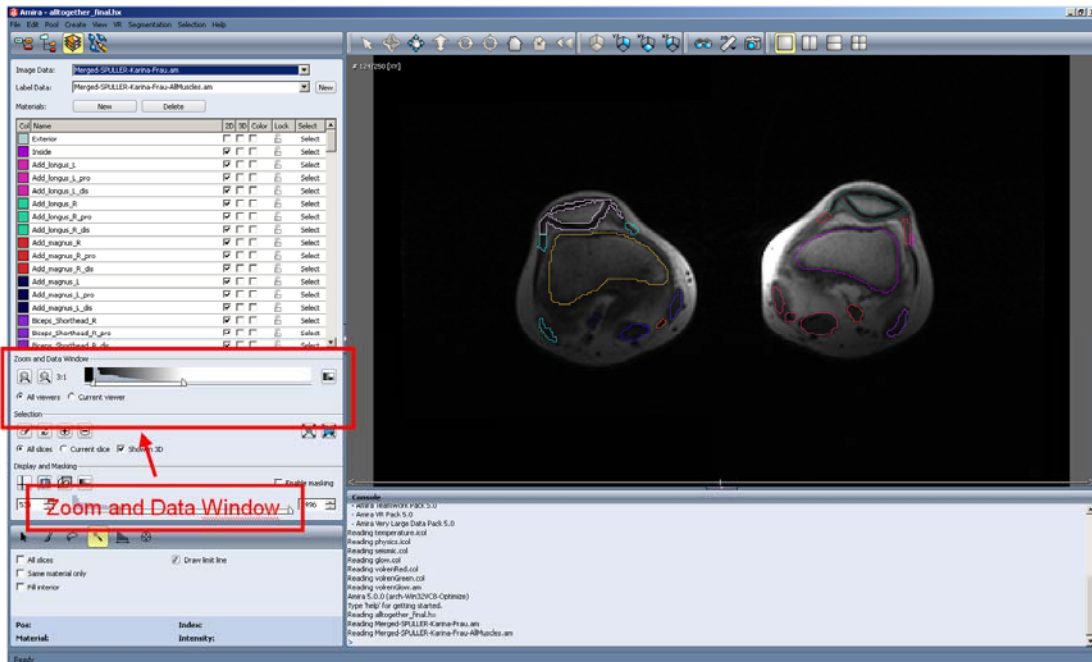


Figure 28: Location of Zoom and Data Window in Amira 5.0 userinterface

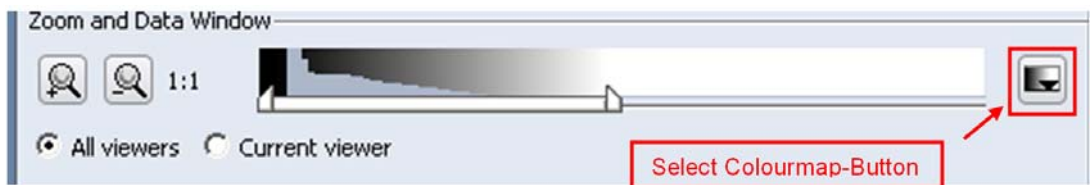


Figure 29: Detailed Zoom and Data Window

The histogram that can be seen in figure 29 displays the distribution of values that represent the different greyscales in the image. In the background of the histogram the different greyscales can be seen so it is easier to cancel or amplify the desired values. The two sliders below the histogram can be used to adjust the data range for the display. So it was possible to cancel some levels of grey that were not necessary for the identification. The only thing that had to be done was to drag the range slider in an area that gave the best results for the segmentation. The images in the display were rescaled automatically after the selection.

It was also possible to set the colourmap of the images by using the so called “Select Colourmap” – button. This button is selected in figure 29. For this work it was not necessary to change the colourmap because the greyscale – setting gave the best results for the differentiation of the muscles.

In figure 30 there are some examples for good and bad settings of the colour data histogram.

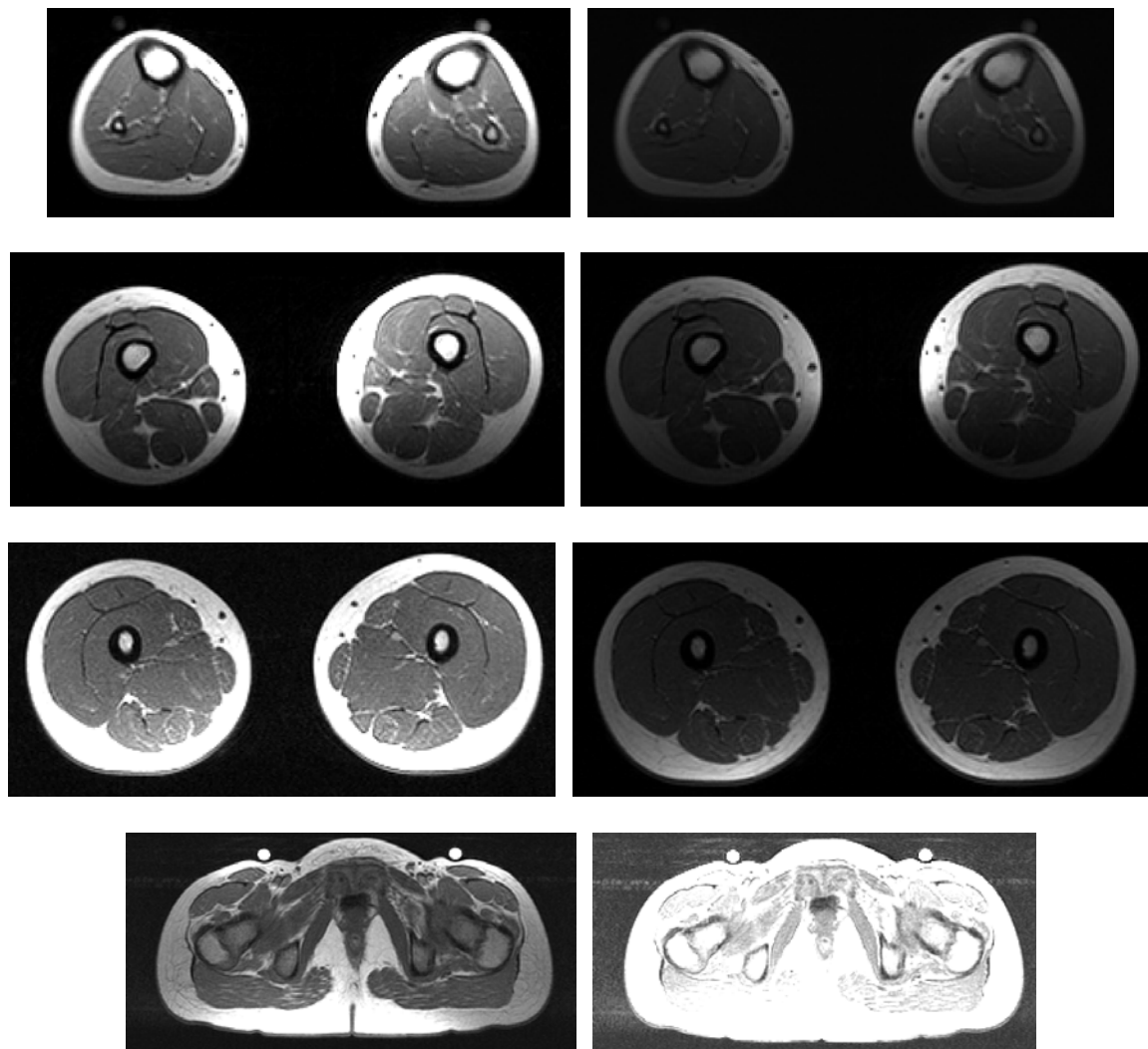


Figure 30: Examples for good (left side) and bad (right side) contrasts in MR - images

4.2 Procedural method of Segmentation in Amira 5.0

The segmentation of the MR – images was also done using the 3D image processing software Amira version 5.0 from Mercury Computer Systems. In this software there was the possibility of selecting areas – the so called segmentation - on digital figures – especially MR-images – and creating 3-dimensional figures relating to the marked areas. The process of segmentation that was done in this work is described in the following paragraphs.

During the segmentation a label was assigned to each pixel or voxel – which was the 3 dimensional equivalent of a pixel - of the image. This label describes to which region or material the pixel belongs for example the femur, M. abductor magnus or the distal tendon of M. peroneus. Another important label was the so called “Exterior” which included all the surrounding that did not belong to a muscle, bone or tendon. The whole information generated during the segmentation was stored in a separate data object called a LabelField. The segmentation was the

prerequisite for a surface model generation and the processing of the desired 3 dimensional muscle models for this work.

First the different stacks of images were put together to one big stack. For this reason there were some nitro capsules placed as markers (figure 31) on the legs of the children during the whole examination. These markers could also be seen on the MR – images and gave a better orientation for combining the different stacks. The result of the stacking was one big stack with images over the whole legs of the children. This made it easier to follow the course of the bones, muscles and tendons over the whole leg. So it was easier to get smooth contours of the different objects and there were no overlaps. With the segmentation tool the different tissues such as bones, muscles and tendons were selected in the slices. The generated big step was imported in Amira.

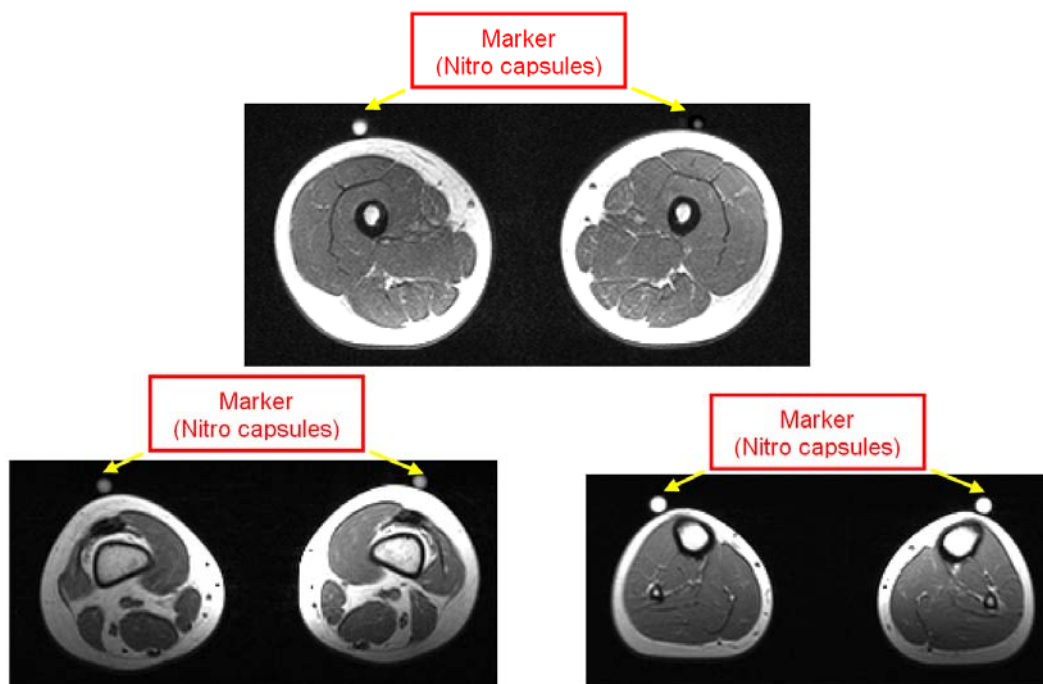


Figure 31: Markers (Nitro capsules) as they appeared on the MR – images

After that a LabelField icon had to be created. This was done by a right click on the data file and choosing LabelField from the Labelling section. A new icon – the LabelField – appeared and simultaneously the image segmentation editor was displayed. This editor operated in a 2 – viewer mode by default and a 2D viewer for the segmentation and a 3D viewer for checking the results is displayed. The editor can be seen in figure 32.

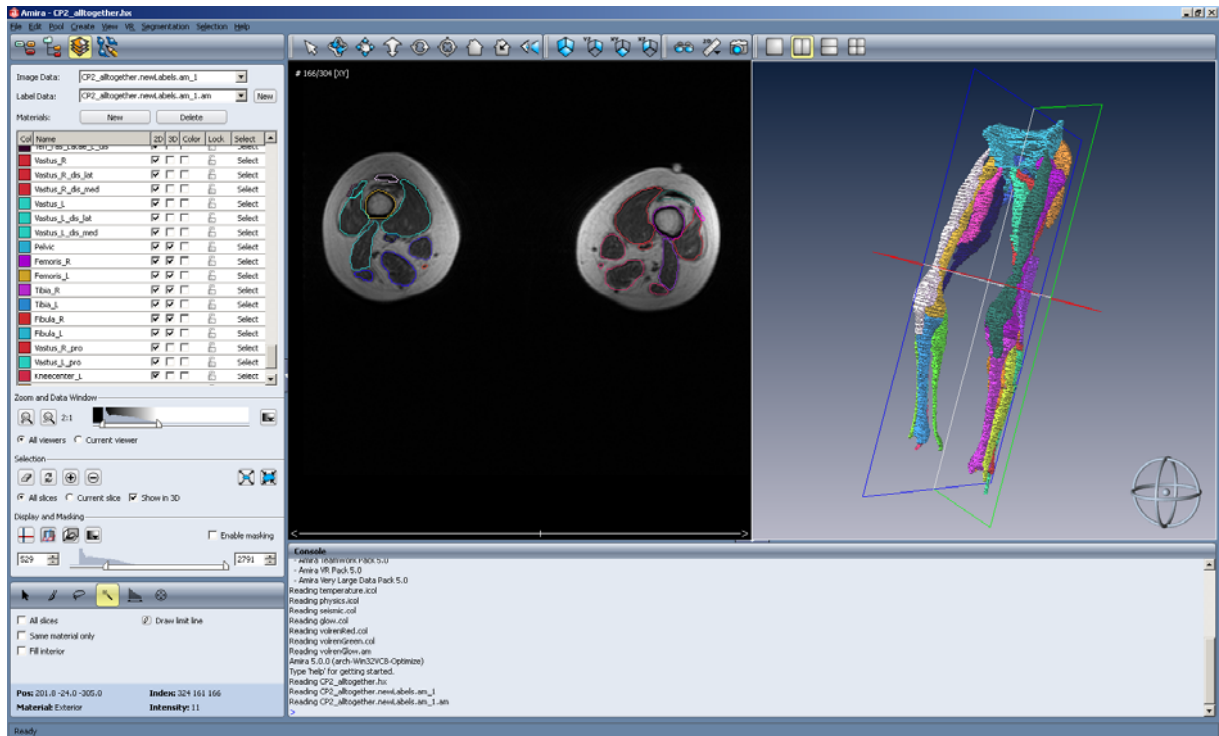


Figure 32: Amira 5.0 Editor with 2 – and 3 – dimensional view

The first step in the segmentation process was to generate a new material in Amira 5.0 for each part of the legs. For the lower limb there were 152 different materials which included all of the muscles, bones, tendons and some centre points that had to be selected for the following analyses.

A new material was generated by a right click into the material list (figure 34) and choosing New Material in the menu that appeared. After that the new material was in the list and it was renamed for better recognition.

When all of the materials were defined the real separation work started. By using one of the marking tools (figure 34) – for example the brush – all of the voxels that belonged to one tissue were selected. After the selection the marked area was assigned to the desired material by using the “Plus” - button under the selection label. In figure 33 there are some examples for the selecting and adding routine.

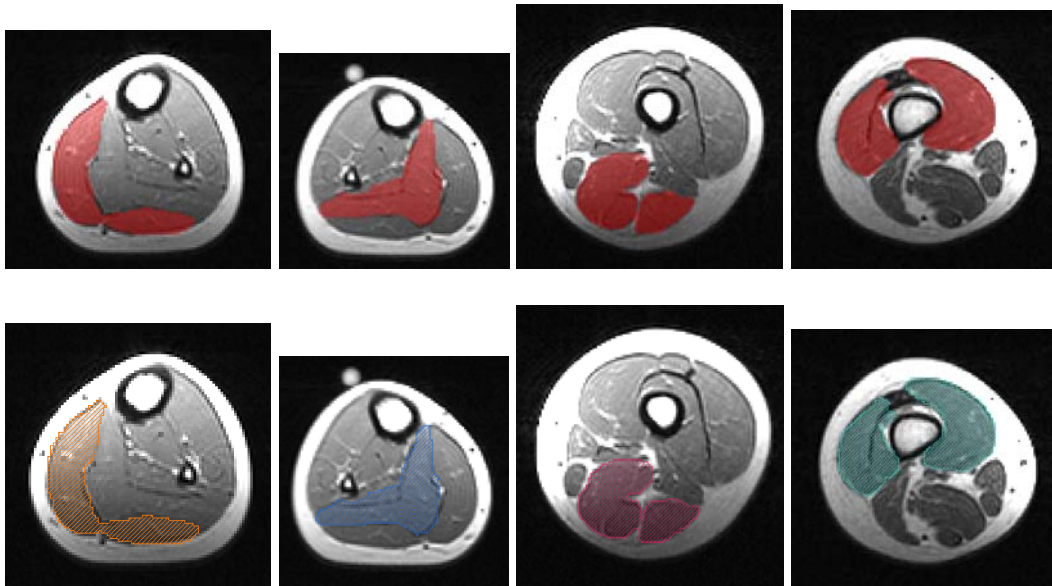


Figure 33: Examples for selecting and adding routine; in the first line the muscles are selected and the figures below show the same muscles after they were assigned to the correct material. The selected muscles are starting from left: M. Gastrocnemius, M.Soleus, M.Hamstring, M.Vastus

If there was a wrong selection there were two possibilities of correction. The first was to subtract some voxels of an existing selection. The desired voxels had to be selected by using one of the marking tools. When the selection was done the selection was subtracted from the designated material by using the “Minus” – button. The second possibility was to delete the selection by using the “Erase” – button. The described buttons and their location in the Amira 5.0 user interface can be seen in figures 34 and 35.

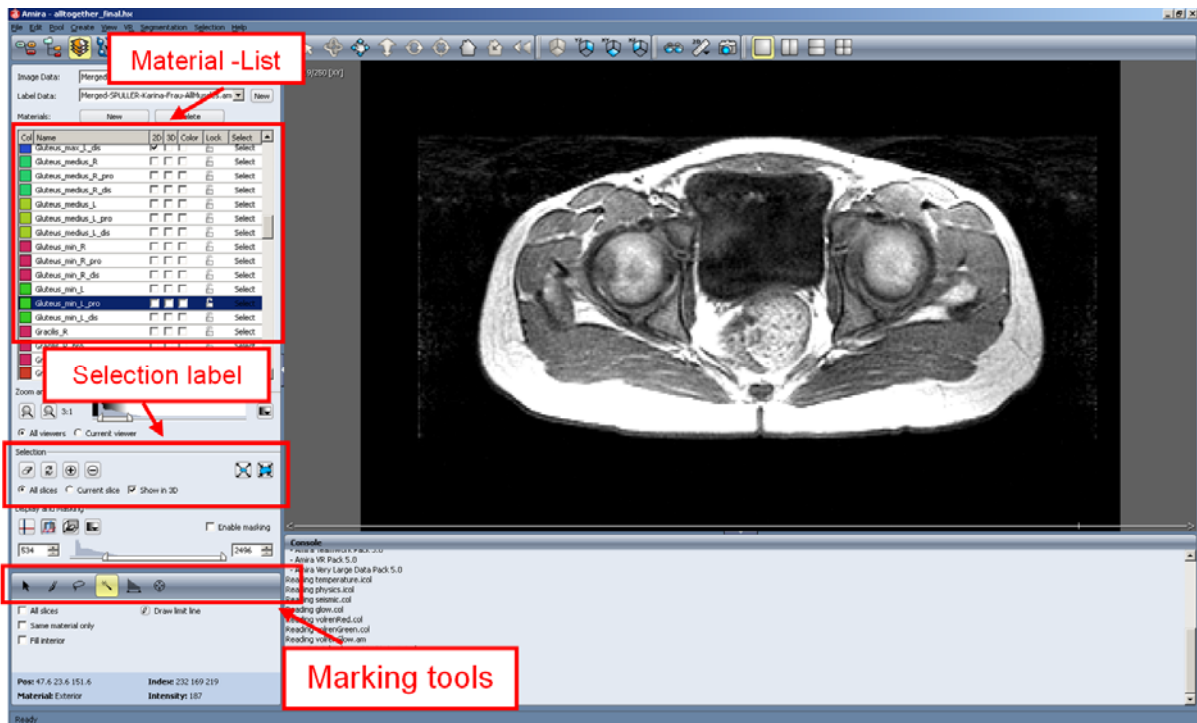


Figure 34: Amira user interface with material list, selection label and marking tools

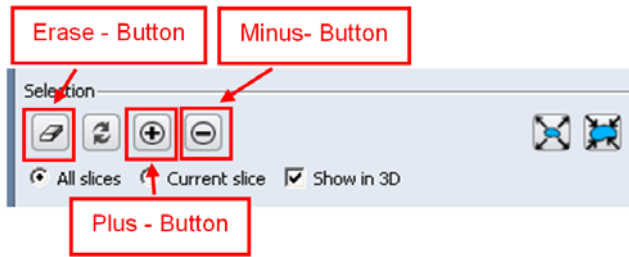


Figure 35: Detailed Selection Label

This selecting and adding routine was always done for a whole structure such as the complete femur. The result of the selection could be seen in the 3D viewer. The displayed shape was always compared with the target state of the muscle, bone or tendon in the human body.

When one part was finished the selection of the next part was performed. So in the end of the segmentation the 46 muscles, the corresponding tendons and the seven bones were defined as different materials that represent 3-dimensional models of the different parts of the lower limb.

5 Moving artefacts

During the segmentation work a problem with the quality of some MR-slices appeared. There were moving artefacts in some of the slices. These artefacts can be seen in the following images.

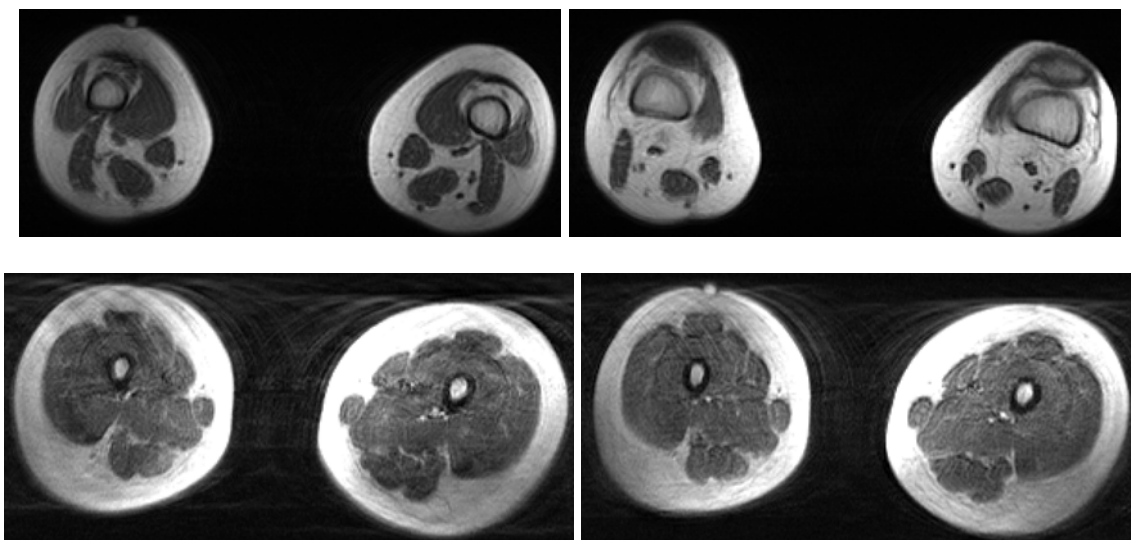


Figure 36: Moving artefacts in MR - images

This failure occurred because the children moved their legs during the examination so there were a kind of moving shadows in some slices. It looked like if there were two different superposed legs on the slices. The outlines of the single parts of the lower limb like bones and muscles were a little bit blurred and so it was difficult to identify the right position of the desired anatomic structures.

This problem was solved by extrapolating the form and position of the relevant muscles and bones using the slices before and after the ones that were not pin sharp. For this extrapolation the “3-dimensional display” function was used. With this sight it was possible to verify if the position of the current selection was right or not. So the structures were built up sequential by selecting one layer after the other and between two selections there was always a crosscheck with the 3-dimensional model to see if the position was right.

Another possibility of solving this problem was the automatic interpolation function in Amira 5.0. To use this function the wanted body part was selected in the last clear image. After scrolling through the slices that were not pin sharp the same part was selected in the next clear image. Then the interpolation function was activated by choosing “Selection” in the menu bar and “Interpolate” in the appearing drop down menu. Afterwards it could be seen that the interpolated contours were selected in all the images that were in between the both that had been selected manually. This automatic function was just used if a manual interpolation was impossible because the manual method was more exact than the automatic one.

6. Localization of the bones:

The first step in the whole segmentation process was to locate the bones in the MR-images. This was necessary to get a first orientation in the images. The bones that had to be located were:

Anatomical name	Labelling in Amira 5.0 (always a object for Left and Right)
Femur	Femoris_L, Femoris_R
Tibia	Tibia_L, Tibia_R
Fibula	Fibula_L, Fibula_R
Pelvis	Pelvis

Table 2: Bones of the lower limb and pelvis

The 3-dimensional visualisation of the bones gave a first frame that was helpful for the following location of the muscles because all of the muscles are fixed to the bones.

As the images are T1 - weighted and bone marrow is a fat containing tissue bones should appear as bright areas in the slices. The compact bone which is a kind of outer jacket of the bones is very dense and so it appeared as a very dark area in the images inside of the legs. In figure 37 there are some examples how bones looked in the MR-images.

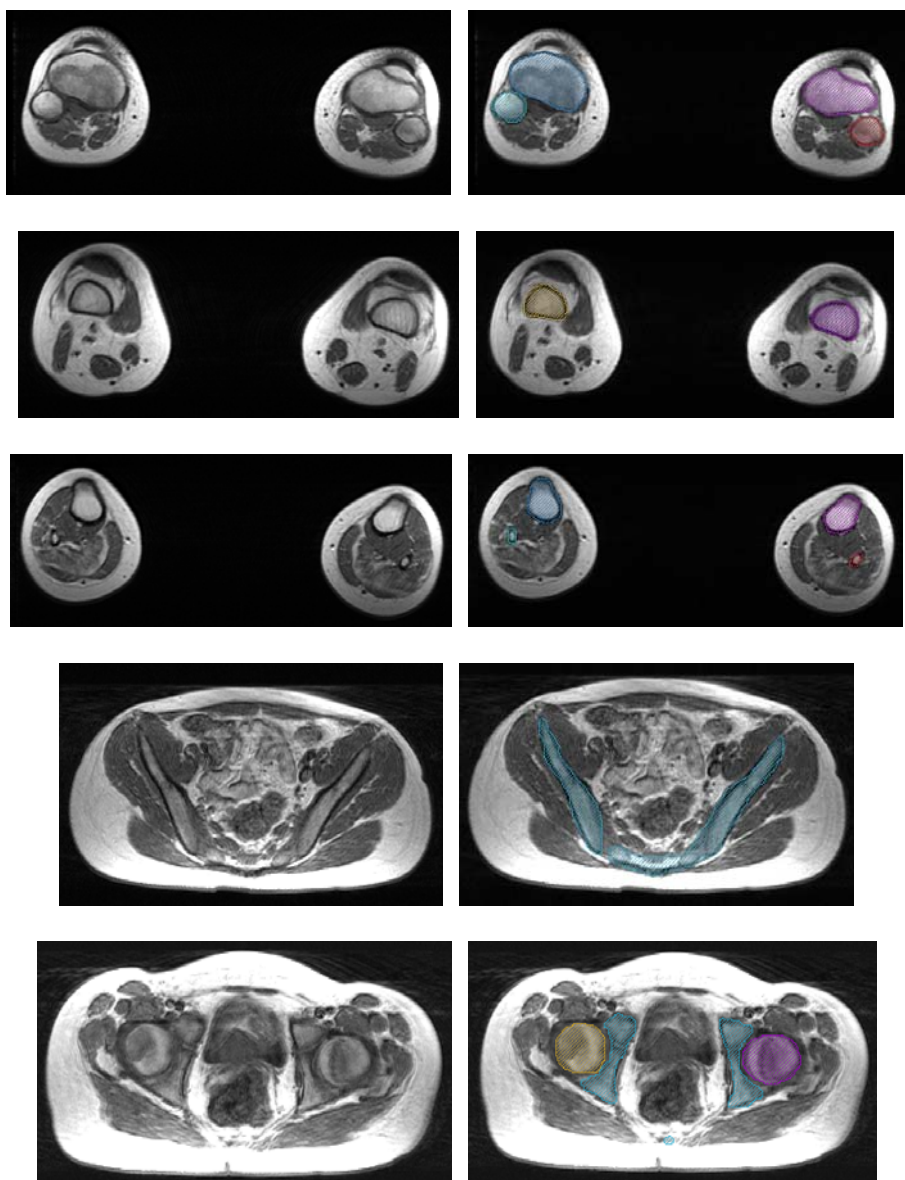


Figure 37: Bones in MR – images; left side: MR – images with bones, right side bones are marked as coloured areas; starting from the top: tibia and fibula, femur, tibia and fibula, pelvis, pelvis and femur

In the majority of the figures the borders between bones and muscles were very clear and so it was not too difficult to find out what was bone and what muscle.

In figure 38 and 39 there is a schematic demonstration of the segmentation of the right femur of the CP child.

As a first step the fragments of the right femur were marked in all of the MR – images. Figure 38 show some of these marked images. The femur is marked as a red area in each slice and there is just the right leg and the right side of the pelvic displayed.

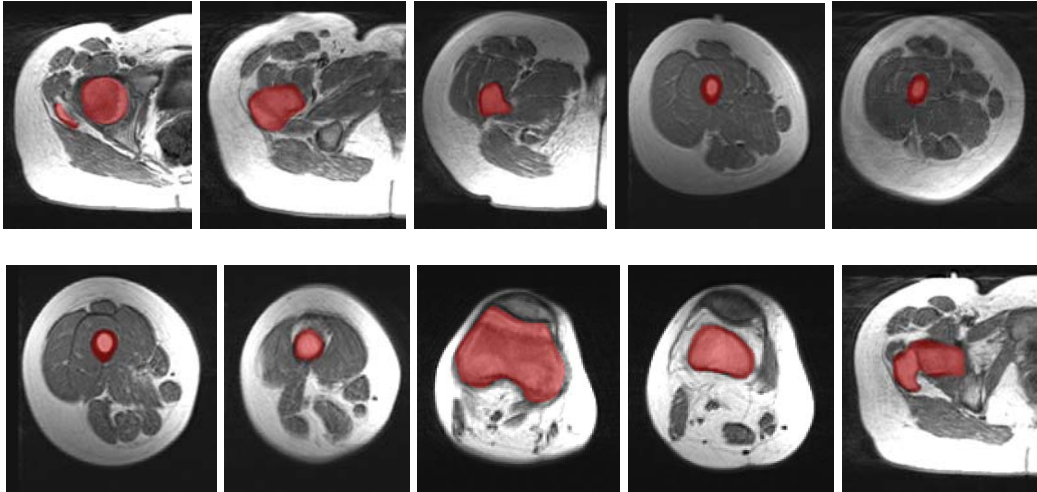


Figure 38: Series of MR – images from CP – child with red marked right femur

After selecting the bone the selected areas were added to the “Femori_R” material. The 3 dimensional result of the segmentation can be seen in figure 39.

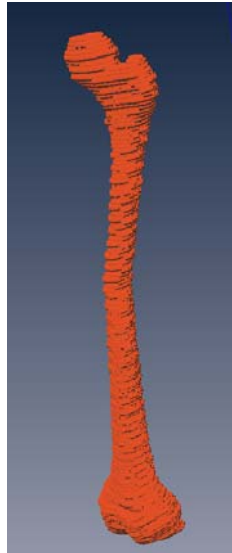


Figure 39: Three dimensional model of the right femur of the CP - child

The identification process that is shown above was done for all of the desired bones. Finally all the bones were identified and the result of the segmentation can be seen in figure 40.

6.1 Segmentation results

The three - dimensional Segmentation result of the bones can be seen in figure 39. The first series is for the CP-child and the second one from the healthy child.

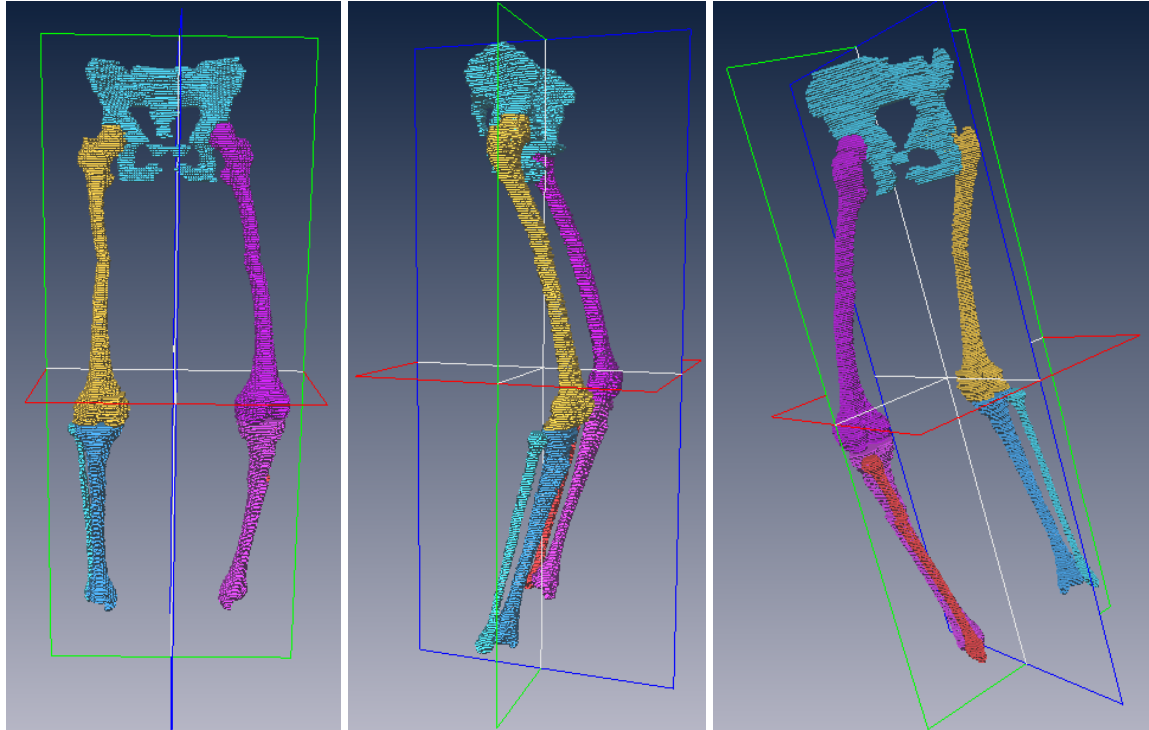


Figure 40: Three different views of the modelled bones from the CP - girl

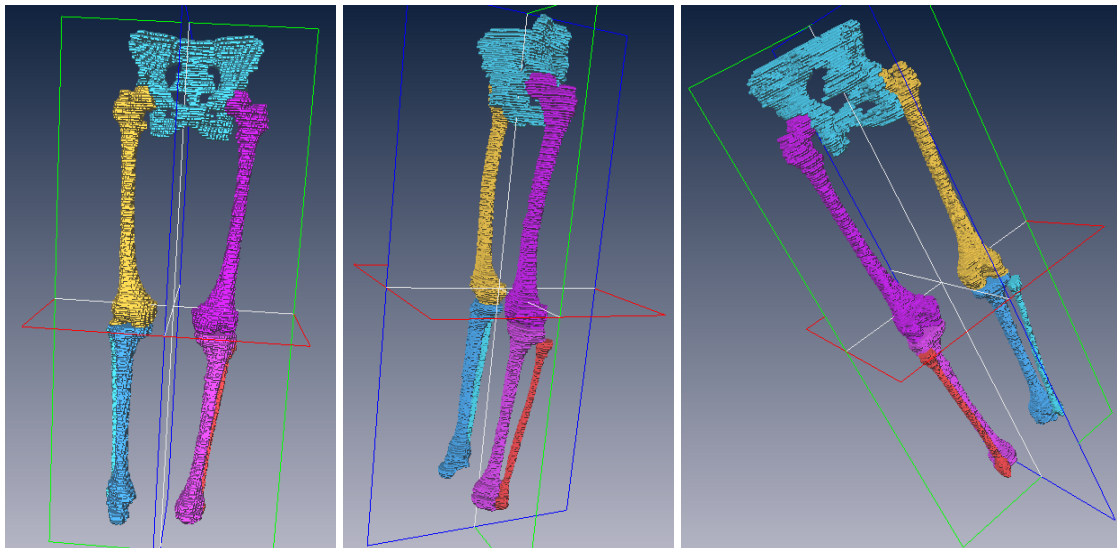


Figure 41: Three different views of the modelled bones from the healthy girl

7. Localization of the muscles

After the identification of the whole skeleton of the lower limb all of the muscles had to be identified and separated. The segmentation procedure was the same as it was done with the bones.

Muscles generate forces and these forces are transmitted to the bones over tendons. So the muscles of the lower limb are responsible for the moving of the lower extremities and as a result of this they cause the gait of a human being. If the muscles do not act in the right way the gait of the human is not as it should be. The pathological gait is one problem that occurs with cerebral palsy. Hence it was necessary to analyse all of the muscles of the lower limb. So all of the desired muscles had to be separated to calculate and compare the muscle parameters later on.

There were 23 muscles and muscle groups in each leg. The numbers and names of the muscles were chosen referring to Wickiewicz et al in “Muscle architecture of the Human lower Limb” [6]. In total there were 46 muscles or muscle groups that had to be identified.

The muscles and muscle groups that had to be detected were:

Anatomical name	Labelling in Amira 5.0 (always a object for Left and Right)
M. Adductor longus	Add_longus_L, Add_longus_R
M. Adductor magnus	Add_magnus_L, Add_magnus_R
M. Biceps femoris short head	Biceps_Shorthead_L, Biceps_Shorthead_R
M. Extensor digitorum longus	Ex_digi_L, Ex_digi_R
M. Flexor digitorum longus	Flex_digi_longus_L, Flex_digi_longus_R
M. Flexor hallucis longus	Flex_hall_longus_L, Flex_hall_longus_R
M. Gastrocnemius	Gastrocnemius_L, Gastrocnemius_R
M. Gluteus maximus	Gluteus_max_L, Gluteus_max_R
M. Gluteus medius	Gluteus_medius_L, Gluteus_medius_R
M. Gluteus minimus	Gluteus_min_L, Gluteus_min_R
M. Gracilis	Gracilis_L, Gracilis_R
M. Hamstring (including M. Semitendinosus, M. Semimembranosus and M. Biceps femoris long head)	Hamstring_L, Hamstring_R
M. Iliopsoas	Iliopsoas_L, Iliopsoas_R
M. Pectineus	Pectinius_L, Pectinius_R
M. Peroneus	Peroneus_L, Peroneus_R
M. Piriformis	Piriformis_L, Piriformis_R
M. Rectus femoris	Rectus_femoris_L, Rectus_femoris_R
M. Sartorius	Sartorius_L, Sartorius_R
M. Soleus	Soleus_L, Soleus_R
M. Tibialis anterior	Tibialis_ant_L, Tibialis_ant_R
M. Tibialis posterior	Tibialis_post_L, Tibialis_post_R
M. Tensor fasciae latae	Ten_Fas_Latae_L, Ten_Fas_Latae_R
M. Vastus (including M. Vastus medialis, M. Vastus intermedius and M. Vastus lateralis)	Vastus_L, Vastus_R

Table 3: Muscles of the lower limb

As said before the MR-images were T1 – weighted. Muscles are tissues that contain water and other liquids and this kind of tissues appear as dark areas in T1

– weighted images. Therefore in the available MR – slices the colour of the muscles should be somewhere between a darker grey and black.

Skeletal muscles are covered by a mantle of connective tissue. So between the different muscles there is either a thin fat film or there is the mantle of connective tissue from each muscle. In T1-weighted MR-images fat appears as a bright area. Connective tissue contains water and other liquids. So in MR-images connective tissue can be identified as dark areas or dark lines. The conclusion of these facts for the muscle segmentation was that the borders of the muscles should either be brighter or very dark areas.

With this knowledge and some anatomic guidelines it was possible to start the segmentation of the muscles. A good way of finding all of the different muscles that should be located in the legs was to look on which slices the borders between the several muscles were very clear. After the identification of all of the muscle parts in one slice it was possible to build up the muscles by using the 3-dimensional display function.

Another good approach was to start with the smaller muscles because then the identification of the bigger ones was easier.

For a better imagination of the way muscles look in MR – images figure 42 shows some MR – slices of the lower limb. On the left side there is always the raw MR – image and on the right side all of the muscles that had to be identified are marked.

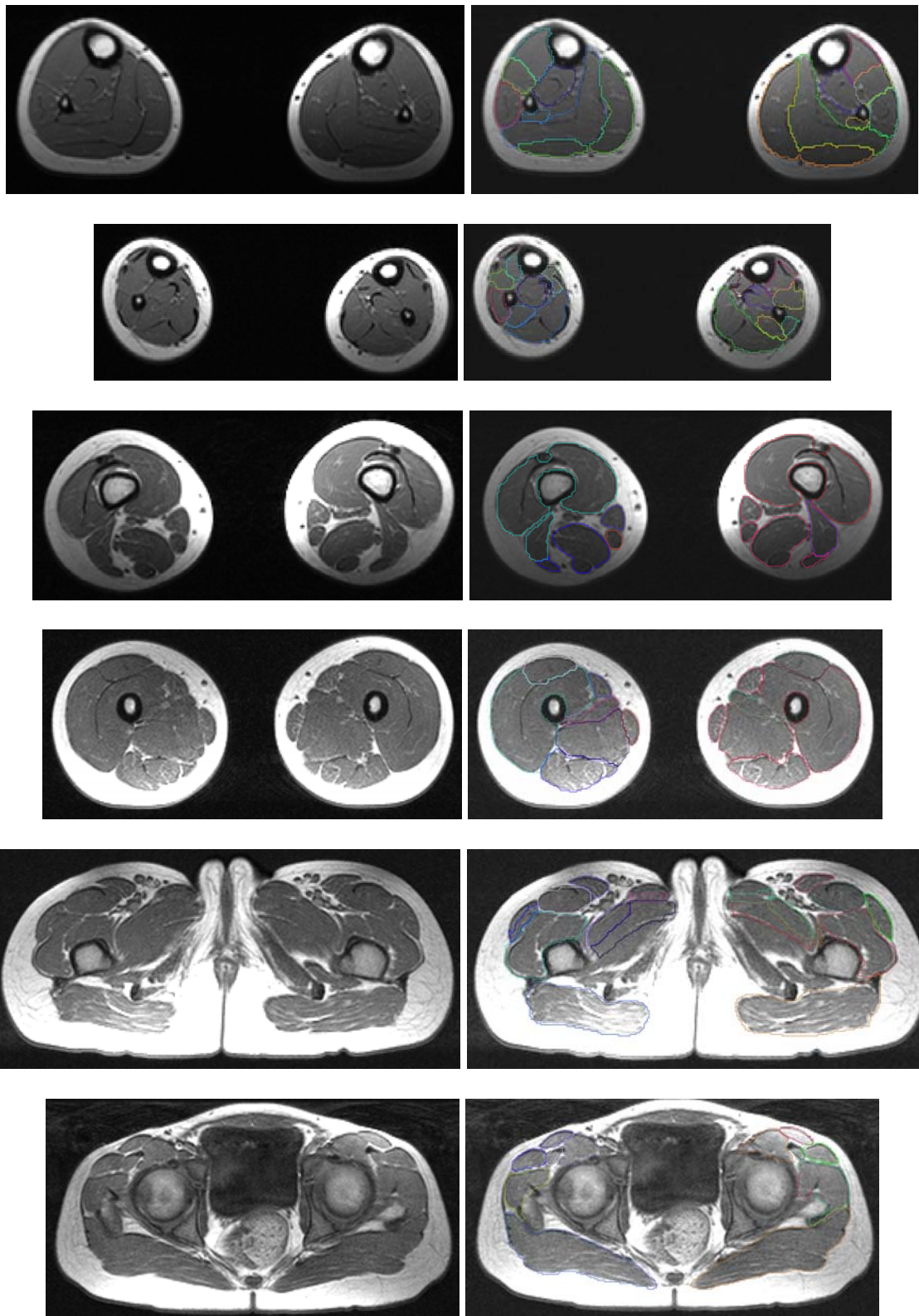


Figure 42: Muscles in MR – images of the lower limb

7.1 Problems that occurred during the separation of the muscles

One problem was that the children moved during the recording of the data and so some of the images were not pin sharp. In these images it was difficult to identify the right location of the muscles. This problem was solved by extrapolating the contour of the affected muscles as described in chapter 5.

Another problem was that on the proximal end of the examined area the images ended before some of the muscles were complete. For this reason it was not possible to compare the volume of these muscles.

The affected muscles were:

- M. gluteus maximus
- M. gluteus medius

The location of these muscles can be seen in chapter 2.4.

7.2 Segmentation Results:

In figure 43 there is an overview of the 3 dimensional results of the muscle segmentation of some important muscles. Starting at the top the following muscles are displayed: M. Vastus, M. Hamstring, M. Gastrocnemius, M. Tibialis anterior, M. Gluteus maximus, M. Iliopsoas, M. Rectus femoris. There is always a figure of the muscles of the CP-girl and for comparison the same muscles of the healthy girl. The figures always show the right and the left muscle belly without the tendons and the white line in between the two muscles represents the median body plane. Finally there is a general 3 – dimensional overview of all of the muscles.

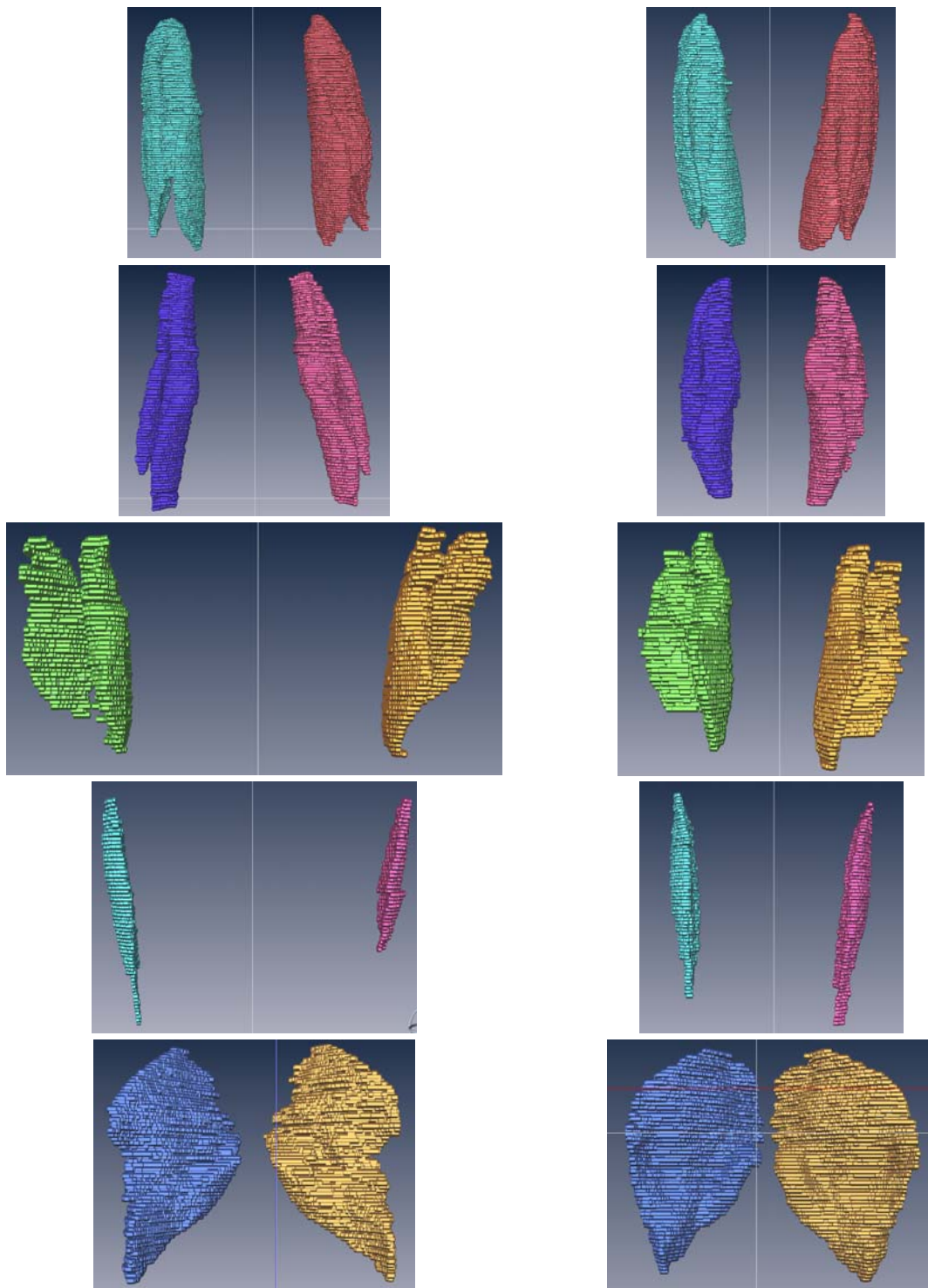


Figure 43: Muscle segmentation results; starting at the top the following muscles are displayed: M. Vastus, M. Hamstring, M. Gastrocnemius, M. Tibialis anterior, M. Gluteus maximus, M. Iliopsoas; left side CP-child right side healthy child

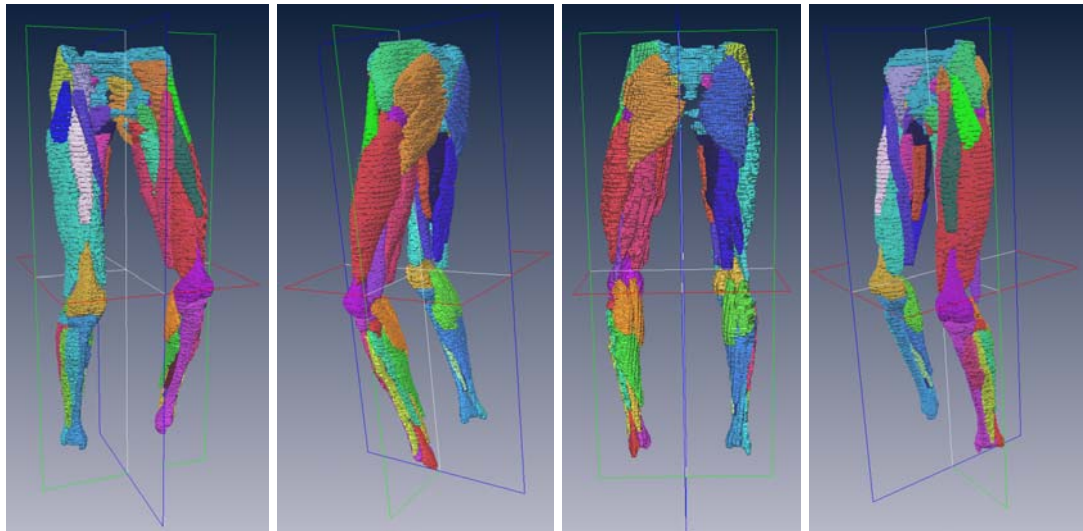


Figure 44: Muscle separation results CP – child

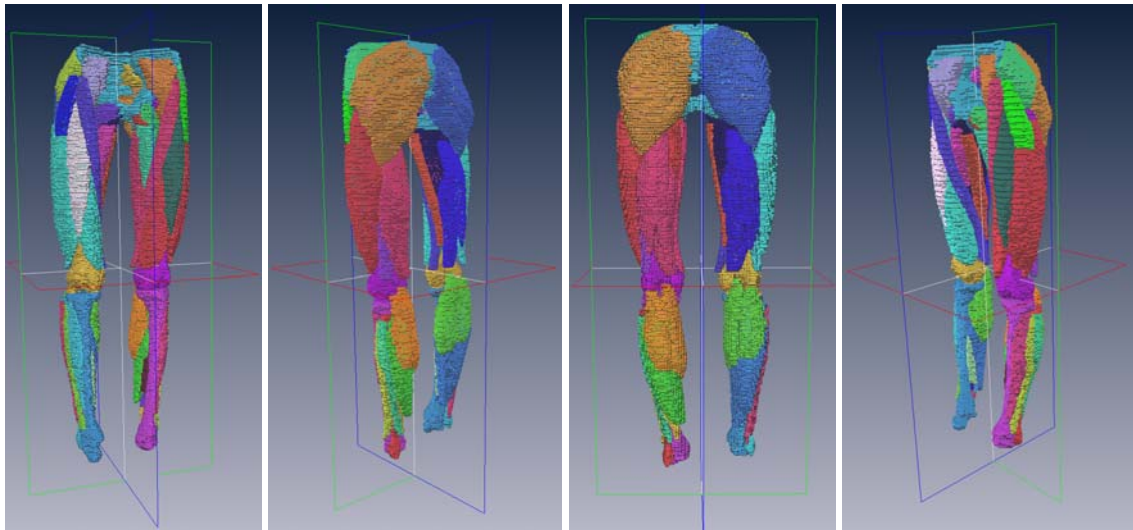


Figure 45: Muscle separation results healthy child

8. Separation of the tendons

For the movement of the lower limbs the force that is generated in the muscles has to be transmitted to the bones. This power transmission is the main function of the tendons. Tendons consist of fibrous connective tissue that is capable of withstanding tension. Tendons have just the capability to exert a pulling force. There is no possibility to transmit a compressive force with tendons. For this reason tendons and muscles always work together and so tendons also had to be identified in this work.

Normally tendons start somewhere inside of the muscle and the end of the tendon is usually a connection point on a bone. There is no defined point where the muscle ends and the tendon starts. So normally there is a smooth transition between the muscle and the tendon. In some cases it was impossible to identify what was tendon and what was muscle and so the following useful simplification was done:

If it was not possible to identify the tendon in between of the muscle then at first the muscle tissue was defined. When there was no more muscle tissue that could be identified the tendon was started. So there was a clear transition from the muscle to the tendon. This simplification did not affect the volume of the muscles in a relevant way because there were just very small parts of muscle tissue that were lost through it.

Each muscle should have a tendon on the origin side and one at the insertion points. So for each muscle there was a proximal and a distal tendon. In relation to what Wickiewicz et al said in “Muscle architecture of the Human lower Limb” [6] there were 92 tendons that had to be identified. It was not necessary to identify all of the tendons that are located in the lower limbs because not all of them are necessary to simulate the gait of a human being. For example the patellar ligament was combined with the distal tendon of the rectus femoris.

Anatomical name	Labelling in Amira 5.0 (always a object for Left and Right)
Distal tendon of M. Adductor longus	Add_longus_L_dis, Add_longus_R_dis
Proximal tendon of M. Adductor longus	Add_longus_L_pro, Add_longus_R_pro
Proximal tendon of M. Adductor magnus	Add_magnus_L_pro, Add_magnus_R_pro
Distal tendon of M. Adductor magnus	Add_magnus_L_dis, Add_magnus_R_dis
Proximal tendon of M. Biceps femoris short head	Biceps_Shorthead_L_pro, Biceps_Shorthead_R_pro
Distal tendon of M. Biceps femoris short head	Biceps_Shorthead_L_dis, Biceps_Shorthead_R_dis
Proximal tendon of M. Extensor digitorum longus	Ex_digi_L_pro, Ex_digi_R_pro
Distal tendon of M. Extensor digitorum longus	Ex_digi_L_dis, Ex_digi_R_dis
Proximal tendon of M. Extensor digitorum longus	Flex_digi_longus_L_pro, Flex_digi_longus_R_pro
Distal tendon of M. Extensor digitorum longus	Flex_digi_longus_L_dis, Flex_digi_longus_R_dis
Proximal tendon of M. Flexor hallucis longus	Flex_hall_longus_L_pro, Flex_hall_longus_R_pro
Distal tendon of M. Flexor hallucis longus	Flex_hall_longus_L_dis, Flex_hall_longus_R_dis
Proximal tendon of M. Gastrocnemius	Gastrocnemius_L_pro, Gastrocnemius_R_pro
Distal tendon of M. Gastrocnemius	Gastrocnemius_L_dis, Gastrocnemius_R_dis
Proximal tendon of M. Gluteus maximus	Gluteus_max_L_pro, Gluteus_max_R_pro
Distal tendon of M. Gluteus maximus	Gluteus_max_L_dis, Gluteus_max_R_dis
Proximal tendon of M. Gluteus medius	Gluteus_medius_L_pro, Gluteus_medius_R_pro
Distal tendon of M. Gluteus medius	Gluteus_medius_L_dis, Gluteus_medius_R_dis
Proximal tendon of M. Gluteus minimus	Gluteus_min_L_pro, Gluteus_min_R_pro
Distal tendon of M. Gluteus minimus	Gluteus_min_L_dis, Gluteus_min_R_dis
Proximal tendon of M. Gracilis	Gracilis_L_pro, Gracilis_R_pro
Distal tendon of M. Gracilis	Gracilis_L_dis, Gracilis_R_dis
Proximal tendon of M Hamstring (including M. Semitendinosus, M. Semimembranosus and M. Biceps femoris long head)	Hamstring_L_pro, Hamstring_R_pro

Anatomical name	Labelling in Amira 5.0 (always a object for Left and Right)
Distal tendon of M Hamstring (including M. Semitendinosus, M. Semimembranosus and M. Biceps femoris long head)	Hamstring_L_dis, Hamstring_R_dis
Proximal tendon of M. Iliopsoas	Iliopsoas_L_pro, Iliopsoas_R_pro
Distal tendon of M. Iliopsoas	Iliopsoas_L_dis, Iliopsoas_R_dis
Proximal tendon of M. Pectineus	Pectinius_L_pro, Pectinius_R_pro
Distal tendon of M. Pectineus	Pectinius_L_dis, Pectinius_R_dis
Proximal tendon of M. Peroneus	Peroneus_L_pro, Peroneus_R_pro
Distal tendon of M. Peroneus	Peroneus_L_dis, Peroneus_R_dis
Proximal tendon of M. Piriformis	Piriformis_L_pro, Piriformis_R_pro
Distal tendon of M. Piriformis	Piriformis_L_dis, Piriformis_R_dis
Proximal tendon of M. Rectus femoris	Rectus_femoris_L_pro, Rectus_femoris_R_pro
Distal tendon of M. Rectus femoris	Rectus_femoris_L_dis, Rectus_femoris_R_dis
Proximal tendon of M. Sartorius	Sartorius_L_pro, Sartorius_R_pro
Distal tendon of M. Sartorius	Sartorius_L_dis, Sartorius_R_dis
Proximal tendon of M. Soleus	Soleus_L_pro, Soleus_R_pro
Distal tendon of M. Soleus	Soleus_L_dis, Soleus_R_dis
Proximal tendon of M. Tibialis anterior	Tibialis_ant_L_pro, Tibialis_ant_R_pro
Distal tendon of M. Tibialis anterior	Tibialis_ant_L_dis, Tibialis_ant_R_dis
Proximal tendon of M. Tibialis posterior	Tibialis_post_L_pro, Tibialis_post_R_pro
Distal tendon of M. Tibialis posterior	Tibialis_post_L_dis, Tibialis_post_R_dis
Proximal tendon of M. Tensor fasciae latae	Ten_Fas_Latae_L_pro, Ten_Fas_Latae_R_pro
Distal tendon of M. Tensor fasciae latae	Ten_Fas_Latae_L_dis, Ten_Fas_Latae_R_dis
Distal lateral tendon of M. Vastus (including M. Vastus medialis, M. Vastus intermedius and M. Vastus lateralis)	Vastus_L_dis_lat, Vastus_R_dis_lat
Distal medial tendon of M. Vastus (including M. Vastus medialis, M. Vastus intermedius and M. Vastus lateralis))	Vastus_L_dis_med, Vastus_R_dis_med
Proximal tendon of M. Vastus (including M. Vastus medialis, M. Vastus intermedius and M. Vastus lateralis)	Vastus_L_pro, Vastus_R_pro
Proximal tendon of M. Vastus (including M. Vastus medialis, M. Vastus intermedius and M. Vastus lateralis)	Vastus_L_pro, Vastus_R_pro

Table 4: Tendons of the lower limb

In the existing MR – images tendons appeared as very dark areas and they always followed the corresponding muscle tissue. Normally the change over from muscle to tendon was the following way: The muscle which was a grey area was finished and in the next slice the tendon - belonging to the muscle - which was a black area started.

Figure 46 shows some examples for tendons in MR – images. On the left side there are the original MR – images and on the right side there are the same images with the tendons marked as coloured areas.

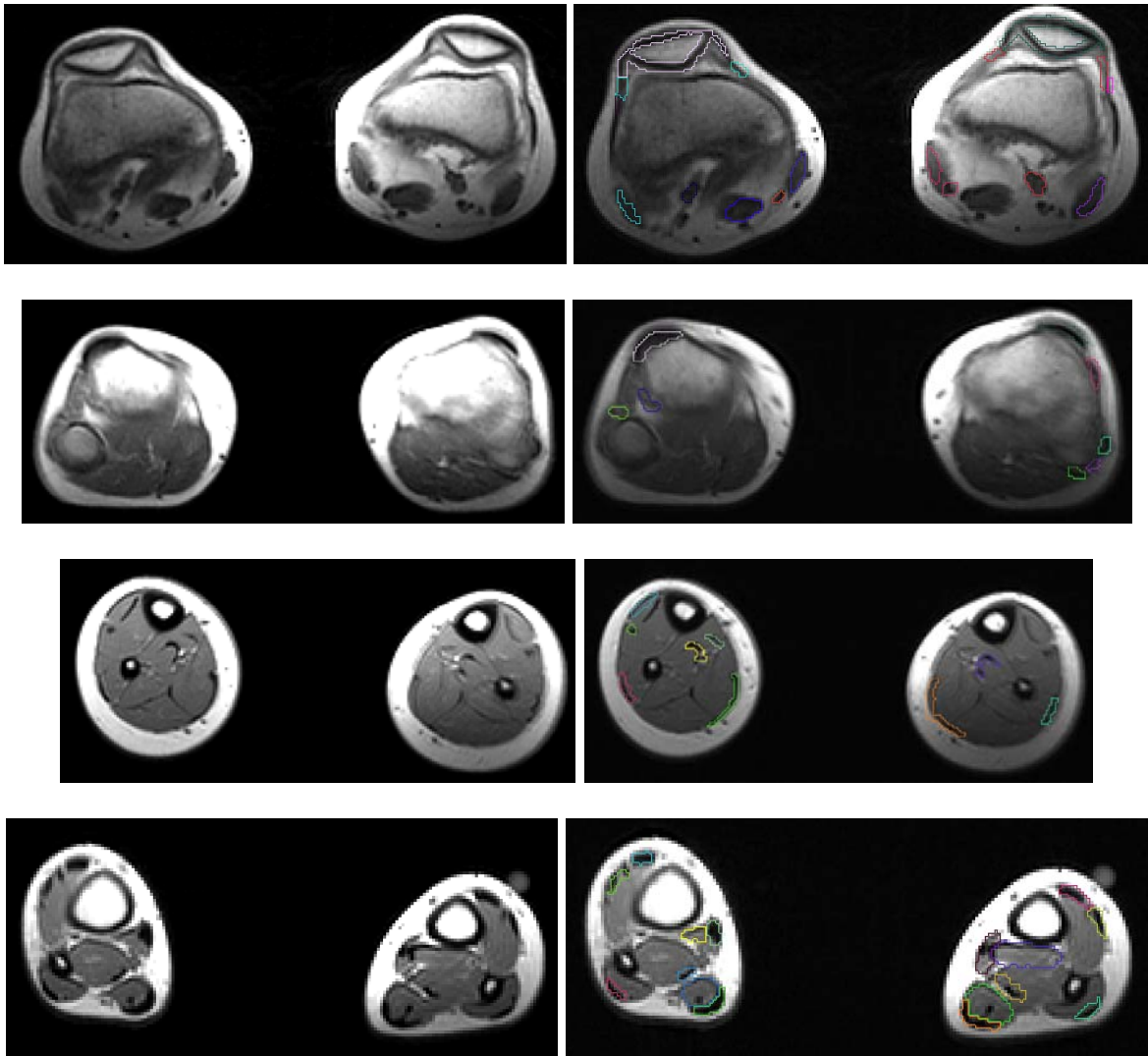


Figure 46: Tendons in MR-images on the left side there are the raw MR – images and on the right side the tendons of M. Gastrocnemius, M.Tibialis anterior, M.Tibialis posterior, M. Extensor digitorum longus, M. Flexor hallucis longus and M. Flexor digitorum longus are selected.

The transition from muscle to tendon can be seen in figures 47 and 48.

As a first example there is the transition from the M. Vastus to its distal tendons. The images start on left side of the first row and end on the right side of the second row. They do not build up a sequential row because there were some images left out to decrease the number of figures. The hatched areas are parts of the muscle and the other areas are the related tendons.

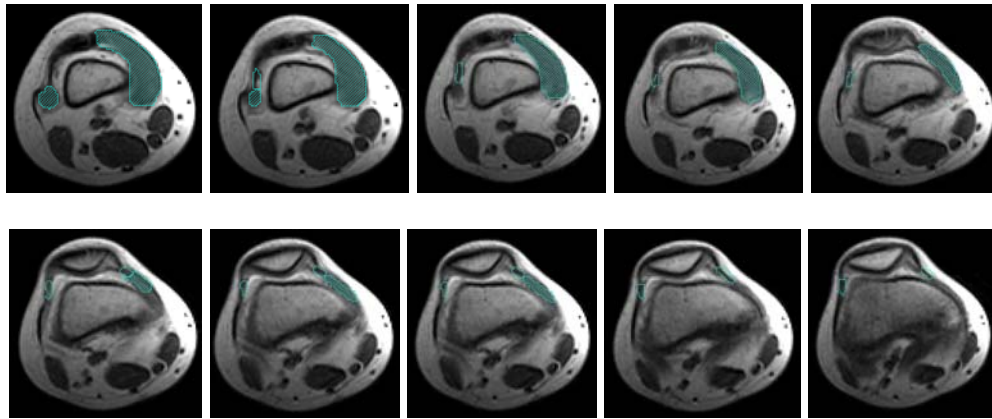


Figure 47: Transition muscle to tendon at M. Vastus - distal end

As a second example the transition from M. Extensor digitorum longus to its distal tendons was taken. The images start again on left side of the first row and end on the right side of the second row. They do not build up a sequential row because there were some images left out to decrease the number of figures. The hatched areas are parts of the muscle and the other areas are the related tendons. In this example the tendon starts inside the muscle.

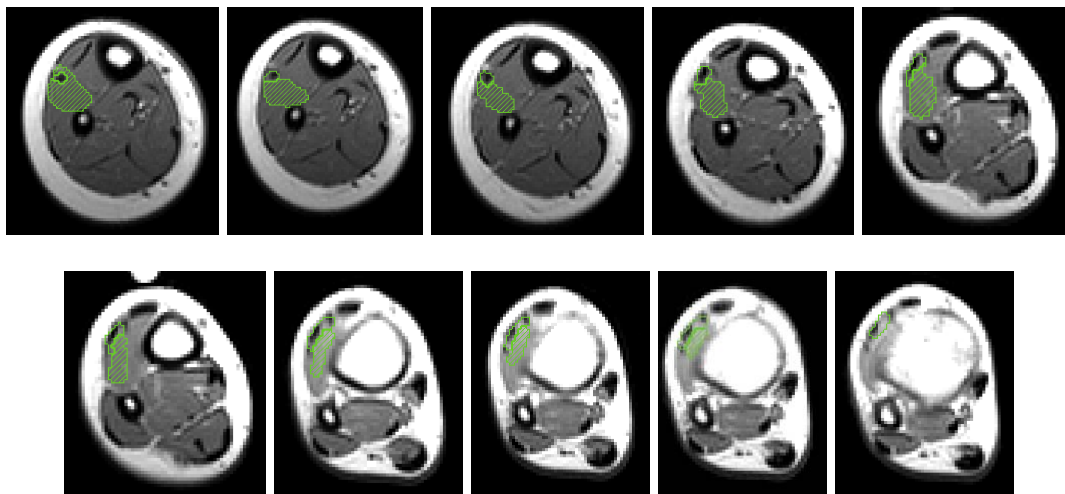


Figure 48: Transition muscle to tendon at M Extensor digitorum longus – distal end

8.1 Problems that appeared while the segmentation of tendons

During the segmentation a problem with some tendons in the shank occurred. There are some muscles in the shank that act on the feet and so there are some tendons that go all the way down from the shank to the end of the feet and even down till the toes. One of these tendons for example is the tendon of M. flexor digitorum longus which starts in the middle of the tibia and ends at digitus minimus, digitus II, digitus III and digitus IV. Another of these tendons was the tendon of M. flexor hallucis longus which starts at the middle of the fibula and ends at the hallux. (Figure 8 shows the insertion and origin of M. flexor digitorum longus and M. flexor hallicus longus)

The existing MR – images did not go down to the end of the toes. Another thing was that there are a lot of bones in the feet and these bones were very dominating in the images of the feet. For these reasons it was impossible to identify the whole length of the tendons of some muscles. The consequence of this was that it was not possible to compare the tendon length of these muscles.

The affected tendons were:

- Distal tendon of M. peroneus
- Distal tendon of M. extensor digitorum longus
- Distal tendon of M. flexor digitorum longus
- Distal tendon of M. flexor hallucis longus
- Distal tendon of M. tibialis anterior
- Distal tendon of M. tibialis posterior

The location, insertion and origin of these muscles can be seen in the figures of chapter 2.4.

8.2 Tendon separation results

The 3 dimensional tendon segmentation results are displayed in figures 49 and 50. The first series is from the CP – child and the second one from the healthy child. Three of the figures include the bones of the lower limb for a better orientation. In the last one they are left out and so it is easier to see all of the tendons in this figure. The corresponding distal and proximal tendons always have the same colour.

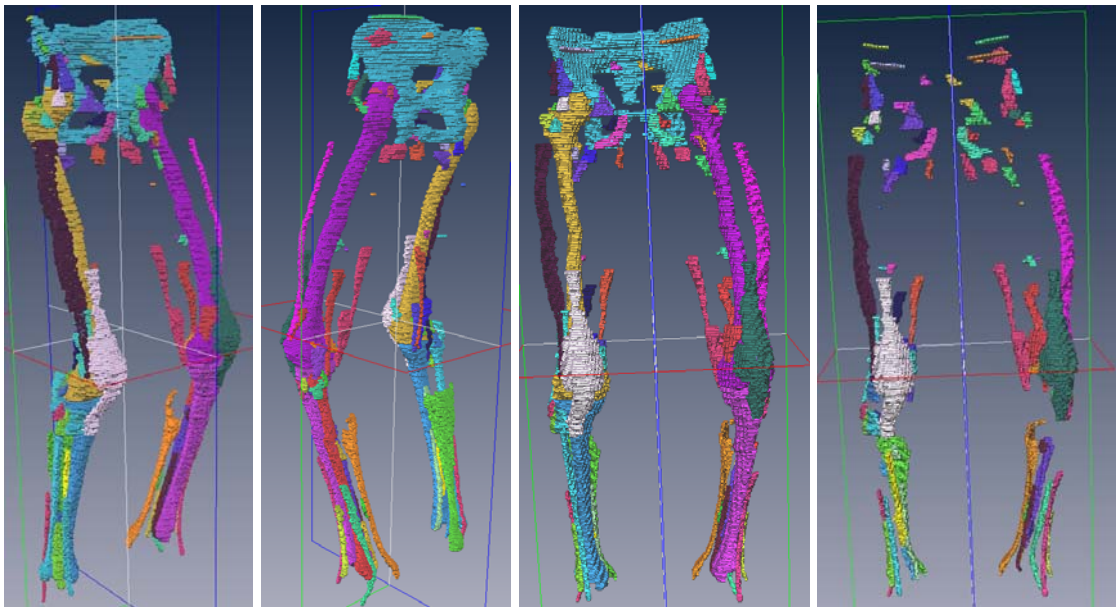


Figure 49: Tendon segmentation results from the CP - child

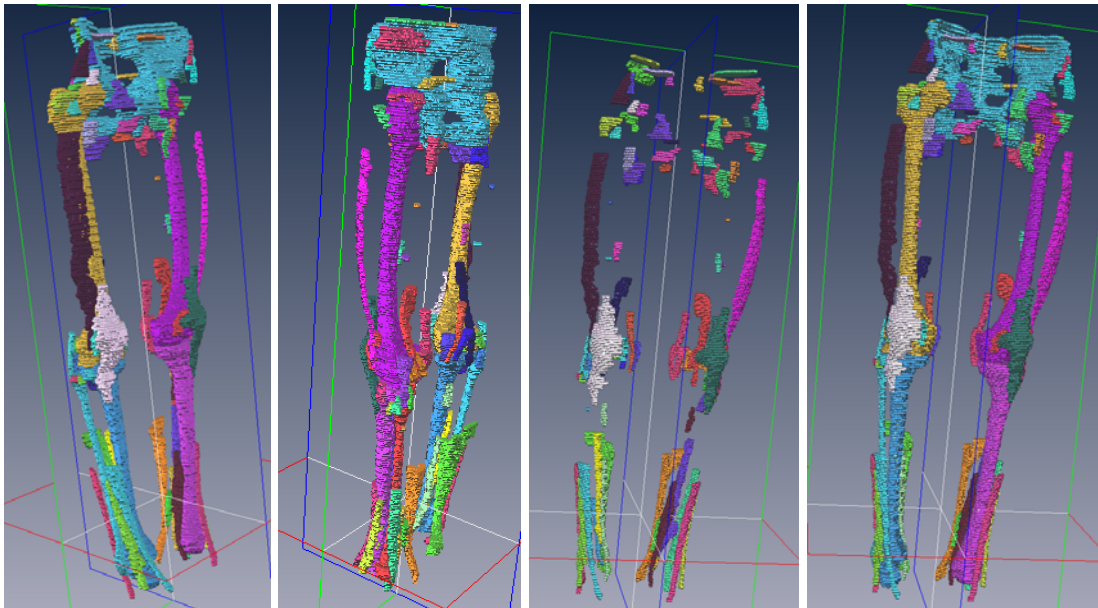


Figure 50: Tendon segmentation results from the healthy child

9 Muscle parameters

9.1 Muscle tendon Model

As explained before there are different kinds of muscles such as unipennated and bipennated muscles. These two types of muscles can be seen in figures 51 and 52. In the figures there is a schematic illustration of the muscle belly, the tendons and the so called pennation angle α .

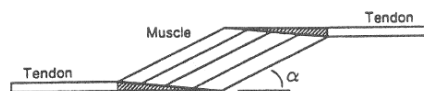


Figure 51: schematic model of a unipennated muscle, Hoy and Zajac 1990

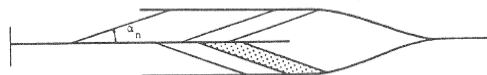


Figure 52: schematic model of a bipennated muscle, Spoor et. al. 1989

For a better imagination of the different muscle parameters and to see how a muscle can be modelled as a technical object there is a muscle tendon model in figure 53. This model was taken out of “Biomechanik” from Roland Pawlik [10].

The muscle is modelled as contractile Element (CE) with the activity $q(t)$ and a parallel elastic element (PE) with the stiffness k^{PE} . The tendon is modelled as an elastic tendon with the stiffness k^T .

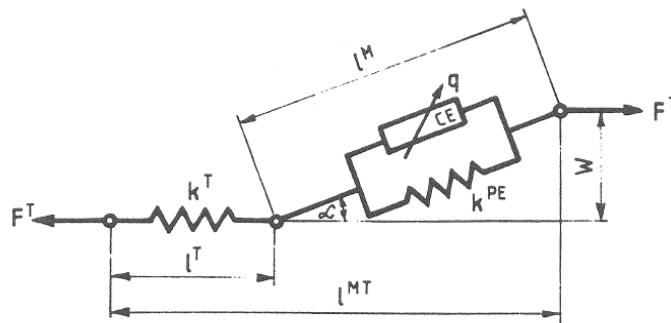


Figure 53: Muscle - tendon model, Biomechanik Roland Pawlik

Parameters in the model:

F^T	Tendon force
F^{CE}	force of contractile element (CE)
F^{PE}	force of passive element (PE)
F^M	overall muscle force
l^M	muscle fibre length
l^M_0	muscle fibre length at the maximum isometric muscle force the so called optimal fibre length which occurs at the optimal joint angles
α	pennation angle
α_0	pennation angle at l^M_0
l^T	tendon length
l^{MT}	complete length of tendon and muscle
W	muscle thickness

It is supposed that the active muscle force F^{CE} just depends on the activation of the muscle q , the muscle fibre length l^M and the relative speed of the muscle fibre ends v^M .

The contractile element is modelled as a ratio between the muscle force F^{CE} and the muscle force for the optimal fibre length F^{CE}_0 .

$$\frac{F^{CE}}{F^{CE}_0} = A_f \left(\frac{(g(l^M) + A_f)v_0^M}{v^M + A_f v_0^M} - 1 \right)$$

The optimal muscle force is the force for the optimal fibre length under isometric conditions. The optimal force is calculated in the following way:

$$F^{CE}_0 = \sigma_0 \cdot PCSA$$

In this equation σ_0 is the maximum muscle tension for optimal fibre length under isometric conditions. It is supposed that this parameter is constant for all muscles and in relation to Pawlik [10] it will be set to $\sigma_0 = 45 \text{ N/cm}^2$ for future calculations. PCSA is the so called physiological cross sectional area which simply means the muscle cross section rectangular to the muscle fibre direction.

Another factor for the determination of the muscle force is v^M_0 which is the maximal muscle contraction speed. This is the contraction speed for the optimal fibre length when there is no muscle force from the outside. The maximum contraction speed depends on the percentage of fast switching muscle fibres in the different muscles. There can be found some suggestions for it in the literature.

A_f is the so called Hill-Parameter and it describes the speed of decreasing muscle power when the contraction speed increases.

g is a function of the optimal fibre length and the existing muscle fibre length under isometric conditions.

The parallel elastic element describes the passive behaviour of the muscle and the surrounding connective tissue. If the muscle fibre length gets bigger than the optimal fibre length there is a resistance against the movement. This resistance is described by the parallel elastic element in the model.

The tendon also produces a resistance against the muscle shortening which is similar to the behaviour of the parallel elastic element when the tendon length becomes bigger than the tendon slack length. This tendon slack length is the tendon length without a muscle activity.

9.2 Calculation of the muscle parameters

After the segmentation work was done the desired parameters had to be calculated. For this reason the results of the segmentation had to be saved as a Matlab file in Amira 5.0. When this was done the parameters were calculated by using a Matlab program that was written by Reinhard Hainisch. The parameters that could be calculated using the data that was generated out of the 3 dimensional muscle models were muscle fibre length, tendon length, muscle volume and tendon volume. The calculated length parameters were the real ones that and not the optimal which relate to the optimal joint angles

9.3 Results of the Calculation

9.3.1 General Explanation for the results

Muscle volume, muscle length, tendon volumes and tendon length were calculated using a Matlab program.

For this reason the Amira 5.0 model was stored as a matlab file. With the matlab program the different muscles and tendons of the model were separated and in the end there was a 3 dimensional body for each part. After this process the calculation of the parameters started.

This was done by calculating the volume of the elements which was equal to the muscle or tendon volume. The length parameters were calculated as the length of the midline of the generated 3 dimensional bodies.

For the scaling of the results it was important to know the voxel size of the MRI – data and the distance between the different MR – slices. These parameters can be seen in chapter 3.

For the calculations that should be done in the future it was important to know that the calculated length parameters were the real ones and not the optimal ones as said before. The optimal fibre length that will be needed in the future is the muscle fibre length that belongs to the optimal joint angles. The joint angles during the recording of the MRI – data were not the optimal ones and so the difference has to be calculated in the future. The schema of the calculation of the optimal fibre length is explained in chapter 10.

The main target was to compare the results of children with cerebral palsy and age matched healthy children to check if there were any differences. To make the results comparable the results had to be normalised.

The volumes were normalised by the volume of the right M.Vastus of the children and the lengths were normalised by the height of the children. The height and weight of the two girls that were treated in this work can be seen in the following table.

Subject	Height	Weight	Age
	cm	kg	years
CP2	146	37	11
Healthy	124	24	9

Table 5: Weight, height and age of both subjects for this thesis

There were some muscle and tendon parameters from other children calculated in the work of Md.Z.Karim from TU – Vienna. In his work there were four healthy children and one with cerebral palsy.

In order to get better results the parameters of the CP – child from this work and the one from the work of Md.Z.Karim from TU – Vienna were compared to an average of all of the healthy children (four from Md.Z.Karim and one from this work).

There were some more parameters from two healthy adults that were taken out of the work of the work of J.A. Friedrich and R.A. Brand. These parameters were also normalised in the same way and they can be seen in the next tables. There was also a calculated average of the two adults which can also be seen in the following tables.

9.3.2 Special results of the calculation

In tables 7 and 8 there are just the parameters of the following muscles (table 6):

Short term for muscle	Anatomic muscle name
TA	M. Tibialis anterior
GN	M. Gastrocnemius
SL	M. Soleus
RF	M. Rectus femoris
HAM	M. Hamstring
VAS	M. Vastus
BF	M. Biceps femoris
GM	M. Gluteus maximus

Table 6: Short terms for some selected muscles

They were selected because those muscles are the most important ones for the human gait.

Explanation of the columns from the following tables

Muscle: Names of the selected muscles; complete names can be seen in table 6

Norm_Avg_Healthy: normalised averaged data from all of the healthy children

CP1: normalised data from the CP – child modelled by Md.Z.Karim

CP2: normalised data from the CP – child modelled in this work

Adults_Ref: Data taken out of the work from J.A. Friedrich and R.A. Brand [1]; and normalisation of this data. S1 and S2 were two different healthy adult subjects in the study of Friedrich and Brand [1].

Norm_Avg_Adults: Averaged data of the two healthy adult subjects

Norm_S1/Norm_S2: Normalised data from the two subjects S1 and S2 from the studies of J.A. Friedrich and R.A. Brand [1].

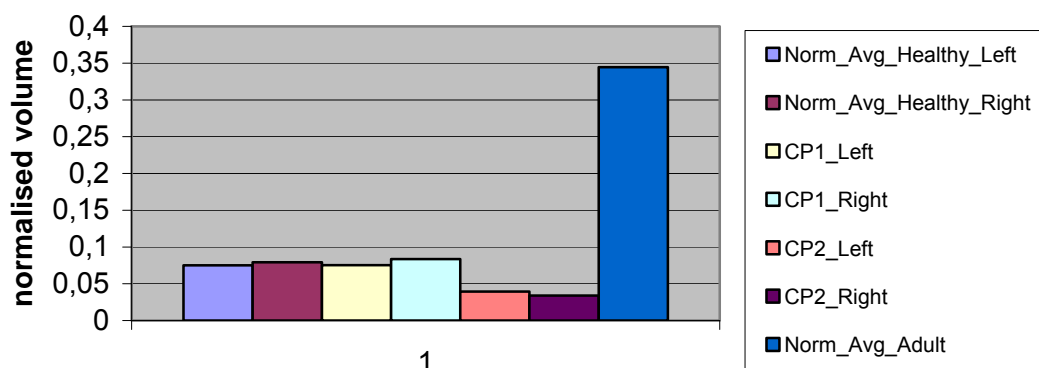
Compared normalised muscle volume data

Muscle	Norm_Avg_Healthy		CP1		CP2		Adults_Ref				Norm_Avg_Adults
	Left	Right	Left	Right	Left	Right	S1	Norm_S1	S2	Norm_S2	
TA	0,075	0,0793	0,0754	0,0836	0,0394	0,034	130	0,252918	58	0,43609	0,344504257
GN	0,199	0,2044	0,1465	0,1708	0,0958	0,0959	110	0,214008	38	0,285714	0,249861034
SL	0,2366	0,261	0,1987	0,2804	0,1575	0,1537	575	1,118677	172	1,293233	1,205955063
RF	0,173	0,1707	0,1504	0,1567	0,091	0,1162	238	0,463035	60	0,451128	0,45708142
HAM	0,3423	0,3427	0,3206	0,3227	0,2246	0,249	776	1,509728	180	1,353383	1,431555543
VAS	0,9475	1	0,9356	1	0,9095	1	514	1	133	1	1
BF	0,0619	0,061	0,0659	0,0687	0,0598	0,0547	100	0,194553	52	0,390977	0,292764986
GM	0,5596	0,5199	0,5122	0,5947	0,3455	0,3547	288	0,560311	109	0,819549	0,689930078

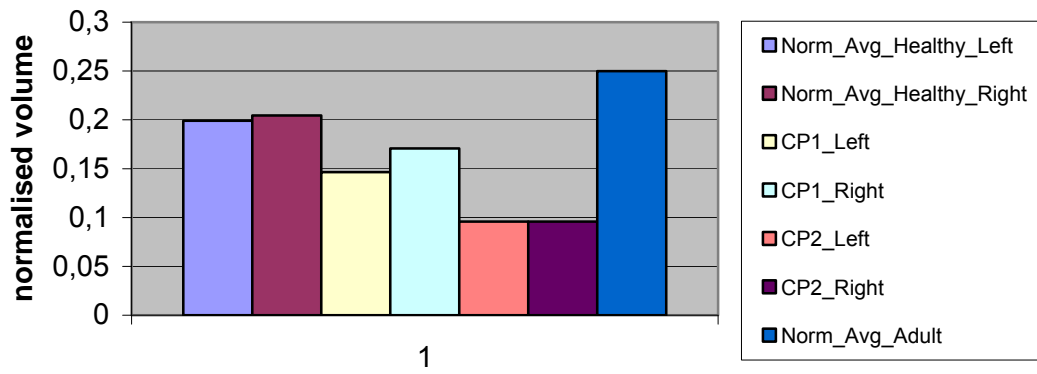
Table 7: Comparison of muscle volume data (**Muscle:** Names of the selected muscles; complete names can be seen in table 6; **Norm_Avg_Healthy:** normalised averaged data from all of the healthy children; **CP1:** normalised data from the CP – child modelled by Md.Z.Karim; **CP2:** normalised data from the CP – child modelled in this work; **Adults_Ref:** Data taken out of the work from J.A. Friedrich and R.A. Brand [1]; and normalisation of this data. S1 and S2 were two different healthy adult subjects in the study of Friedrich and Brand [1]; **Norm_Avg_Adults:** Averaged data of the two healthy adult subjects)

In the following diagrams there is a visual comparison for the normalised volume data of each muscle.

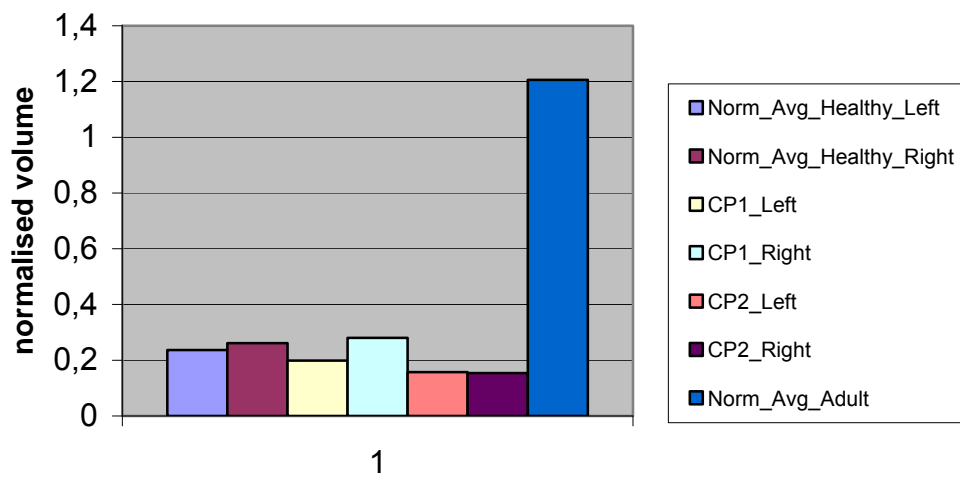
Comparison of M. Tibialis anterior



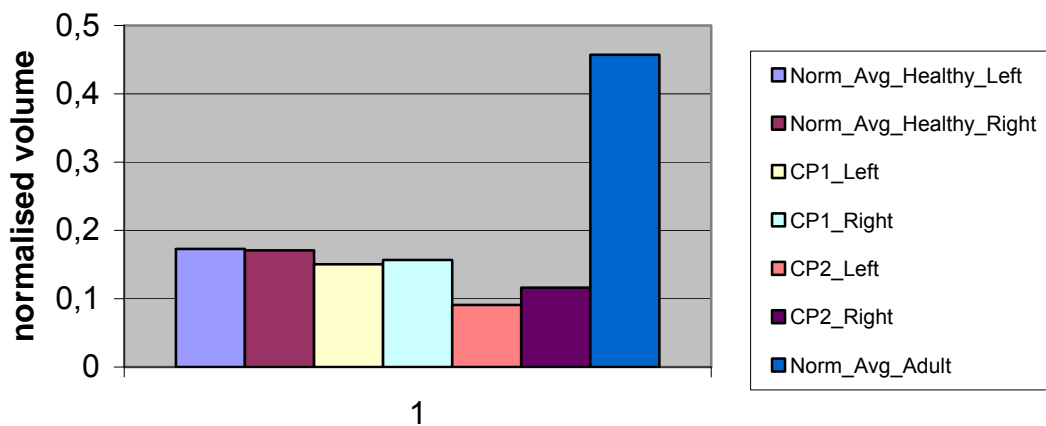
Comparison of M. Gastrocnemius



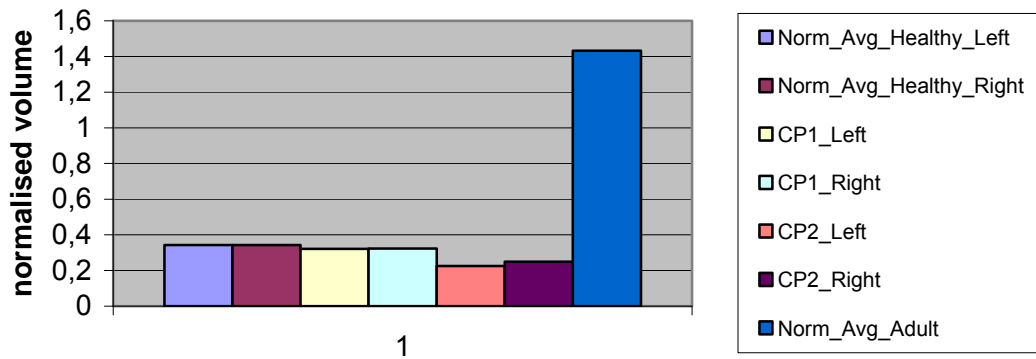
Comparison of M. Soleus



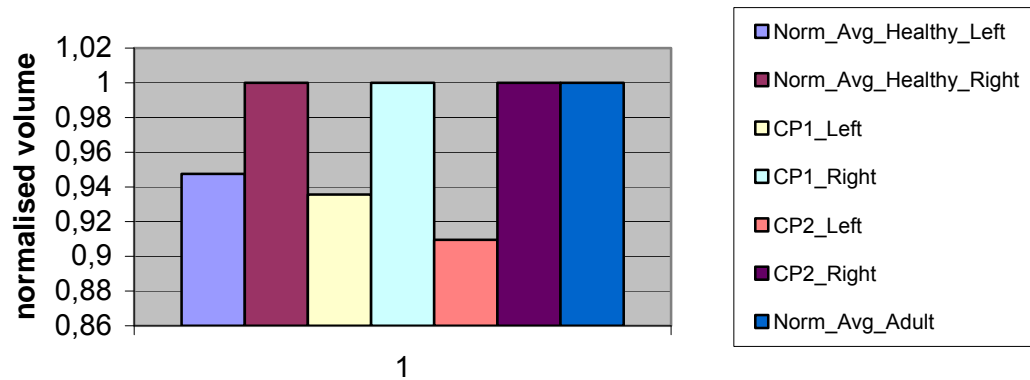
Comparison of M. Rectus femoris



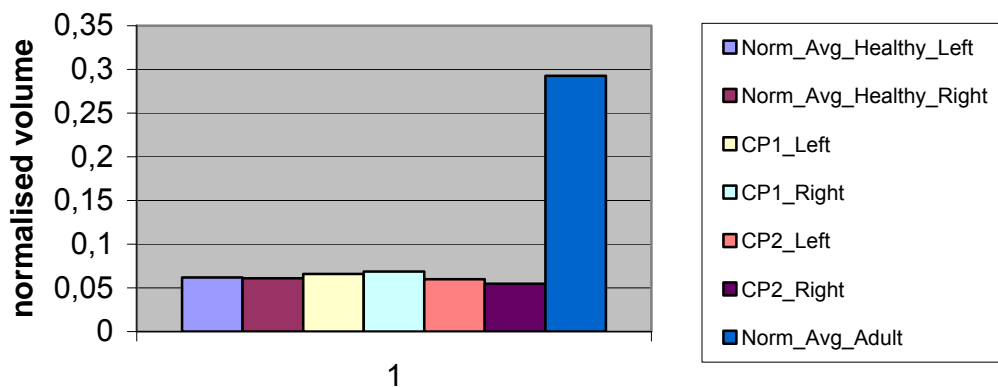
Comparison of M. Hamstrings



Comparison of M. Vastus



Comparison of M. Biceps femoris



Comparison of M. Gluteus maximus

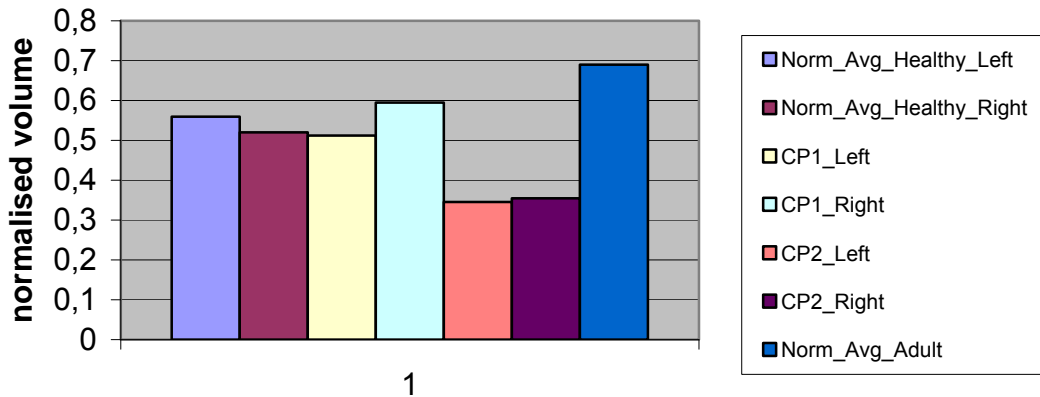


Figure 54: Diagrams of normalised volume parameters of some selected muscles from different subjects

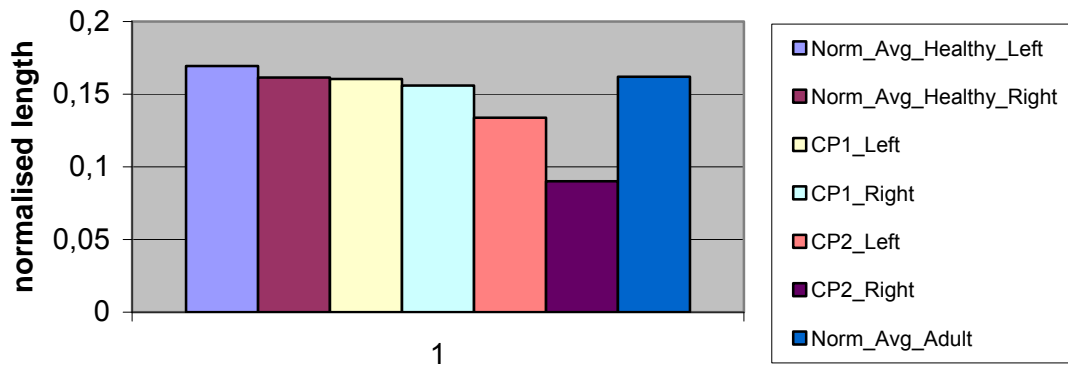
Compared normalised muscle length data

Muscle	Norm_Avg_Healthy		CP1		CP2		Adults_Ref				Norm:Avg_Adults
	Left	Right	Left	Right	Left	Right	S1	Norm_S1	S2	Norm_S2	
TA	0,1694	0,1614	0,1605	0,156	0,134	0,0901	0,29	0,15847	0,278	0,16548	0,161973068
GN	0,1484	0,1549	0,1323	0,134	0,111	0,1093	0,23	0,125683	0,205	0,12202	0,123853435
SL	0,1787	0,1875	0,1785	0,201	0,165	0,1609	0,37	0,202186	0,305	0,18155	0,191866706
RF	0,18	0,1848	0,1805	0,187	0,174	0,1829	0,332	0,181421	0,295	0,1756	0,178508002
HAM	0,1872	0,1924	0,1783	0,182	0,201	0,2019	0,29	0,15847	0,275	0,16369	0,161080211
VAS	0,2271	0,2234	0,2334	0,228	0,259	0,261	0,305	0,166667	0,295	0,1756	0,171130952
BF	0,1136	0,1209	0,1142	0,132	0,111	0,1071	0,205	0,112022	0,24	0,14286	0,1274395
GM	0,1643	0,1656	0,1987	0,186	0,16	0,1706	0,165	0,090164	0,16	0,09524	0,092701015

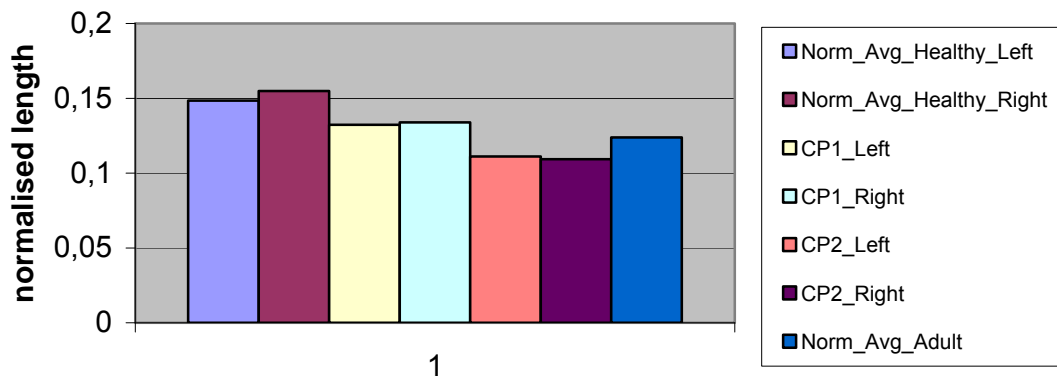
Table 8: Comparison of muscle length data (**Muscle**: Names of the selected muscles; complete names can be seen in table 6; **Norm_Avg_Healthy**: normalised averaged data from all of the healthy children; **CP1**: normalised data from the CP – child modelled by Md.Z.Karim; **CP2**: normalised data from the CP – child modelled in this work; **Adults_Ref**: Data taken out of the work from J.A. Friedrich and R.A. Brand [1]; and normalisation of this data. S1 and S2 were two different healthy adult subjects in the study of Friedrich and Brand [1]; **Norm_Avg_Adults**: Averaged data of the two healthy adult subjects)

In the following diagrams there is a visual comparison for the normalised length data of each muscle.

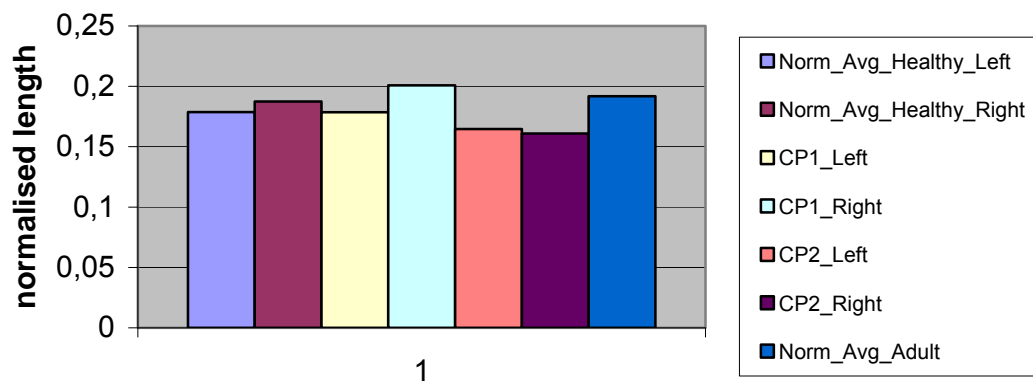
Comparison of M. Tibialis anterior



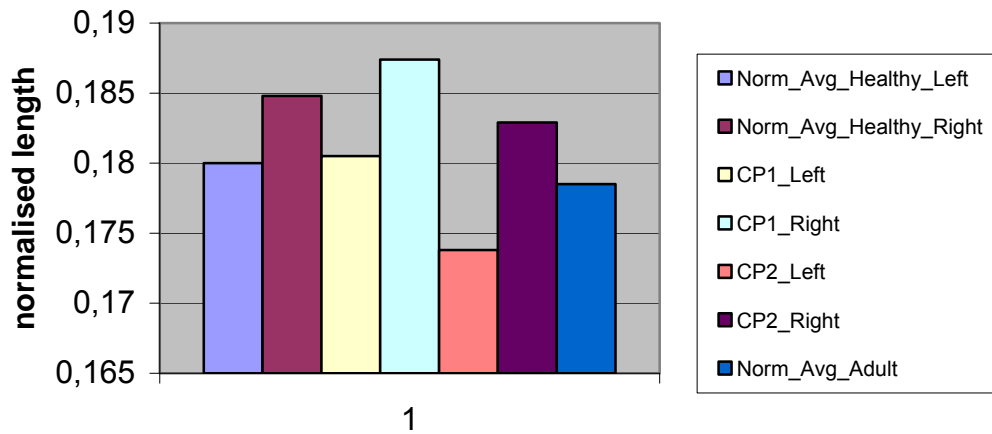
Comparison of M. Gastrocnemius



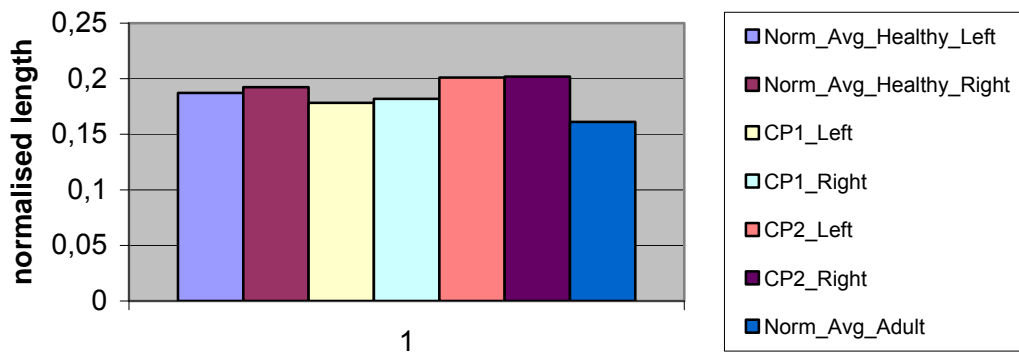
Comparison of M. Soleus



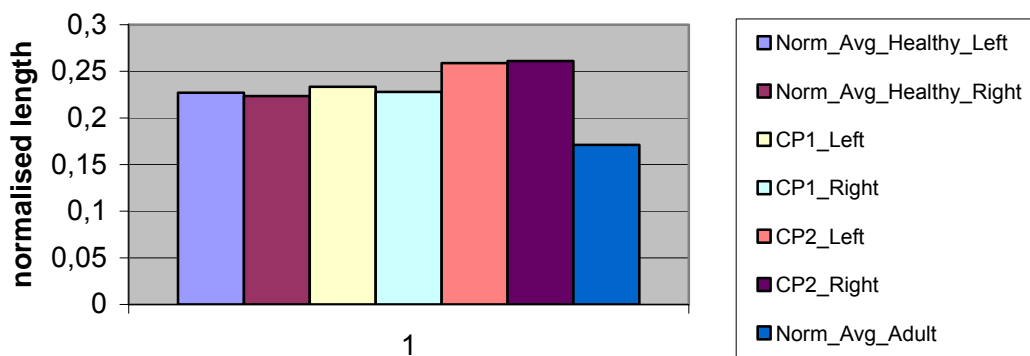
Comparison of M. Rectus femoris



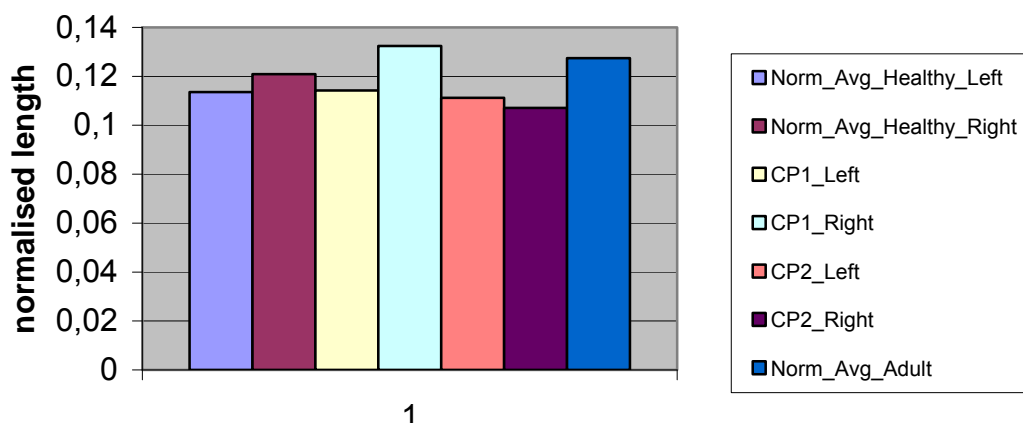
Comparison of M. Hamstrings



Comparison of M. Vastus



Comparison of M. Biceps femoris



Comparison of M. Gluteus maximus

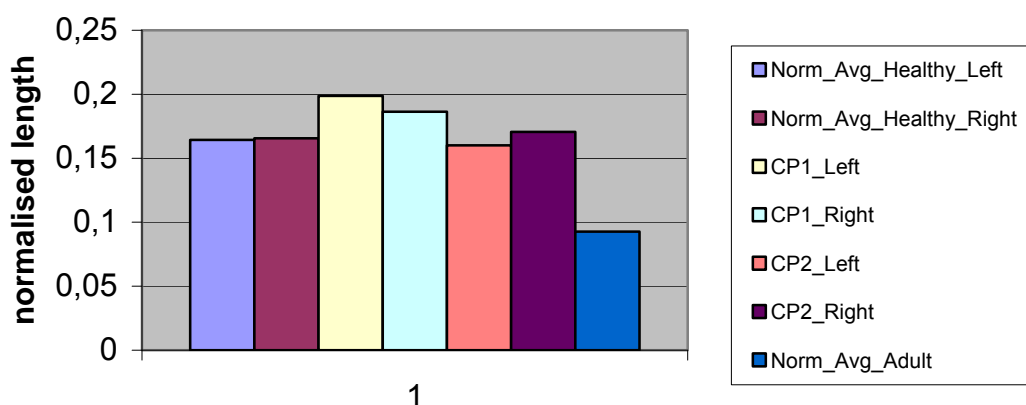


Figure 54: Diagrams of normalised length parameters of some selected muscles from different subjects

As it can be seen in the diagrams there are not too big length or volume differences between the different subjects. The differences of the right and left leg of one subject are also negligible. The length differences between the children and the adult average could be a consequence of the different joint angles. The joint angles of the adult studies from Friedrich et. Al [1] where the optimal joint angles and the joint angles for the data of the children were not optimal ones. These angles will be measured in some future works on this topic.

It seems like the volumes and length of the muscles from CP – kids and healthy children are approximately the same. The obvious gait differences between those two groups are maybe not an affect of volume or length differences. So finally it is supposed that the gait differences are an affect of different muscle activations at healthy children and children with cerebral palsy. The comparison of the parameters from children and healthy adults is not significant at the moment

because there are different joint angles at the moment. It will be necessary to calculate the optimal fibre lengths of the children to get better results for future comparisons.

The complete results of the calculation can be seen in a table in the Appendix. This table contains the normalised muscle and tendon parameters from the lower limb of the two girls that were modelled in this work.

10. Discussion

After the segmentation the muscle and tendon parameters were calculated. The data generated out of the 3 – dimensional models made it possible to calculate the muscle volume, the muscle length, the tendon volume and the tendon length. All of these parameters were calculated and they could be compared.

In the future it should be possible to calculate the muscle force and the physiological cross sectional areas. For these calculations the optimal muscle fibre length will be needed. It is not possible to get this optimal length out of the MRI – data because the joints of the children were not in the optimal joint angles which affect the optimal muscle fibre length. So the first step for the future calculation will be finding out the optimal joint angles to determine the optimal fibre length. This will be done by using some existing literature.

Another important thing for the determination of the optimal fibre length is to find out the centre points of all of the joints of the lower limb. When these centre points are found it will be possible to calculate the difference between the existing fibre length and the optimal fibre length by using the moment arms of the muscle midlines in relation to the centre points concerning the joint angles in the MR – images. The difference between the existing fibre length and the optimal fibre length will be modelled as the change of the length of a sector of a circle along the midline of the different muscles. The centre points of the circles for the calculation are the joint centre points.

When the optimal fibre length will be found the peak isometric force and the physiological cross sectional area of each muscle will be calculated.

The peak isometric force will be calculated the following way:

$$Peak_isometric_force = Maximum_muscle_stress \times \frac{Muscle_Volume}{optimal_muscle_fibre_length}$$

The physiological cross-sectional area (PCSA) of each muscle will be calculated by using the following equation:

$$PCSA = muscle_volume \times \frac{\cos(pennation_angle)}{optimal_muscle_fibre_length}$$

All of these parameters will be calculated in some future works.

The calculated muscle data for this work was quite good but not all of the results could be compared. This was not possible because the existing MR – data was not enough to make complete models of all of the muscles and tendons of the lower limb. As it is mentioned before there are some slices missing to reconstruct the complete distal tendons of the muscles of the shank and some of the muscles that are located in the pelvis.

The quality of the MR – images was quite good and so the results of the modelling should be reliable but in some of the images there were some moving artefacts and so some parts of the muscles had to be modelled by using a kind of interpolation as described in the chapters before.

To get even better results and to improve the comparability of the results there are some suggestions for further works on this topic in the following text.

For a better comparison of the calculated parameters it would be necessary to have MR – images containing the whole lower limb of the patient. The images should start at the sole of the foot to include all the tendons of the muscles from the shank and the should go up till the end of M Gluteus medius and M. Gluteus minimus to get the whole volume of all needed muscles.

To avoid moving artefacts it would be necessary to fix the patients legs during the examination. If this will be done the quality of the images should be even better and the modelling results should be more exact.

Another important thing for studies in the future would be to measure the joint angles during the MRI – data recording. This would be useful for the calculation of the optimal fibre length because the measurement of the joint angles in MR – images is more difficult than it would be on the living subject.

Finally it can be said that the differences in muscle parameters between the healthy child and the CP-child were not too big. For a better comparison it will be necessary to calculate the optimal fibre length for all of the muscles. After this calculation it might be possible to detect some bigger differences. Another possibility is that the obvious gait differences are just a result of different muscle activation in healthy and diseased lower limbs and not a problem of different muscle volumes or muscle lengths. The solution for this has to be found out in future works.

11. Table of figures:

Figure 1: Left side: Planes (Anatomy and human movement, 2006) and right side: Axes (Der Körper des Menschen, 1995) in the human body	8
Figure 2: General anatomical terms of location (trunk and extremities),	9
Figure 3: Arrangements of fibres within muscles	11
Figure 4: Bones of the thigh – Femur, left ventral view on the left side and dorsal view on the right, Netter 1999.....	12
Figure 5: Bones of the shank – Fibula and Tibia, right shank, ventral view on the left and dorsal view on the right, Netter 1999	13
Figure 6: Muscle insertion points on the pelvis and femur, ventral view, origins are marked as red areas and insertion points are marked blue, Netter 1999	14
Figure 7: Muscle insertion points on the pelvis and femur, dorsal view, origins are marked as red areas and insertion points are marked blue, Netter 1999	15
Figure 8: Muscle insertion points on the shank, ventral view on the left and dorsal view on the right, origins are marked as red areas and insertion points are marked blue, Netter 1999.....	16
Figure 9: Muscles and tendons of the thigh; ventral view; surface layer on the left and middle layer on the right, Netter 1999.....	17
Figure 10: Muscles and tendons of the thigh; ventral view; deepest layer, Netter 1999	18
Figure 11: Muscles and tendons of the thigh and the pelvis; lateral view, Netter 1999.....	19
Figure 12: Muscles and tendons of the thigh and the pelvis; ventral view; surface layer on the left and deeper layer on the right, Netter 1999.....	20
Figure 13: Muscular cross – sections of the thigh, Netter 1999.....	21
Figure 14: Muscles and tendons of the shank; dorsal view; surface layer, Netter 1999.....	22
Figure 15: Muscles and tendons of the shank; dorsal view; middle layer, Netter 1999.....	23
Figure 16: Muscles and tendons of the shank; dorsal view; deepest layer, Netter 1999.....	24
Figure 17: Muscles and tendons of the shank; ventral view; surface layer, Netter 1999.....	25
Figure 18: Muscles and tendons of the shank; ventral view; deepest layer, Netter 1999.....	26
Figure 19: Muscles and tendons of the shank; lateral view, Netter 1999	27
Figure 20: Muscular cross - section of the shank, Netter 1999.....	28
Figure 21: Schematic numeration of MR – image stack in the transverse plane.....	29
Figure 22: Point and direction of view for MR – images and anatomical terms (Der Körper des Menschen, 1995).....	30
Figure 23: Directions in a MR-image of the pelvic	31
Figure 24: Directions in a MR-image of the thigh.....	31
Figure 25: Schematic Location of the MRI series	33
Figure 26: T1 – weighted (left image) and T2 – weighted (right image) image of the knee and the surrounding muscles, National Library of Medicine (http://www.nlm.nih.gov/research/visible/mri.html).....	34
Figure 27: T1 – weighted (left image) and T2 – weighted (right image) image of the ankle and the surrounding muscles, National Library of Medicine (http://www.nlm.nih.gov/research/visible/mri.html).....	34
Figure 28: Location of Zoom and Data Window in Amira 5.0 userinterface	36
Figure 29: Detailed Zoom and Data Window	36
Figure 30: Examples for good (left side) and bad (right side) contrasts in MR - images	37
Figure 31: Markers (Nitro capsules) as they appeared on the MR – images	38
Figure 32: Amira 5.0 Editor with 2 – and 3 – dimensional view	39
Figure 33: Examples for selecting and adding routine; in the first line the muscles are selected and the figures below show the same muscles after they were assigned to the correct material. The selected muscles are starting from left: M. Gastrocnemius, M.Soleus, M.Hamstring, M.Vastus	40
Figure 34: Amira user interface with material list, selection label and marking tools.....	40
Figure 35: Detailed Selection Label	41
Figure 36: Moving artefacts in MR - images	41
Figure 37: Bones in MR – images; left side: MR – images with bones, right side bones are marked as coloured areas; starting from the top: tibia and fibula, femur, tibia and fibula, pelvis, pelvis and femur	43
Figure 38: Series of MR – images from CP – child with red marked right femur.....	44
Figure 39: Three dimensional model of the right femur of the CP - child	44

Figure 40: Three different views of the modelled bones from the CP - girl.....	45
Figure 41: Three different views of the modelled bones from the healthy girl	45
Figure 42: Muscles in MR – images of the lower limb.....	48
Figure 43: Muscle segmentation results; starting at the top the following muscles are displayed: M. Vastus, M. Hamstring, M. Gastrocnemius, M. Tibialis anterior, M. Gluteus maximus, M. Iliopsoas; left side CP-child right side healthy child	50
Figure 44: Muscle separation results CP – child.....	51
Figure 45: Muscle separation results healthy child	51
Figure 46: Tendons in MR-images on the left side there are the raw MR – images and on the right side the tendons of M. Gastrocnemius, M. Tibialis anterior, M. Tibialis posterior, M. Extensor digitorum longus, M. Flexor hallicus longus and M. Flexor digitorum longus are selected.....	54
Figure 47: Transition muscle to tendon at M. Vastus - distal end.....	55
Figure 48: Transition muscle to tendon at M Extensor digitorum longus – distal end	55
Figure 49: Tendon segmentation results from the CP - child.....	56
Figure 50: Tendon segmentation results from the healthy child	57
Figure 51: schematic model of a unipennated muscle, Hoy and Zajac 1990	57
Figure 52: schematic model of a bipennated muscle, Spoor et. al. 1989	57
Figure 53: Muscle - tendon model, Biomechanik Roland Pawlik	58
Figure 54: Diagrams of normalised volume parameters of some selected muscles from different subjects	64
Figure 54: Diagrams of normalised length parameters of some selected muscles from different subjects	67

12. Table of Tables

Table 1: MRI parameters.....	32
Table 2: Bones of the lower limb and pelvis.....	42
Table 3: Muscles of the lower limb.....	46
Table 4: Tendons of the lower limb.....	53
Table 5: Weight, height and age of both subjects for this thesis.....	60
Table 6: Short terms for some selected muscles.....	60
Table 7: Comparison of muscle volume data (Muscle : Names of the selected muscles; complete names can be seen in table 6; Norm_Avg_Healthy : normalised averaged data from all of the healthy children; CP1 : normalised data from the CP – child modelled by Md.Z.Karim; CP2 : normalised data from the CP – child modelled in this work; Adults_Ref : Data taken out of the work from J.A. Friedrich and R.A. Brand [1]; and normalisation of this data. S1 and S2 were two different healthy adult subjects in the study of Friedrich and Brand [1]; Norm_Avg_Adults : Averaged data of the two healthy adult subjects).....	61
Table 8: Comparison of muscle length data (Muscle : Names of the selected muscles; complete names can be seen in table 6; Norm_Avg_Healthy : normalised averaged data from all of the healthy children; CP1 : normalised data from the CP – child modelled by Md.Z.Karim; CP2 : normalised data from the CP – child modelled in this work; Adults_Ref : Data taken out of the work from J.A. Friedrich and R.A. Brand [1]; and normalisation of this data. S1 and S2 were two different healthy adult subjects in the study of Friedrich and Brand [1]; Norm_Avg_Adults : Averaged data of the two healthy adult subjects).....	64

13. Bibliography:

- [1] Friedrich, J.A. and Brand, R.A., Muscle fibre architecture in the human lower limb. Technical Note, J.Biomech. 23: 91-95, 1990
- [2] Nikola Bojanovic, Erstellung eines 3D-CAD Modells der unteren Extremitäten eines Kindes basierend auf Magnetresonanzaufnahmen, TU-Vienna, 2004
- [3] Murray WM. et al. Building biomechanical models based on medical image data: an assessment of model accuracy. Wells et al.(Eds.) : Springer-Verlag Berlin Heidelberg, MICCAI'1998, LNCS 1496 : 539-549, 1998
- [4] Spoor CW. et al. Knee muscle moment arms from MRI and tendon travel. J Biomech. 25(2): 201-206, 1992
- [5] Arnold AS. et al. Accuracy of muscle moment arms estimated from MRI-based musculoskeletal models of lower extremity. Computer Aided Surgery 5: 108-119, 2000
- [6] Wickiewicz TL, Roy RR, Powell PL, Edgerton VR, Muscle architecture of the lower limb, Clinical Orthopaedics and Related Research 179: 275-283, 1983
- [7] Nigel Palastanga, Derek Field, Roger Soames, Anatomy and human movement structure and function, fifth edition, 2006
- [8] Adolf Faller, Der Körper des Menschen, 12. Auflage, 1995
- [9] Frank H. Netter, M.D., Atlas der Anatomie des Menschen, 2. Ausgabe, 1999
- [10] Pawlik R., Biomechanik des Radfahrens – Untersuchung der maximalen menschlichen Leistungsabgabe, TU-Vienna, 1992
- [11] Margit Gföhler, Marcus G. Pandy, Ing. Mag. Andreas Kranzl, Proposal for funding of the research project Computational Modeling of Crouch Gait in Children with Cerebral Palsy, 2006

14. Appendix

Calculated muscle volume, muscle length, tendon volume and tendon length of the CP-child and the healthy child.

Muscle Volume Data

Name	Volume_healthy_child	Volume_norm_healthy_child	Volume_CP1	CP1_norm
	m ³		m ³	
Add_longus_L	3,556219790E-05	7,870240598E-02	4,851071340E-05	8,753632511E-02
Add_longus_L_pro	1,308811320E-06	2,896519505E-03	6,683670000E-07	1,206050930E-03
Add_longus_L_dis	4,327521300E-07	9,577201588E-04		0,000000000E+00
Add_longus_R	4,110353615E-05	9,096589582E-02	5,103141180E-05	9,208486004E-02
Add_longus_R_pro	1,556852175E-06	3,445456669E-03	1,304907000E-07	2,354670863E-04
Add_longus_R_dis	3,852549450E-07	8,526045317E-04		0,000000000E+00
Add_magnus_R	1,431960966E-04	3,169060967E-01	1,930657647E-04	3,483821688E-01
Add_magnus_R_pro	1,108267650E-07	2,452697968E-04		0,000000000E+00
Add_magnus_R_dis	6,227408700E-06	1,378182668E-02	3,921086400E-06	7,075498788E-03
Add_magnus_L	1,443756100E-04	3,195164681E-01	1,748129802E-04	3,154454922E-01
Add_magnus_L_pro	1,926274725E-07	4,263022658E-04		0,000000000E+00
Add_magnus_L_dis	5,042617808E-06	1,115977575E-02	3,816057300E-06	6,885976499E-03
Biceps_Shorthead_R	2,143442410E-05	4,743634665E-02	3,811919790E-05	6,878510470E-02
Biceps_Shorthead_R_pro	1,847112750E-07	4,087829946E-04	2,660737200E-06	4,801231321E-03
Biceps_Shorthead_R_dis	1,646569080E-06	3,644008409E-03		0,000000000E+00
Biceps_Shorthead_L	1,628097953E-05	3,603130110E-02	3,655012680E-05	6,595375656E-02
Biceps_Shorthead_L_pro	5,805211500E-08	1,284746555E-04	7,001940000E-08	1,263481926E-04
Biceps_Shorthead_L_dis	9,895246875E-07	2,189908900E-03	2,807141400E-06	5,065413905E-03
Ex_digi_R	3,156715690E-05	6,986101378E-02	3,167104770E-05	5,714958477E-02
Ex_digi_R_pro	3,667838175E-07	8,117262322E-04	8,306847000E-07	1,498949013E-03
Ex_digi_R_dis	3,493681830E-06	7,731838356E-03	6,963747600E-06	1,256590207E-02
Ex_digi_L	2,684118699E-05	5,940200888E-02	3,411217860E-05	6,155454222E-02
Ex_digi_L_pro	2,005436700E-07	4,438215370E-04	3,946548000E-07	7,121443586E-04
Ex_digi_L_dis	3,625618455E-06	8,023826209E-03	8,351404800E-06	1,506989352E-02
Flex_digi_longus_R	8,446582733E-06	1,869306237E-02	6,394044300E-06	1,153788723E-02
Flex_digi_longus_R_pro	7,441225650E-07	1,646811493E-03		0,000000000E+00
Flex_digi_longus_R_dis	5,203580490E-06	1,151600093E-02	4,328472000E-07	7,810615545E-04
Flex_digi_longus_L	8,319923573E-06	1,841275403E-02	9,239378100E-06	1,667221833E-02
Flex_digi_longus_L_pro	7,282901700E-07	1,611772950E-03		0,000000000E+00
Flex_digi_longus_L_dis	3,609786060E-06	7,988787666E-03	1,642273200E-06	2,963439428E-03
Flex_hall_longus_R	1,791435494E-05	3,964611072E-02	2,619362100E-05	4,726571025E-02
Flex_hall_longus_R_pro	3,694225500E-08	8,175659893E-05		0,000000000E+00
Flex_hall_longus_R_dis	3,103149420E-06	6,867554310E-03	1,941447000E-07	3,503290796E-04
Flex_hall_longus_L	1,738133098E-05	3,846647979E-02	2,434765500E-05	4,393471244E-02
Flex_hall_longus_L_pro	3,430352250E-08	7,591684186E-05		0,000000000E+00
Flex_hall_longus_L_dis	1,219094415E-06	2,697967765E-03	9,548100000E-08	1,722929900E-04
Gastrocnemius_R	9,180678114E-05	2,031768278E-01	9,470123850E-05	1,708859306E-01
Gastrocnemius_R_pro	3,148007873E-06	6,966830180E-03	1,575436500E-06	2,842834335E-03
Gastrocnemius_R_dis	1,089796523E-05	2,411819668E-02	1,311908940E-05	2,367305682E-02
Gastrocnemius_L	8,427847732E-05	1,865160009E-01	8,120977320E-05	1,465409311E-01
Gastrocnemius_L_pro	1,361585970E-06	3,013314646E-03	1,737754200E-06	3,135732418E-03
Gastrocnemius_L_dis	9,327919388E-06	2,064354123E-02	1,177599000E-05	2,124946876E-02
Gluteus_max_R	2,581498392E-04	5,713092735E-01	3,296131428E-04	5,947783738E-01
Gluteus_max_R_pro	1,741563450E-07	3,854239664E-04		0,000000000E+00
Gluteus_max_R_dis	5,541338250E-08	1,226348984E-04		0,000000000E+00
Gluteus_max_L	2,157454079E-04	4,774643775E-01	2,838841092E-04	5,122615178E-01
Gluteus_max_L_pro	2,031824025E-07	4,496612941E-04		0,000000000E+00
Gluteus_max_L_dis	3,166479000E-08	7,007708479E-05		0,000000000E+00
Gluteus_medius_R	8,836323523E-05	1,955559449E-01	1,286065416E-04	2,320671713E-01
Gluteus_medius_R_pro	2,015991630E-06	4,461574399E-03		0,000000000E+00
Gluteus_medius_R_dis	1,752118380E-06	3,877598692E-03		0,000000000E+00
Gluteus_medius_L	7,988498771E-05	1,767928054E-01	1,358981073E-04	2,452246126E-01

Muscle Volume Data

Name	Volume_healthy_child	Volume_norm_healthy_child	Volume_CP1	CP1_norm
	m ³		m ³	
Gluteus_medius_L_pro	1,361585970E-06	3,013314646E-03		0,000000000E+00
Gluteus_medius_L_dis	1,936829655E-06	4,286381687E-03		0,000000000E+00
Gluteus_min_R	1,661345982E-05	3,676711049E-02	1,551566250E-05	2,799761087E-02
Gluteus_min_R_pro	2,683590953E-06	5,939032936E-03	2,768949000E-07	4,996496709E-04
Gluteus_min_R_dis	1,211178218E-06	2,680448493E-03	2,673468000E-07	4,824203719E-04
Gluteus_min_L	1,356572378E-05	3,002219108E-02	2,065254030E-05	3,726697373E-02
Gluteus_min_L_pro	2,108347268E-06	4,665965896E-03	2,450679000E-07	4,422186743E-04
Gluteus_min_L_dis	1,182152160E-06	2,616211166E-03	4,392126000E-07	7,925477539E-04
Grasilis_R	2,520781157E-05	5,578719925E-02	4,957055250E-05	8,944877729E-02
Grasilis_R_pro	7,414838325E-07	1,640971736E-03	1,655004000E-07	2,986411826E-04
Grasilis_R_dis	2,517350805E-06	5,571128241E-03	1,336734000E-06	2,412101860E-03
Grasilis_L	2,657467501E-05	5,881219341E-02	4,003200060E-05	7,223670760E-02
Grasilis_L_pro	6,227408700E-07	1,378182668E-03	1,973274000E-07	3,560721793E-04
Grasilis_L_dis	1,878777540E-06	4,157907031E-03	1,120310400E-06	2,021571082E-03
Hamstring_R	1,495871067E-04	3,310499883E-01	1,788550092E-04	3,227392288E-01
Hamstring_R_pro	2,849831100E-06	6,306937631E-03	1,931898900E-06	3,486061497E-03
Hamstring_R_dis	1,224371880E-06	2,709647279E-03	2,103764700E-06	3,796188879E-03
Hamstring_L	1,416207733E-04	3,134197617E-01	1,776742275E-04	3,206085388E-01
Hamstring_L_pro	2,965935330E-06	6,563886942E-03	1,925533500E-06	3,474575298E-03
Hamstring_L_dis	1,453941608E-06	3,217706143E-03	2,272447800E-06	4,100573161E-03
Iliopsoas_R	4,553396802E-05	1,007708479E-01	1,142493819E-04	2,061600487E-01
Iliopsoas_R_pro	1,541019780E-06	3,410418127E-03		0,000000000E+00
Iliopsoas_R_dis	1,303533855E-06	2,884839991E-03	4,169337000E-07	7,523460562E-04
Iliopsoas_L	3,952029665E-05	8,746204158E-02	1,110825954E-04	2,004456645E-01
Iliopsoas_L_pro	1,263952868E-06	2,797243635E-03		0,000000000E+00
Iliopsoas_L_dis	1,031744408E-06	2,283345013E-03	5,315109000E-07	9,590976442E-04
Pectinius_R	1,565823866E-05	3,465311843E-02	6,442421340E-05	1,162518234E-01
Pectinius_R_pro	2,015991630E-06	4,461574399E-03	2,355198000E-07	4,249893753E-04
Pectinius_R_dis	1,936829655E-06	4,286381687E-03		0,000000000E+00
Pectinius_L	1,633111544E-05	3,614225648E-02	6,150567750E-05	1,109854010E-01
Pectinius_L_pro	2,213896568E-06	4,899556178E-03	3,882894000E-07	7,006581592E-04
Pectinius_L_dis	1,936829655E-06	4,286381687E-03		0,000000000E+00
Peroneus_R	2,448743760E-05	5,419294557E-02	3,818285190E-05	6,889996669E-02
Peroneus_R_pro	4,881655125E-07	1,080355057E-03		0,000000000E+00
Peroneus_R_dis	4,842074138E-06	1,071595422E-02		0,000000000E+00
Peroneus_L	2,963296598E-05	6,558047185E-02	3,045525630E-05	5,495572070E-02
Peroneus_L_pro	1,240204275E-07	2,744685821E-04	5,124147000E-07	9,246390462E-04
Peroneus_L_dis	3,976569878E-06	8,800513899E-03	4,503520500E-06	8,126486027E-03
Piriformis_R	9,217092623E-06	2,039827143E-02	1,317637800E-05	2,377643262E-02
Piriformis_R_pro	6,939866475E-07	1,535856108E-03	2,864430000E-07	5,168789699E-04
Piriformis_R_dis	9,103627125E-07	2,014716188E-03	1,339916700E-06	2,417844959E-03
Piriformis_L	9,106265858E-06	2,015300164E-02	1,077662220E-05	1,944613547E-02
Piriformis_L_pro	3,958098750E-07	8,759635599E-04	2,991738000E-07	5,398513686E-04
Piriformis_L_dis	6,781542525E-07	1,500817566E-03	4,455780000E-07	8,040339532E-04
Rectus_femoris_R	7,061512043E-05	1,562777388E-01	8,687497920E-05	1,567636485E-01
Rectus_femoris_R_pro	4,512232575E-07	9,985984583E-04	6,779151000E-07	1,223280229E-03
Rectus_femoris_R_dis	1,458427453E-05	3,227633730E-02	1,699880070E-05	3,067389531E-02
Rectus_femoris_L	6,981558449E-05	1,545082925E-01	8,337719190E-05	1,504519819E-01
Rectus_femoris_L_pro	5,805211500E-07	1,284746555E-03	4,678569000E-07	8,442356509E-04
Rectus_femoris_L_dis	1,433623367E-05	3,172740014E-02	2,167100430E-05	3,910476562E-02
Sartorius_R	4,446000389E-05	9,839406681E-02	7,524857610E-05	1,357841054E-01
Sartorius_R_pro	3,905324100E-07	8,642840458E-04	1,877793000E-07	3,388428803E-04

Muscle Volume Data

Name	Volume_healthy_ child	Volume_norm_ healthy_child	Volume_CP1	CP1_norm
	m ³		m ³	
Sartorius_R_dis	1,208539485E-06	2,674608736E-03	1,133041200E-06	2,044543481E-03
Sartorius_L	4,552077436E-05	1,007416491E-01	7,914420090E-05	1,428136594E-01
Sartorius_L_pro	3,509514225E-07	7,766876898E-04	3,087219000E-07	5,570806676E-04
Sartorius_L_dis	1,058131733E-06	2,341742584E-03	6,301746000E-07	1,137133734E-03
Soleus_R	1,112252136E-04	2,461516001E-01	1,554207891E-04	2,804527860E-01
Soleus_R_pro	6,966253800E-07	1,541695865E-03	3,723759000E-07	6,719426609E-04
Soleus_R_dis	3,000238853E-06	6,639803784E-03	3,946548000E-07	7,121443586E-04
Soleus_L	1,069029698E-04	2,365860780E-01	1,101246027E-04	1,987169915E-01
Soleus_L_pro	7,388451000E-07	1,635131979E-03	5,697033000E-07	1,028014840E-03
Soleus_L_dis	8,285620050E-07	1,833683719E-03	2,005101000E-07	3,618152789E-04
Tibialis_ant_R	3,695808740E-05	8,179163747E-02	4,636239090E-05	8,365973283E-02
Tibialis_ant_R_pro	6,755155200E-07	1,494977809E-03	5,665206000E-07	1,022271741E-03
Tibialis_ant_R_dis	5,156083305E-06	1,141088531E-02	4,548078300E-06	8,206889422E-03
Tibialis_ant_L	3,326386190E-05	7,361597758E-02	4,178566830E-05	7,540115551E-02
Tibialis_ant_L_pro	2,744281800E-07	6,073347349E-04	5,633379000E-07	1,016528641E-03
Tibialis_ant_L_dis	3,976569878E-06	8,800513899E-03	4,007019300E-06	7,230562479E-03
Tibialis_post_R	2,932423427E-05	6,489722028E-02	4,506066660E-05	8,131080507E-02
Tibialis_post_R_pro	1,055493000E-06	2,335902826E-03	5,315109000E-07	9,590976442E-04
Tibialis_post_R_dis	6,678631958E-06	1,478042513E-02	6,285832500E-06	1,134262184E-02
Tibialis_post_L	3,328761049E-05	7,366853539E-02	4,382896170E-05	7,908822550E-02
Tibialis_post_L_pro	8,628655275E-07	1,909600561E-03	2,768949000E-07	4,996496709E-04
Tibialis_post_L_dis	3,588676200E-06	7,942069610E-03	4,869531000E-06	8,786942489E-03
Ten_Fas_Latae_R	1,662929222E-05	3,680214903E-02	2,842787640E-05	5,129736621E-02
Ten_Fas_Latae_R_pro	1,944745853E-06	4,303900958E-03	7,638480000E-08	1,378343920E-04
Ten_Fas_Latae_R_dis	1,076602860E-05	2,382620883E-02	2,505103170E-05	4,520393747E-02
Ten_Fas_Latae_L	1,642083235E-05	3,634080822E-02	2,610132270E-05	4,709916036E-02
Ten_Fas_Latae_L_pro	1,609626825E-06	3,562251810E-03	1,209426000E-07	2,182377873E-04
Ten_Fas_Latae_L_dis	1,098768213E-05	2,431674842E-02	2,028334710E-05	3,660077417E-02
Vastus_R	4,518565533E-04	1,000000000E+00	5,541780894E-04	1,000000000E+00
Vastus_R_dis_lat	1,211178218E-06	2,680448493E-03	2,094216600E-06	3,778959580E-03
Vastus_R_dis_med	7,625936925E-07	1,687689792E-03	3,255902100E-06	5,875190958E-03
Vastus_L	4,225191254E-04	9,350735809E-01	5,185350321E-04	9,356830268E-01
Vastus_L_dis_lat	1,084519058E-06	2,400140154E-03	1,028012100E-06	1,855021192E-03
Vastus_L_dis_med	7,705098900E-07	1,705209063E-03	1,915985400E-06	3,457345999E-03

Muscle Length Data

Name	Length_healthy	Norm_L_healthy	Length_CP1	Norm_L_CP1
	m		m	
Add_longus_L	0,130879626	0,105548085	0,188268628	0,134477592
Add_longus_L_pro	0,027073303	0,021833309	0,006229177	0,004449412
Add_longus_L_dis	0,023388108	0,018861377		0
Add_longus_R	0,127172161	0,102558194	0,191932419	0,137094585
Add_longus_R_pro	0,024531244	0,019783261	0,003184142	0,002274387
Add_longus_R_dis	0,021927785	0,017683698		0
Add_magnus_R	0,218889672	0,176523929	0,272154092	0,19439578
Add_magnus_R_pro	0	0		0
Add_magnus_R_dis	0,136221412	0,109855977	0,08747487	0,06248205
Add_magnus_L	0,206764458	0,166745531	0,241334583	0,172381845
Add_magnus_L_pro	0	0		0
Add_magnus_L_dis	0,138332923	0,111558809	0,132448557	0,094606112
Biceps_Shorthead_R	0,113828166	0,091796908	0,185473968	0,132481406
Biceps_Shorthead_R_pro	0	0	0,068179381	0,048699558
Biceps_Shorthead_R_dis	0,057082654	0,046034399		0
Biceps_Shorthead_L	0,105937401	0,085433388	0,159965883	0,114261345
Biceps_Shorthead_L_pro	0	0	0	0
Biceps_Shorthead_L_dis	0,049971907	0,040299925	0,053457041	0,038183601
Ex_digi_R	0,23176292	0,186905581	0,264851084	0,189179346
Ex_digi_R_pro	0,014731817	0,011880498	0,026014088	0,018581491
Ex_digi_R_dis	0,125859092	0,101499268	0,155517464	0,111083903
Ex_digi_L	0,216876116	0,174900094	0,271891941	0,19420853
Ex_digi_L_pro	0,006427183	0,005183212	0,012352549	0,008823249
Ex_digi_L_dis	0,142647784	0,115038535	0,188660895	0,134757782
Flex_digi_longus_R	0,106588491	0,08595846	0,117895062	0,084210758
Flex_digi_longus_R_pro	0,032981869	0,026598281		0
Flex_digi_longus_R_dis	0,145331931	0,11720317	0,03109016	0,022207257
Flex_digi_longus_L	0,127946271	0,103182477	0,130564997	0,093260712
Flex_digi_longus_L_pro	0,028521109	0,023000894		0
Flex_digi_longus_L_dis	0,162407578	0,130973853	0,158992319	0,113565942
Flex_hall_longus_R	0,196097003	0,158142745	0,254973211	0,182123722
Flex_hall_longus_R_pro	0	0		0
Flex_hall_longus_R_dis	0,112373658	0,090623918	0,009592622	0,006851873
Flex_hall_longus_L	0,166460507	0,134242345	0,25034502	0,178817872
Flex_hall_longus_L_pro	0	0		0
Flex_hall_longus_L_dis	0,087676466	0,070706827	0,003262756	0,00233054
Gastrocnemius_R	0,161951307	0,130605892	0,187551784	0,13396556
Gastrocnemius_R_pro	0,035763582	0,028841598	0,063078392	0,045055995
Gastrocnemius_R_dis	0,206979455	0,166918915	0,280837333	0,200598095
Gastrocnemius_L	0,156119909	0,125903152	0,185288903	0,132349216
Gastrocnemius_L_pro	0,019538635	0,015756964	0,057629258	0,041163756
Gastrocnemius_L_dis	0,21286054	0,171661726	0,232459247	0,166042319
Gluteus_max_R	0,203009337	0,163717207	0,260832306	0,18630879
Gluteus_max_R_pro	0	0		0
Gluteus_max_R_dis	0	0		0
Gluteus_max_L	0,19327613	0,155867847	0,278233429	0,198738164
Gluteus_max_L_pro	0	0		0
Gluteus_max_L_dis	0	0		0
Gluteus_medius_R	0,107752468	0,086897152	0,152933191	0,109237994
Gluteus_medius_R_pro	0	0		0
Gluteus_medius_R_dis	0,029732281	0,023977646		0
Gluteus_medius_L	0,102385668	0,082569087	0,159596144	0,113997245
Gluteus_medius_L_pro	0	0		0
Gluteus_medius_L_dis	0,025687383	0,020715632		0

Muscle Length Data

Name	Length_healthy	Norm_L_healthy	Length_CP1	Norm_L_CP1
	m		m	
Gluteus_min_R	0,074301504	0,059920568	0,122806856	0,087719183
Gluteus_min_R_pro	0,031531819	0,025428886	0	0
Gluteus_min_R_dis	0,026327273	0,021231672	0,009982082	0,007130059
Gluteus_min_L	0,061962298	0,049969595	0,082719378	0,05908527
Gluteus_min_L_pro	0,026625444	0,021472132	0	0
Gluteus_min_L_dis	0,025639567	0,02067707	0,011438046	0,008170033
Grasilis_R	0,184612846	0,148881328	0,231888684	0,165634774
Grasilis_R_pro	0,013449849	0,010846652	0,006176943	0,004412102
Grasilis_R_dis	0,093338416	0,075272916	0,073049828	0,052178448
Grasilis_L	0,191242508	0,154227829	0,221685614	0,158346867
Grasilis_L_pro	0,015436715	0,012448963	0,006762789	0,004830563
Grasilis_L_dis	0,079240721	0,063903807	0,074272455	0,053051754
Hamstring_R	0,223248005	0,180038714	0,25473206	0,181951472
Hamstring_R_pro	0,044488007	0,035877425	0,034609243	0,024720888
Hamstring_R_dis	0,040668849	0,032797459	0,049190671	0,035136194
Hamstring_L	0,214194242	0,172737292	0,249665467	0,178332476
Hamstring_L_pro	0,046440533	0,037452043	0,041727027	0,029805019
Hamstring_L_dis	0,039770452	0,032072945	0,050726283	0,036233059
Iliopsoas_R	0,13303219	0,107284024	0,180435197	0,128882284
Iliopsoas_R_pro	0	0		0
Iliopsoas_R_dis	0,031206725	0,025166713	0,003953888	0,002824206
Iliopsoas_L	0,128709785	0,103798214	0,190210348	0,135864534
Iliopsoas_L_pro	0	0		0
Iliopsoas_L_dis	0,029088343	0,023458341	0,010873918	0,007767084
Pectinius_R	0,098252542	0,079235921	0,13280633	0,094861665
Pectinius_R_pro	0,036443647	0,029390038	0,006558267	0,004684476
Pectinius_R_dis	0,038742841	0,031244226		0
Pectinius_L	0,073198389	0,059030959	0,148942135	0,106387239
Pectinius_L_pro	0,034068879	0,027474903	0,010690629	0,007636163
Pectinius_L_dis	0,025865051	0,020858912		0
Peroneus_R	0,217699913	0,175564446	0,275711442	0,196936744
Peroneus_R_pro	0,018995651	0,015319073		0
Peroneus_R_dis	0,173358344	0,139805116		0
Peroneus_L	0,234362095	0,189001689	0,24923216	0,178022972
Peroneus_L_pro	0,003210581	0,002589178	0,019630823	0,014022016
Peroneus_L_dis	0,178991612	0,144348074	0,218022171	0,155730122
Piriformis_R	0,045946362	0,037053518	0,053497845	0,038212746
Piriformis_R_pro	0,018848637	0,015200513	0	0
Piriformis_R_dis	0,024138172	0,019466268	0,007593912	0,005424223
Piriformis_L	0,051020236	0,041145352	0,0482714	0,034479572
Piriformis_L_pro	0,013220224	0,010661471	0	0
Piriformis_L_dis	0,019952645	0,016090842	0	0
Rectus_femoris_R	0,239379911	0,193048315	0,262446217	0,187461584
Rectus_femoris_R_pro	0,01015907	0,008192799	0,02041901	0,014585007
Rectus_femoris_R_dis	0,156746213	0,126408237	0,175203923	0,12514566
Rectus_femoris_L	0,233796157	0,188545288	0,252815314	0,180582367
Rectus_femoris_L_pro	0,013488301	0,010877662	0,009693609	0,006924007
Rectus_femoris_L_dis	0,158907412	0,128151139	0,176010662	0,125721902
Sartorius_R	0,32658841	0,26337775	0,381278712	0,272341937
Sartorius_R_pro	0,028768596	0,02320048	0,003998565	0,002856118
Sartorius_R_dis	0,043729902	0,03526605	0,03557915	0,025413679
Sartorius_L	0,326133588	0,263010958	0,358450116	0,256035797
Sartorius_L_pro	0,022060879	0,017791032	0,006607527	0,004719662
Sartorius_L_dis	0,035733171	0,028817073	0,021790333	0,015564524

Muscle Length Data

Name	Length_healthy	Norm_L_healthy	Length_CP1	Norm_L_CP1
	m		m	
Soleus_R	0,198930712	0,160427993	0,281176717	0,200840512
Soleus_R_pro	0,03939484	0,031770033	0,008060648	0,005757606
Soleus_R_dis	0,040972376	0,033042238	0,016805881	0,012004201
Soleus_L	0,208138117	0,16785332	0,249930892	0,178522066
Soleus_L_pro	0,032242571	0,026002074	0,013472499	0,009623214
Soleus_L_dis	0,024870282	0,020056679	0,006306407	0,004504576
Tibialis_ant_R	0,206291004	0,166363713	0,225089014	0,160777867
Tibialis_ant_R_pro	0,022748235	0,01834535	0,025597913	0,018284224
Tibialis_ant_R_dis	0,159797411	0,12886888	0,15610409	0,111502921
Tibialis_ant_L	0,186030107	0,15002428	0,218381983	0,15598713
Tibialis_ant_L_pro	0,01164897	0,009394331	0,01558821	0,011134436
Tibialis_ant_L_dis	0,176963333	0,142712365	0,165184126	0,117988661
Tibialis_post_R	0,173294523	0,139753647	0,242609516	0,173292512
Tibialis_post_R_pro	0,020250997	0,016331449	0,010635012	0,007596437
Tibialis_post_R_dis	0,165425358	0,133407547	0,152552668	0,108966191
Tibialis_post_L	0,187567598	0,151264192	0,225088843	0,160777745
Tibialis_post_L_pro	0,013618668	0,010982797	0,006268403	0,00447743
Tibialis_post_L_dis	0,146299155	0,11798319	0,205662836	0,146902026
Ten_Fas_Latae_R	0,109899587	0,088628699	0,126113503	0,090081073
Ten_Fas_Latae_R_pro	0,055448622	0,04471663	0,003261502	0,002329644
Ten_Fas_Latae_R_dis	0,27454456	0,221406903	0,301858822	0,215613444
Ten_Fas_Latae_L	0,09391466	0,075737629	0,122284478	0,087346056
Ten_Fas_Latae_L_pro	0,036189316	0,029184933	0,003436862	0,002454902
Ten_Fas_Latae_L_dis	0,280606365	0,226295455	0,314762402	0,224830287
Vastus_R	0,302404773	0,243874817	0,326769674	0,23340691
Vastus_R_dis_lat	0,047866076	0,038601674	0,077995298	0,055710927
Vastus_R_dis_med	0,032923567	0,026551264	0,050790278	0,03627877
Vastus_L	0,289393813	0,233382108	0,319314502	0,228081787
Vastus_L_dis_lat	0,04604616	0,037134	0,051712821	0,036937729
Vastus_L_dis_med	0,031039226	0,025031634	0,038536395	0,027525997